NOVA SCHOOL OF SCIENCE & TECHNOLOGY

DEPARTMENT OF ELECTRICAL AND COMPUTER ENGINEERING

MARGARIDA MARIA GUIMARÃES DA COSTA PEREIRA

Bsc in Electrical and Computer Engineering

ENERGY POTENTIAL OF A COMMUNITY

MASTER IN ELECTRICAL AND COMPUTER ENGINEERING

NOVA University Lisbon

September, 2023

NOVA SCHOOL OF
SCIENCE & TECHNOLOGY

DEPARTMENT OF ELECTRICAL
AND COMPUTER ENGINEERING

ENERGY POTENTIAL OF A COMMUNITY

MARGARIDA MARIA GUIMARÃES DA COSTA PEREIRA

Bsc in Electrical and Computer Engineering

Adviser: Pedro Miguel Ribeiro Pereira
Assistant Professor, NOVA University Lisbon

Examination Committee

Rapporteur: Rui Lopes
Assistant Professor, FCT-NOVA

Adviser: Pedro Miguel Ribeiro Pereira
Assistant Professor, NOVA University Lisbon

MASTER IN ELECTRICAL AND COMPUTER ENGINEERING

NOVA University Lisbon
September, 2023

Energy potential of a community

Acknowledgements

Foremost, I want to express my appreciation to my Dissertation advisor, Professor Pedro Pereira. His support, guidance, and belief in my abilities have been the cornerstone of my research endeavors. His mentorship has not only provided me with the necessary expertise but also instilled in me the confidence to tackle complex challenges, ultimately shaping the very foundation of this work.

Turning to my family, particularly my mother and uncles, I am profoundly indebted to them for their support that has extended beyond the boundaries of mere words. Their encouragement, both emotionally and practically, has been the bedrock of my academic journey. Their belief in my potential and their sacrifices on my behalf have been a constant source of inspiration, serving as the driving force behind my pursuit of achievement.

Furthermore, I wish to extend my appreciation to my friends, whose encouragement, motivation, and camaraderie have been a wellspring of strength during the most challenging phases of this research journey. Their presence, be it through late-night study sessions, discussions, or words of encouragement, has served as a reminder that I am part of a supportive community that shares in my aspirations.

In closing, I want to emphasize that the support I have received, regardless of its scale, has been an essential and irreplaceable component of this academic accomplishment. The collective influence of my Dessirtation advisor, my family, and my friends has left an indelible mark on my academic path, and for this, I am genuinely and profoundly appreciative.

"The saddest aspect of life right now is that science gathers knowledge faster than society gathers wisdom." -Isaac Asimov

Abstract

This thesis considers the growing concern over carbon emissions and the European Union's commitment to achieving carbon neutrality by 2050 through national climate and energy plans. These plans have led to a shift away from fossil fuels toward renewable energy sources, with residential Photovoltaic (PV) systems emerging as a sought-after solution. These decentralized energy systems offer greater efficiency and eco-friendliness.

However, the adoption of PV systems also presents challenges related to solar resource availability, energy storage, and energy exchange in decentralized scenarios. This study explores these challenges and focuses on maximizing the energy consumption to maximize the benefits of PV systems.

The study's findings indicate that Energy Communities (EC) with energy storage perform better in terms of PV consumption compared to individual approaches. ECs demonstrate a high PV consumption due to surplus PV energy being shared among houses. Importantly, the study found no adverse effects on transformers, even in a worst-case scenario, suggesting that decentralized PV systems can be integrated into existing infrastructure seamlessly.

Additionally, the study demonstrated the distribution transformers in these communities do not experience any noteworthy adverse effects. Even in the most unfavorable scenario, where individual PV systems lack storage, the highest observed increase in transformer demand was merely 16.74 kVA, which falls comfortably within acceptable thresholds.

In summary, this research underscores the potential of PV systems in achieving carbon neutrality within the framework of national climate and energy plans. It also provides valuable insights into the advantages and challenges of decentralized energy systems, offering a path toward more sustainable and efficient energy consumption.

Keywords: Photovoltaic energy, Energy Communities, Battery systems, Transformer aging, SSR and SCR

Resumo

Esta tese considera a crescente preocupação com as emissões de carbono e o compromisso da União Europeia em atingir a neutralidade carbónica até 2050, através dos planos nacionais de clima e energia. Estes planos conduziram a uma transição longe dos combustíveis fósseis em direção a fontes de energia renovável, com os sistemas residenciais de PV emergindo como uma solução muito procurada. Estes sistemas descentralizados de energia oferecem maior eficiência e amigabilidade para o ambiente.

No entanto, a adoção de sistemas de PV também apresenta desafios relacionados com a disponibilidade de recursos solares, armazenamento de energia e troca de energia em cenários descentralizados. Este estudo explora esses desafios e concentra-se na otimização do consumo de energia para maximizar os benefícios dos sistemas de PV.

Os resultados do estudo indicam que as EC com armazenamento de energia têm um melhor desempenho em termos de consumo de PV em comparação com abordagens individuais. As ECs demonstram um elevado consumo de energia PV devido à partilha de energia excedente de PV entre as habitações. Importante ainda, o estudo não encontrou efeitos adversos nos transformadores, mesmo no pior cenário, sugerindo que os sistemas de PV descentralizados podem ser integrados na infraestrutura existente de forma harmoniosa.

Adicionalmente, o estudo demonstrou que os transformadores de distribuição nestas comunidades não sofrem quaisquer efeitos adversos significativos. Mesmo no cenário mais desfavorável, onde os sistemas de PV individuais não têm armazenamento, o aumento mais elevado observado na procura de transformadores foi apenas de 16,74 kVA, o que se situa confortavelmente dentro dos limites aceitáveis.

Em resumo, este estudo destaca o potencial dos sistemas de PV para atingir a neutralidade carbónica no âmbito dos planos nacionais de clima e energia. Também fornece informações valiosos sobre as vantagens e desafios dos sistemas de energia descentralizada, oferecendo um caminho em direção a um consumo de energia mais sustentável e eficiente.

Palavras-chave: Energia fotovoltaica, Comunidades de energia, Sistemas bateria, Envelhecimento transformador, SSR e SCR

Contents

List of Figures

List of Tables

List of Listings

Glossary

Commons-Based Peer Production Commons-based peer production (CBPP) is an emerging innovative model of production characterized by peer to peer collaboration for the creation or maintenance of shared resources, which are freely accessible and reusable by anyone. In CBPP, the creative energy of communities of individuals is coordinated through software platforms mostly without traditional hierarchical organisation or financial compensation. [1] *(pp. xviii, 12)*

Energy Communities Energy communities organise collective and citizen-driven energy actions that help pave the way for a clean energy transition, while moving citizens to the fore. They contribute to increasing public acceptance of renewable energy projects and make it easier to attract private investments in the clean energy transition. At the same time, they have the potential to provide direct benefits to citizens by increasing energy efficiency, lowering their electricity bills and creating local job opportunities. [2] *(pp. v, xviii, 5)*

microgrid A small network of electricity consumer, producers and prosumers who have a local source of electricity that can be connected to the national grid but is also able to function independently *(pp. xi, 12–14, 20, 21)*

prosumer Someone that both produces and consumes energy *(pp. 20, 25, 34, 52, 53, 72)*

Acronyms

3D Three Dimensions *(p. 39)*

AC Alternate Current *(pp. 42–44)*
APS Action-based Pricing Strategy *(pp. 14, 17)*

BS Bill Sharing *(pp. 14, 16)*

CBPP Commons-Based Peer Production *(p. 12)*
CES Community Energy Storage *(pp. 28)*

DC Direct Current *(p. 42)*
DER Decentralized Energy Resources *(pp. 8–10)*
DG Distributed Generation *(p. 20)*
DoD Depth of Discharge *(p. 50)*

EC Energy Communities *(pp. v, vi, xii, 2–5, 10–12, 20–22, 26, 27, 30, 32–34, 39, 45, 47–49, 52, 53, 56, 65, 72–75, 83)*
EU European Union *(pp. 2, 21)*

ICT Information and Communication Technologies *(p. 13)*
ID Identification *(p. 39)*

KiBaM Kinetic Battery Model *(pp. xi, 23)*
kWh killo-Watt hour *(p. 20)*

MMR Mid-Market Rate *(pp. 14, 16, 18, 34, 53)*

NES National Electric System *(p. 1)*
NGE Net Grid Exchange *(p. 29)*

NPV Net Present Value *(p. 11)*
nZEB Nearly Zero Energy Building *(pp. 18, 19)*

P2P Peer-to-Peer *(pp. xi, xii, 4, 5, 12–16, 21, 25, 28, 30, 34, 36, 47, 49, 53, 54, 66, 69, 70, 72, 74, 83)*
PV Photovoltaic *(pp. v, vi, xi, 1–12, 14–18, 20–23, 25–30, 32–54, 56, 57, 59, 60, 62, 65–72, 74, 75)*
PVGIS Photovoltaic Geographical Information System *(pp. 32, 41, 54, 55, 60)*

RES Renewable Energy System *(p. 2)*
RLS Recursive Least Square *(p. 17)*

SCR Self Consumption Rate *(pp. 29, 65, 67–70, 74, 75)*
SOC State Of Charge *(pp. 24, 74)*
SoC State of Charge *(pp. 34, 35, 48–52)*
SSR Self Sufficiency Rate *(pp. 29, 65, 67, 68, 70, 74)*

VPP Virtual Power Plant *(p. 20)*

Wp Watt peek *(p. 59)*
WTP Willingness To Pay *(p. 3)*

1 Introduction

In the course of time the concern regarding the carbon footprint has been increasing and several goals have been set. All Member States of the European Union elaborated and presented a national climate and energy plan, mapping the actions that would take place between 2021-2030 in effort to reach carbon neutrality by the year 2050 [3]. In scope of the established plans, most of the Member States have imposed restrictions on the production and usage of fossil fuels changing the direction of energy solutions towards renewable energies.

A sought-after solution are residential PV systems. Various approaches have emerged for the utilization of PV systems, ranging from individual consumers to entire communities. The usage of PV systems as a decentralized energy system allows for more optimal use of renewable energy and increases eco-efficiency [4].

When considering a decentralized energy scenario, it is also necessary to consider the struggles that emerge with such systems. Focusing on PV systems, it is possible to extrapolate that most difficulties are related to the availability of the natural resource in question, the solar radiation, the paradigm of energy storage and the exchange of energy. Therefore, it is necessary to exploit the most out of the energy produced and optimize the consumption process.

In Portugal, an effort is being made to erase the distinction between production in ordinary regime and special regime, additionally erasing the need for two distinct electricity production licensing procedures simplifying the National Electric System (NES) [3] which alongside government incentives for PV systems, are enabling the demand for renewable energy systems to increase along with innovation and more effective technology. With that demand comes the need for system optimization.

1.1 Motivation

In order to achieve the rotary established by the European Ecological Pact and reach a curtailment of emissions of no less than 55% by 2030, a significant transformation is needed in the energetic module [3].

The rapid expansion of PV systems as a key renewable energy source has brought forth the need to explore critical aspects such as dimensioning, battery integration, and the emergence of energy communities.

Accordingly to Öko Institute [5], rooftop solar installations, whether PV systems or solar panels, are a fundamental step in the increase of renewable energies. Ritter, Bauknecht, and Kaya also state that the solar installations should become standard for European countries and claim the obligation should be implemented by stages starting as soon as mid 2023. This statement is backed by a proposal for amending European Union (EU) Directives regarding the use of renewable energy, energy performance of buildings and energy efficiency [6], in which Article 9a states that new buildings are obliged to ensure "solar energy generation" optimization based on their solar irradiation. This action is ensured to be deployed by 31 of December of 2029 in all residential buildings. While buildings [7], are responsible for 40% of energy consumption, buildings with PV systems can generate up to 25% of the EU's electricity consumption [8].

Figure 1.1 displays which European countries currently have solar mandates. Countries represented in green have mandates that involve existing buildings, in light green mandates encompass new and/or renovated buildings, in orange countries have mandatory installation of Renewable Energy System (RES) technology and lastly, in red are countries with no current mandates.

Figure 1.1: Countries where solar mandates are in place, taken from Commission [9].

With the goal of increasing the profitability of PV systems, this study examines four distinct scenarios of PV installations: (1) PV systems with and without battery systems, (2) the establishment of an EC and (3) the aggregation of neighbouring ECs so as to make a multi-EC. These scenarios will be evaluated based on specific parameters including energy community size and battery system types. To quantitatively assess the disparities among the different scenarios, multiple performance indicators are taken into account.

1.2 Problems with the Current State

The transition towards sustainable and renewable energy sources is a key priority for countries worldwide. However, the variation in solar mandates across European countries poses significant challenges in policy implementation, enforcement, and the need for harmonization. Achieving widespread adoption of PV systems requires consideration of various critical aspects due to their rapid expansion as a renewable energy source.

The integration of batteries with PV systems is a promising approach to store excess energy and ensure continuous power supply. However, this approach faces challenges related to high costs, limited battery lifespan and environmental concerns.

ECs represent an innovative approach to decentralized energy generation and distribution. Legal and regulatory frameworks need to be adapted to accommodate the characteristics of EC, and technical interoperability must be achieved to enable integration with existing energy infrastructures. Additionally, developing appropriate market models and encourage active community involvement are crucial to the long-term viability of EC.

The idea of aggregating neighboring ECs to form multi-ECs offers potential benefits in terms of increased efficiency and broader impact. However, this approach presents its own set of challenges. Addressing issues related to scalability and operational challenges becomes essential to capitalize on the advantages of multi-ECs.

1.3 Objectives

The primary objectives of this dissertation encompass a study and modeling of various aspects related to battery capacity optimization, energy community size determination, and scalability analysis.

One of the primary focuses is the assessment of various factors that can influence the EC effectiveness and find the EC parameters who contribute the most. These factors include energy demand, scalability, optimal PV integration, households' orientation, Willingness To Pay (WTP), and the impact of transformer age. This analysis provided valuable insights into the design and operation of energy communities, facilitating their effective and sustainable deployment.

Consequently, in order to determine the appropriate battery capacity for each PV system scenario, a model was created that ensures the overall feasibility of the system. By developing appropriate models, this research aims to enhance the lifespan of batteries and reduce associated costs, making battery integration economically viable for PV systems. By identifying the optimal battery capacity, it was possible to maximize the efficiency and longevity of PV systems while ensuring cost-effectiveness.

Furthermore, the scalability of ECs and the potential benefits of aggregating multiple energy communities were studied, so as to evaluate the feasibility and advantages of scaling up EC networks. This study takes into account the previous concerns regarding battery capacity optimization, energy community size, and other relevant factors.

1.4 Dissertation Structure

The first chapter of this dissertation serves as an introduction to the study, outlining the problem statement, objectives, and significance of the study.

Chapter 2 discusses the existing literature including up-to-date studies on the topic of PV rooftop generation and the integration of these systems with energy storage systems and the the integration and implementation of ECs. Additionally, the subject of the different P2P markets approaches and their ramifications is discussed along with their possible equations. Moreover, Chapter 2 provides insight to a model for the dimensioning of an adequate battery for PV systems. Furthermore, this chapter will also focus on possible work limitations in the implementation of these systems

The primary aim of the third chapter is to provide a comprehensive explanation of the methodology employed throughout this dissertation, elaborating on the specific approaches in the research. Multiple flowcharts are shown in order to better demonstrate the steps involved in modeling of the ECs and the overall study. Additionally, a timeline is provided showcasing the subsequent steps involved in this study.

Chapter 4, will take a closer and more comprehensive look at the implementation of the methodology employed. This chapter will provide a thorough examination of the step-by-step processes, tools, and techniques utilized to carry out the study.

Moving on to Chapter 5, it will delve into the case study that consolidates the methodology. Within this chapter, it will not only describe the chosen case study in detail but also provide the results obtained throughout the study. This section will shed light on the practical application and real-world implications of the methodologies and theories discussed in earlier chapters.

Finally, Chapter 6 will serve as the concluding section of the dissertation. Here, it will consolidate the key findings, insights, and contributions of the study.

2

State of the Art

This literature review provides an insightful analysis of the interconnected elements of Photovoltaic (PV) generation. By examining dimensioning practices, battery integration, and the evolving concept of Energy Communities (EC)s, this review aims to shed light on the transformative potential and future prospects of PV systems in shaping a sustainable and decentralized energy landscape. Dimensioning plays a pivotal role in optimizing the performance and cost-effectiveness of PV systems.

In parallel, battery integration has become increasingly crucial for the stability and flexibility of PV systems. This review explores the challenges and opportunities in integrating energy storage systems with PV installations, and discusses the impact of such integration on self-consumption and grid resilience. Lastly, the emergence of ECs, which promote energy sharing and Peer-to-Peer (P2P) trading within local neighborhoods, is explored. The review delves into the technological, regulatory, and social aspects of ECs, highlighting their potential to drive renewable energy adoption and democratize the energy sector.

2.1 Calculating PV Generation

PV Module Production

The initial stage in establishing a residential PV roof plant where the goal is to increase self-consumption, involves calculating the energy production necessary to meet maximal load requirements. Using Rosell and Ibáñez's equation to calculate the PV generation, it requires the temperature of the module's cell [10]. Chapter 3 will delve into the acquisition of irradiance data.

The expression needed to calculate the PV generation can be described by Equation 2.1,

$$P_{out} = \frac{G}{G_{STC}} P_{max}[1 + \Upsilon(T_{cell} - T_{STC})] \tag{2.1}$$

where G is the incident irradiation, G_{STC} and T_{STC} refer to the testing conditions of $1000 W m^{-2}$ and 25°C respectively, P_{max} is panel's maximum power, Υ is the module's correction value for temperature and T_{cell} is the cell's temperature.

The temperature of the module's cell can be calculated by Zhang et al.'s Equation 2.2 [10],

$$T_{cell} = T_{amb} + G \cdot \frac{NOCT - 20}{800} \cdot \left(\frac{\eta}{\tau\alpha}\right) \tag{2.2}$$

in which T_{amb} is the ambient temperature, G the total irradiance, α the absorbance of the PV module, τ the transmittance of the PV cell surface and η the efficiency of the PV model.

Wind Speed

However this model does not consider the wind speed action in reducing the cell temperature, therefore in this dissertation the Sandia model, used by Kratochvil, Boyson, and King [12], will be considered.

The calculation of the temperature of the PV module can be described by Equation 2.3,

$$T_{mod} = T_{amb} + G \cdot e^{(a+b \cdot W_{speed})} \tag{2.3}$$

where T_{cell} is the module temperature, a the coefficient that establishes the upper limit for the T_{mmod} when the G is high and W_{speed} is low, b is the coefficient that establishes the rate T_m as W_{speed} increases and W_{speed} is the wind speed. Both coefficients can be found in Table 2.1.

Now it is possible to calculate the temperature of the module's cells by applying Equation 2.4,

$$T_{cell} = T_{mod} + \frac{G}{G_{STC}} \cdot \Delta T \tag{2.4}$$

where G and G_{STC} are the irradiance on the module and the irradiance the module was tested for, respectively, and ΔT is the temperature difference between the cell and the module back surface at the tested irradiance, G_{STC}.

Table 2.1: Empirically calculated coefficients for the calculation of the wind speed, adapted from Kratochvil, Boyson, and King [12].

Module Type	Mount	a	b	$\delta T(C)$
Glass/Cell/Polymer sheet	Open rack	-3.56	-0.0750	3
Glass/Cell/Polymer sheet	Insulated back	-2.81	-0.0455	0

Given that wind speed is provided for a height of ten meters, it is necessary to convert the speed to the height of the various buildings considered. That can be achieved by Equation 2.5 taken from Tahbaz [13],

$$W_{speed} = W_{10} \cdot \left[\frac{h}{10}\right]^{\alpha} \tag{2.5}$$

where W_{10} is the wind speed at a height of 10 meters and α is empirical exponent which depends on the surface roughness, stability and temperature gradient.

Table 2.2: Values for coefficient α in each terrain, adapted from Tahbaz [13].

Terrain Category	Description	Exponent $alpha$
1	Large city centres, in which at least 50% of buildings are higher than 21.3 m, over a distance of at least 0.8 km or 10 times the height of the structure upwind, whichever is greater	0.33
2	Urban and suburban areas, wooded areas, or other terrain with numerous closely spaced obstructions having the size of single-family dwellings or larger, over a distance of at least 460 m or 10 times the height of the structure upwind, whichever is greater	0.22
3	Open terrain with scattered obstacles having heights generally less than 9 m, including flat open country typical of meteorological station surroundings	0.14
4	Flat, unobstructed areas exposed to wind flowing over water for at least 1.6 km, over a distance of 460 m or 10 times the height of the structure inland, whichever is greater	0.10

Inter-Row Spacing

Once the value for the necessary energy production is reached and the PV modules are selected it is necessary to establish the number of modules that it is possible to install in the household's roof. When installing the modules it is necessary to guarantee no shading is cast upon the modules so as to maximize the power output. Diehl [14] calculates the distance needed between each row of modules making it as there is no shading during solar noon using the sun's path using Equation 2.6,

$$D^{'} = \frac{H}{tan(S)} \tag{2.6}$$

where $D^{'}$ is the inter-row distance when considering the solar elevation angle, H is the height of the PV module relative to the roof and S is the solar elevation angle.

After the calculating the distance referring to the solar elevation angle it is necessary to add the correction concerning the solar azimuth, expressed by Equation 2.7,

$$D = D^{'} \cdot cos(A) \tag{2.7}$$

where D is the actual inter-row distance and A is the solar azimuth correction angle.

2.2 System Configuration

Aiming to reach the maximum PV generation, Aghamolaei et al. [15] conducted a study to establish the most effective structural factors to improve solar access of buildings in a urban context. The study focused on residential neighborhoods in Yazd as the experimental setting. The findings of the study revealed that building height, site coverage and street width were the predominant factors influencing solar access. The study also demonstrated that the implementation of a semi-detached architectural form resulted in the highest solar gain, thus maximizing PV generation in urban contexts

In the wake of rapid urbanization, cities, many of which boast a substantial proportion of apartment buildings, have risen to prominence as the foremost contributors to global energy consumption. This surge in urban energy demands poses a significant challenge to both energy sustainability and climate resilience. To effectively address this challenge, it is imperative to develop and implement innovative solutions that harness the potential of Decentralized Energy Resources (DER)s in urban settings. These solutions must not only enhance energy efficiency but also foster a more sustainable and resilient urban energy landscape, thereby contributing to the broader goals of mitigating climate change and ensuring long-term environmental sustainability, Fleischhacker et al. [16]. When contrasting apartment buildings with single-family houses, notable divergences emerge. Firstly, these distinctions encompass the presence of multiple consumers, involving both owners and tenants within the apartment building setting. Secondly, an important aspect involves the imperative for these consumers to mutually agree upon an energy allocation strategy, particularly in the context of sharing communal energy resources. In this thesis scenario, PV systems are being considered and potentially integrated with battery storage. Lastly, the analysis requires an examination of individual objectives and consumer behavior, taking into account the potential for conflicting interests among different parties involved.

By harnessing autonomous agents, Alam, Ramchurn, and Rogers [17] proposes a novel approach to model energy exchanges. These agents, acting on behalf of households, are envisioned to play a pivotal role in coordinating and regulating the exchange of energy between homes. One notable outcome highlighted in the article is the potential for a significant reduction in overall battery usage and lower energy losses through the implementation of cooperative energy exchange systems. By fostering collaboration among community members, this approach seeks to address the unique energy dynamics of remote locales, where conventional energy infrastructure may be limited or impractical.

Fan, Papadaskalopoulos, and Strbac [18] propose a modeling framework for decentralized transmission describing a non-cooperative and game-theoretical decision-making process for each participant, articulated as a bi-level optimization problem. In this context, a model was created, that depict scenarios in which the consumer, strategically pursue their interests without engaging in direct collaboration. These models employs mathematical frameworks to assess and foresee the results of interactions, taking into account

elements such as decision strategies, information imbalances, and possible conflicts of interest among the involved parties. Specifically, the upper level of this framework is designed to maximize the profit of each player, while the lower level is focused on the clearance of the energy market. This is one of the models depicted in Figure 2.1.

Fleischhacker et al. introduces a framework for the collaborative utilization of DER within an apartment building. Through an examination of various models and scenarios, this analysis aids in determining the most effective configuration for practical implementation in real-world scenarios.

Figure 2.1 depicts the relation between the PV plant owner and the consumers along the models employed.

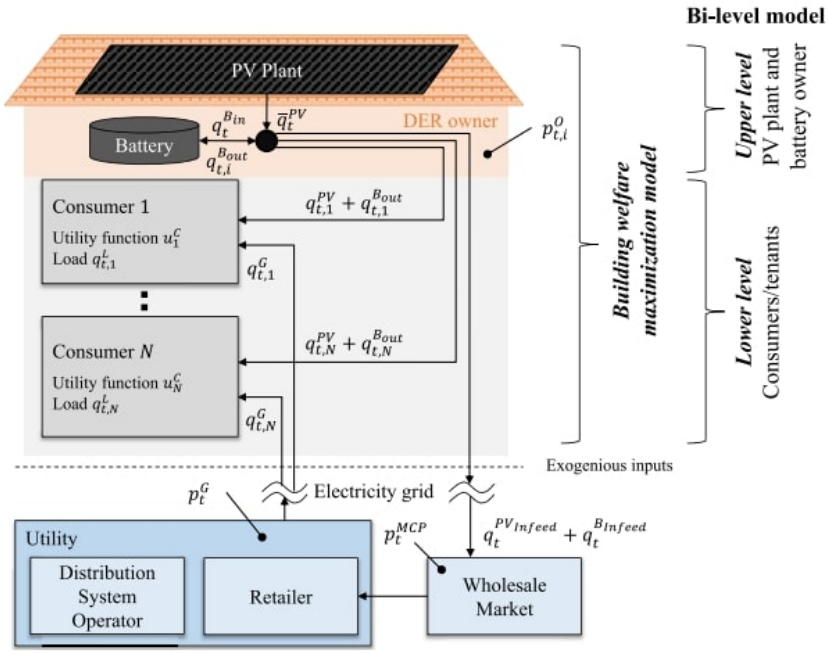

Figure 2.1: Graphical representation of a PV system in a apartment building taken from Fleischhacker et al. [16]

Two models are considered in this study as shown in Figure 2.1. Regarding the pricing of the electricity sold, both discriminatory and uniform price auctions were taken into account. The first model optimizes the building welfare maximizing the local generation. It is also considered that the energy produced is either sold to the consumer, stored in the battery, fed into the national grid or curtailed. The second model focuses on maximizing the DER owner's profit. The DER owner establishes the pricing for the generated electricity and sells to the grid, while consumers had the option to purchase from either the grid or the DER owner.

Since many consumers are driven by more than just financial goals, a consumer's utility function is frequently characterized by a combination of nonlinear and multiple objectives, costs, emission reduction and degree of DER generation. This function can be shown by Equation 2.8,

$$u_i^C(q,p) = -costs_i(q,p) - w_i^E emissions_i(q) + w_i^{DER} der_i(q) \tag{2.8}$$

where w_i^E and w_i^{DER} are the weight factor each consumer i takes for emissions and the DER respectively.

The individual electricity costs can be calculated by Equation 2.9,

$$costs_i(q,p) = \sum_{t \epsilon T} (p_{t,i}^G q_{t,i}^G + p_{t,i}^O \cdot (q_{t,i}^{PV} + q_{t,i}^{Bout})) \tag{2.9}$$

where $p_{t,i}^G$ is the cost of the electricity bought from the grid, $q_{t,i}^G$ is the power flow from the grid to the consumer i, $q_{t,i}^{PV}$ is the power flow from the solar PV plant to the consumer i, $p_{t,i}^O$ is the cost of the DER generation and $q_{t,i}^{Bout}$ is the power flow from the battery to the consumer i.

The emission reductions can be defined as Equation 2.10,

$$emissions_i(q) = \sum_{t \epsilon T} e_t^G q_{t,i}^G \tag{2.10}$$

where e_t^G are the grids emissions.

Lastly, the DER can be described by Equation 2.11.

$$der_i(q) = \sum_{t \epsilon T} (q_{t,i}^{PV} + q_{t,i}^{Bout}) \tag{2.11}$$

Both models prioritize serving consumers based on their valuation of DER, ensuring that those who place the highest value are addressed first, followed by others in descending order of valuation. The outcomes indicate that optimizing building welfare results in energy allocation akin to the bi-level model with a discriminatory price auction. The introduction of prices plays a crucial role in determining how the welfare derived from the DER is shared between consumers and the DER owner. For community-oriented projects like shared battery and PV plants, where owners may also be consumers, maximizing building welfare aligns intuitively. On the other hand, the bi-level model becomes more appealing when an external investor seeks to optimize the investment's rate of return.

2.3 Peer-to-Peer

2.3.1 Energy Communities

Reijnders, van der Laan, and Dijkstra [19] asserts that a novel approach to decentralized energy, shifting the focus from individual households, lies in ECs where energy generation, consumption, and sharing occur within a local context. These communities can adopt either a storage-based or no-storage-based system. This scenario alleviates the necessity of PV systems in households where installation may be impractical or would require additional infrastructure, such as rented homes, apartment buildings or shaded roofs.

Widening the field of study, Fina, Auer, and Friedl [20] examines the profitability and optimal storage capacity for PV systems within EC in comparison to individual buildings. To assess the economic viability of PV sharing in ECs, a model was created to ascertain the highest Net Present Value (NPV) and optimal PV systems. To simulate a realistic environment, four settlement patterns were considered: apartment buildings, historical, rural and mixed areas. Buildings structures and heating systems distributions considered are representative of Austria. Within each settlement pattern, ten buildings were analyzed. In the individual approach, the optimal PV system size and maximum NPV were determined by individually optimizing each building. In the EC approach, optimization was performed considering only buildings within the EC capable of implementing PV systems. Lastly, the pool approach, established the EC for the entirety of buildings, considering properties lacking PV systems implemented as additional load.

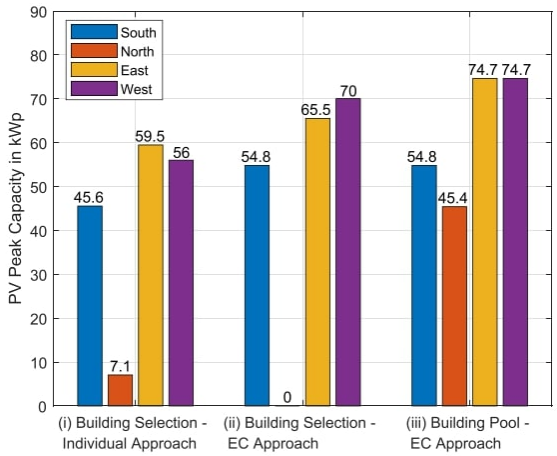

Figure 2.2: Optimal rooftop PV implementation for the various approaches for an apartment area, taken from Fina, Auer, and Friedl [20]

When examining the results depicted in Figure 2.2 for the apartment building area, it becomes evident that adopting the EC approach offers the potential to achieve higher PV generation by excluding areas characterized by low solar irradiation. Additionally, this approach leads to cost reductions associated with implementation.

Due to the community-based strategy, there are sufficient rooftop spaces with higher solar irradiation available. Similarly, the conclusions drawn for the apartment area, as demonstrated in Figure 2.3, hold true for the rural area as well. Notably, the findings for the mixed area, consisting of both single-family and apartment buildings, show that the latter dominates. Establishing an EC would yield significant benefits for apartment buildings, as PV systems could be installed on the rooftops of single family home. With more loads and greater synergy effects, the cost-saving potential increases. Therefore when considering apartment buildings the forecast cost savings are considerably higher as seen in Table 2.3. Across the different approaches, the previous reasoning can be used; since it is possible to chose the better solar irradiation areas instead of being limited by individual buildings, it is possible to optimize the production and consequently cost

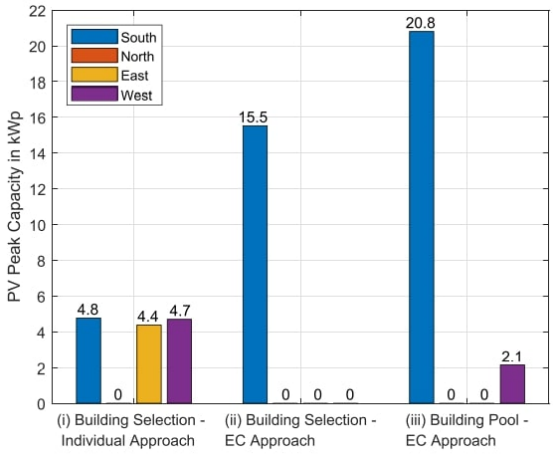

Figure 2.3: Optimal rooftop PV implementation for the various approaches for a rural area, taken from Fina, Auer, and Friedl [20]

reductions.

Table 2.3: Cost reduction taking in account the settlement patterns and approach, adapted from Fina, Auer, and Friedl [20].

	Cost savings in %		
Settlement Pattern	(i) Building selection - Individual approach	(ii) Building selection - EC approach	(iii) Building Pool - EC approach
Apartment building area	8.3	9.2	7.4
Rural area	1.9	6.8	5.4
Mixed area	7.7	8.9	8.5

The findings indicate that when comparing individual buildings to EC, the profitability of optimal PV systems increases within the EC framework. The author highlights the significance of diverse loads in enhancing the potential for cost savings. Throughout the study, Fina, Auer, and Friedl considers that "People cannot be obliged to participate in an EC" [20] resulting in a lower PV generation and trade for the considered scenarios.

As Reijnders, van der Laan, and Dijkstra [19] states, ECs run by citizens represent a viable approach towards achieving decentralized energy solutions. A key distinction between EC and microgrids lies in their spatial limitations, with microgrids constrained by distance.

2.3.2 Multi-microgrids

Having Commons-Based Peer Production (CBPP) systems as a base, this is, using a model that relies on a network of individuals who contribute their skills, resources, and efforts to collectively create and maintain a shared resource, often referred to as the "commons", Giotitsas, Pazaitis, and Kostakis [21] proposes a decentralized P2P network. The P2P network as illustrated in Figure 2.4 is comprised of interconnected microgrids in close proximity capable of operating without the need for a centralized control. Rather than

engaging in price negotiations for the traded energy, the network prioritizes the allocation of the surplus energy where it is needed. This decentralized model, consisting of n microgrids, exhibits a higher resilience and security since, in the case one of its elements collapse, the P2P network can rely on other options to ensure continuous functionality. Open technologies can be employed in the microgrids' Information and Communication Technologies (ICT) component as well as, to some extent, to the production itself reducing costs and enhancing flexibility.

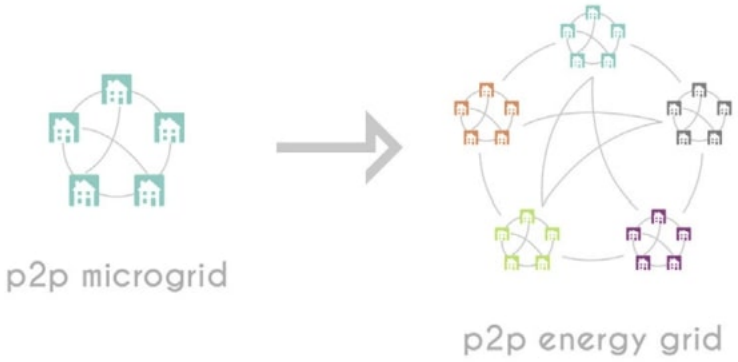

Figure 2.4: Decentralised model for P2P energy trading taken from Giotitsas, Pazaitis, and Kostakis [21].

In a closely related study, Du et al. [22] adopts a similar conceptual framework as Giotitsas, Pazaitis, and Kostakis to enhance energy efficiency within multi-microgrids. The authors employ cooperative game theory to reach what they define as the local optimal solution, this being each element of the multi-microgrids can benefit from partial cost savings. To assess the economic efficacy of multi-microgrids, Du et al. utilizes the IEEE 33-bus distribution system depicted in Figure 2.5. Since each microgrid possesses its unique characteristics, they can achieve their cost savings in different scenarios therefore enabling the multi-microgrids a greater cost saving. When investigating the impact of multi-microgrids penetration on a distribution grid it was possible to verify that when adding multi-microgrids the network, losses would decrease from 4.65% to 4.39%, Du et al. [22]. Additionally it is demonstrated that the various microgrids can provide reliable support to distribution system by effectively regulating the system voltage level. During the simulation period, the majority of the buses experienced voltage increases while maintaining their feasibility region.

2.3.3 Markets

Adopting P2P energy trading means changing the electricity market. Rather than individual households engaging in transactions with energy suppliers, the energy community functions as a collective entity in managing such transaction as it is shown in Figure 2.6.

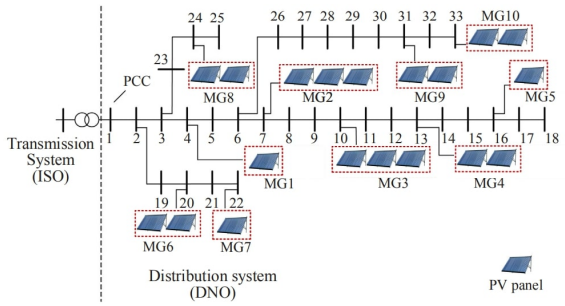

Note: The figure was adapted from [22] to include only PV.

Figure 2.5: IEEE 33-bus distribution system with 10 microgrid, adapted from Du et al. [22].

Long et al. [23] proposes three distinct market approaches for the P2P energy community, Bill Sharing (BS), Mid-Market Rate (MMR), Action-based Pricing Strategy (APS).

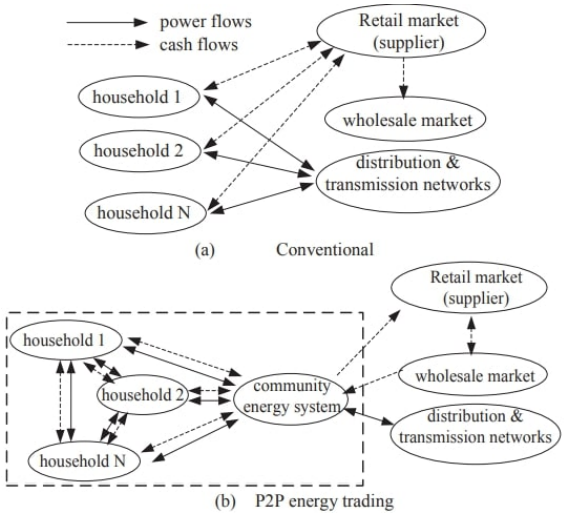

Figure 2.6: (a) Conventional and (b) P2P energy trading of a P2P community, taken from Long et al. [23].

2.3.3.1 BS

In the BS method, the utility meter is placed at the coupling point enabling the electricity bill to be calculated for the entire energy community rather than individual households. Subsequently, the total cost is divided among the households, taking in consideration their respective consumption and energy export. The cost for energy consumption remains the same for every consumer and prosumer while the price for energy exports can vary.

Subsequently, the energy cost of every households needs to be computed. Firstly, Equation 2.12 determines the amount of PV each household consumes by finding the overlapping value between the electricity demand - L^n - and the on-site PV generation - P_{PV}. Where n represents the specific household for which the calculations are being performed, [23].

$$M^n(t) = min\left\{L^n(t), P^n_{PV}(t)\right\} \tag{2.12}$$

Having calculated the portion of the PV generation consumed by each household, it becomes possible to determine the surplus PV energy that can be exported - P^n_{ex} - or the energy needed to be imported - P^n_{im}, shown by Equation 4.9 Equation 4.9,

$$P^n_{im}(t) = L^n(t) - M^n(t) \tag{2.13}$$

$$P^n_{ex}(t) = P^n_{PV}(t) - M^n(t) \tag{2.14}$$

Having calculated the amount of energy each household imports or exports, it is possible to determine the he overall energy import and export for the entire community. It can be expressed by Equation 2.15 and Equation 2.16 respectively,

$$E_{im-tot} = \sum_{n=1}^{N} \cdot \left(\sum_{t=0}^{T} P^n_{im}(t) \cdot t\right) \tag{2.15}$$

$$E_{ex-tot} = \sum_{n=1}^{N} \cdot \left(\sum_{t=0}^{T} P^n_{ex}(t) \cdot t\right) \tag{2.16}$$

considering C_{BFG} as the price of energy bought from the grid and C_{STG} as the price of energy sold to the grid, it is possible to calculate the cost of overall energy exchanges for each household n [23].

$$C_n = \left(\sum_{t=0}^{T} P^n_{im}(t) \cdot t\right) \cdot C_{BFG} - \left(\sum_{t=0}^{T} P^n_{ex}(t) \cdot t\right) \cdot C_{STG} \tag{2.17}$$

In the context of P2P energy trading, following a similar approach to determining the PV consumption for individual households, Equation 2.18 -2.22 [23] represent the PV consumption for individual households for the community, the residual energy demand and surplus PV and the total energy the community imports or exports.

$$M^n(t)^{'} = min\left\{\sum_{n=1}^{N} L^n(t), \sum_{n=1}^{N} P^n_{PV}(t)\right\} \tag{2.18}$$

$$P_{BFG}(t) = \sum_{n=1}^{N} L^n(t) - M^n(t)^{'} \tag{2.19}$$

$$P_{STG}(t) = \sum_{n=1}^{N} P^n_{PV}(t) - M^n(t)^{'} \tag{2.20}$$

$$E_{BFG} = \sum_{t=0}^{T} P_{BFG}(t) \cdot t \tag{2.21}$$

$$E_{STG} = \sum_{t=0}^{T} P_{STG}(t) \cdot t \tag{2.22}$$

Where $P_{BFG}(t)$ and $P_{STG}(t)$ are the imported and exported PV generated power, and E_{BFG} and E_{STG} are the imported and exported energy, respectively.

Given the diversity of electricity demands, a portion of surplus PV is consumed by the neighboring households. In such manner E_{BFG} will present a smaller value than E_{im-tot} and E_{STG} will be smaller than E_{ex-tot}. Equation 2.23 and Equation 2.24 describe the cost of importing and exporting electricity, respectively.

$$C_{im} = C_{BFG} \cdot \frac{E_{BFG}}{E_{im-tot}} \tag{2.23}$$

$$C_{ex} = C_{STG} \cdot \frac{E_{STG}}{E_{ex-tot}} \tag{2.24}$$

When using BS the final electricity cost can be determined by Equation 2.25 [23].

$$C_n^{'} = \left(\sum_{t=0}^{T} P_{im}^{n} \cdot t \right) \cdot C_{im} - \left(\sum_{t=0}^{T} P_{ex}^{n} \cdot t \right) \cdot C_{ex} \tag{2.25}$$

2.3.3.2 MMR

The MMR method adopts a pricing approach in which the energy community members pay a price between between the energy selling price - C_{BFG} - and energy buying price - C_{STG} as indicated by Equation 2.26.

$$C_{P2P} = \frac{C_{BFG} + C_{STG}}{2} \tag{2.26}$$

PV generation as an uncontrollable energy source, can vary throughout the day and time. Therefore PV generation can match, exceed or fall short of the energy demand. In the event that there is insufficient PV generation to meet the demand, the required energy can be acquired from neighboring generations or from the grid. The **{8274546}**, however, considers only the possibility of selling the community surplus PV generation to the grid.

1. PV generation equals demand

While the community PV generation equals the community demand, the cost of electricity is equal to the cost of buying from neighboring households as shown in Equation 2.27 and Equation 2.28,

$$C_{im}^{''}(t) = C_{P2P} \tag{2.27}$$

$$C_{ex}^{''}(t) = C_{P2P} \tag{2.28}$$

where C_{P2P} is the price of P2P energy trading.

2. Higher PV generation than demand

In scenarios where there is surplus community PV generation, the cost of buying electricity remains the same as when the generation matches the load, while the selling cost, assuming no battery system is present, is as determined in Equation 2.29.

$$C''_{ex}(t) = \frac{\sum_{n=1}^{N} L^n(t) \cdot C_{P2P} + \left(\sum_{n=1}^{N} P^n_{PV}(t) - \sum_{n=1}^{N} L^n(t)\right) \cdot C_{STG}}{\sum_{n=1}^{N} P^n_{PV}(t)} \tag{2.29}$$

where $L^n(t)$ is the community load in the time period t and $P^n_{PV}(t)$ id the community PV generation.

3. Lower PV generation than demand

In the case where the demand exceeds the generation, the selling cost remains the same as as when the generation matches the load and the buying cost is determined by Equation 2.30.

$$C''_{ex}(t) = \frac{\sum_{n=1}^{N} P^n_{PV}(t) \cdot C_{P2P} + \left(\sum_{n=1}^{N} L^n(t) - \sum_{n=1}^{N} P^n_{PV}(t)\right) \cdot C_{BFG}}{\sum_{n=1}^{N} L^n(t)} \tag{2.30}$$

Lastly, the electricity bill of individual households can be calculated by Equation 2.31.

$$C''_n = \sum_{t=0}^{T} \left(P^n_{im}(t) \cdot t \cdot C''_{im}(t)\right) - \sum_{t=0}^{T} \left(P^n_{ex}(t) \cdot t \cdot C''_{ex}(t)\right) \tag{2.31}$$

2.3.3.3 APS

With APS method, both the demand and generation prices are determined through auction markets. In this scenario, each household participates in the market by submitting bids for their PV generation and placing offers for other households' PV generation. The offers and bids are managed using pre-defined rules to establish the pricing strategy.

When utilizing APS method, each household begins by declaring a clearing price based on the bidding or offering proposed, as well as a clearing price for the previous time using Recursive Least Square (RLS) estimation.

Depending on the relation between their PV generation and demand, the household role is determined. If the PV generation is smaller than their demand, the household acts a buyer and submits bids for the energy needed to fulfill their demand, with the bidding price serving as the estimated clearing price. Conversely, if there is surplus PV generation, the household becomes a seller and offers their surplus PV generation at the estimated clearing price. The bids are put into ascending order and the clearing prices are determined by the real demand and generation of the community.

Thereafter the difference between the clearing price and the buyers biding prices are calculated and it determines the customer priority to obtain the cheaper prices. The higher

priorities are designated to the smaller absolute value. This process concludes with the calculation of the actual buying and selling prices.

The estimation of the clearing price is given by Equation 2.32,

$$\hat{C}_g^n(t+1) = \hat{C}_g^n(t) + \gamma^n \cdot (C_g^n(t) - \hat{C}_g^n(t)) \tag{2.32}$$

where $\hat{C}_g^n(t)$ is the estimate of the clearing price for the household n, $C_g^n(t)$ is the clearing price at the time and γ^n the filtering rate.

Similarly to the MMR method, the clearing price is determined by three different scenarios.

The case study generated by Long et al. show a decrease to 72.1% of the conventional electricity bill regardless of the method used. With the MMR method, the buying and selling prices vary with time and the availability, making it more cost-effective to purchase electricity when the consumption coincides with the local generation.

2.3.4 Effects on a Distribution Transformer

Distribution transformers play a crucial role in the electricity distribution network. Electricity supplied to clients reliably and effectively is ensured by a transformer in good condition. Distribution transformers need to undergo routine maintenance and inspection in order to identify any faults and stop them from evolving. To provide a steady and dependable supply of energy to consumers, distribution transformer maintenance is crucial.

One of the consequences of PV generation is the impact on the aging process of a Distribution Transformer. With the increased load, the core temperature of the transformer can increase leading to an accelerated aging.

Lopes et al. [24] conducted a case study in Évora, Portugal with the goal of analyzing the effects Nearly Zero Energy Building (nZEB) have on the aging of a distribution transformer. The study involved 19 selected buildings and their real load data.

Figure 2.7 illustrates the equations required to compute the hot-spot temperature, θ_h, of the transformer. This temperature can be obtained by summing the top oil temperature, θ_o with the hot-spot temperature rise above the top oil temperature, $\Delta\theta_h$, using the ambient temperature and the rated load of the transformer as inputs. Consequently, the values for both temperatures can be achieved using the parameters of the distribution transformer module and the real load of the transformer.

To ensure the smooth functioning of the transformer, it is necessary to keep the hot-spot temperature below 140°C and maintain the load below 1.5 times the rated load limit.

Considering the normal life time of a oxygen free insulation as 20.55 years with a hot-spot temperature of 110°C, the computation of the life span of the transformer for different hot-spot temperatures is made possible by Equation 2.33,

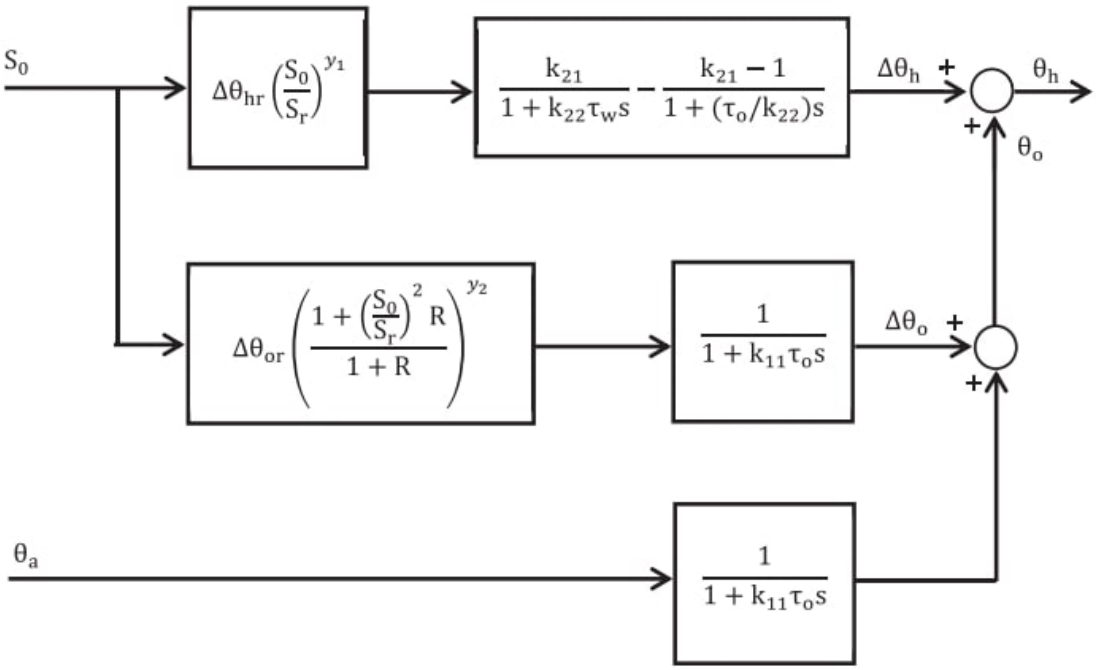

Figure 2.7: Block diagram of heat transfer equations taken from

$$EA = \sum_{n=n_1}^{n_2} F_{AA}(n) \tag{2.33}$$

where n is the amount of increments simulated by Equation 2.34,

$$F_{AA} = e^{\left(\frac{15000}{110+273}\right) - \frac{15000}{\Theta_h(n)+273}} \tag{2.34}$$

where $\Theta_h(n)$ is the hot-spot temperature for each time step.

The findings of the case study reveal that significant variations in the load can elicit either positive or negative effects on the service life of the transformer. If the load changes result in a decrease in the number of interactions between the transformer and the grid, it leads to an increase in the life span. However, if a multitude of nZEBs are present, the transformer may be forced to operate in a manner contrary to its design, which results in a reduction in its lifespan. With a baseline scenario of an equivalent aging of 7.8 days in a year when considering up to 10 nZEBs, the equivalent aging reaches the lowest value of 7.4 days with both 7 and 8 nZEBs. The highest value reached for the equivalent aging was 2277.8 days in a year corresponding to 19 nZEBs connected to the same transformer. Additionally, the authors note that the utilization of battery systems can also have an impact on the aging of the transformer.

2.3.5 Comparing existing Energy Communities

Yeloha, [25], established a functioning energy community by providing the PV systems in the clients house in exchange for energy sharing among their peers. As the project expanded, the community was accessible to anyone who was interested in sharing energy and not just existing clients.

Those who were unable to install PV systems on their roofs could join the community by subscribing, allowing to save 5% to 10% on their energy bills. Partners with suitable roofs could start their subscription with one panel, promising an annual generation of 336 killo-Watt hour (kWh), Young [26]. Yeloha provided its clients with an app that enabled them to track their energy production and savings. The company would also supply algorithms capable of allocating solar capacity to the subscribers and manage the billing processes as seen in Figure 2.8.

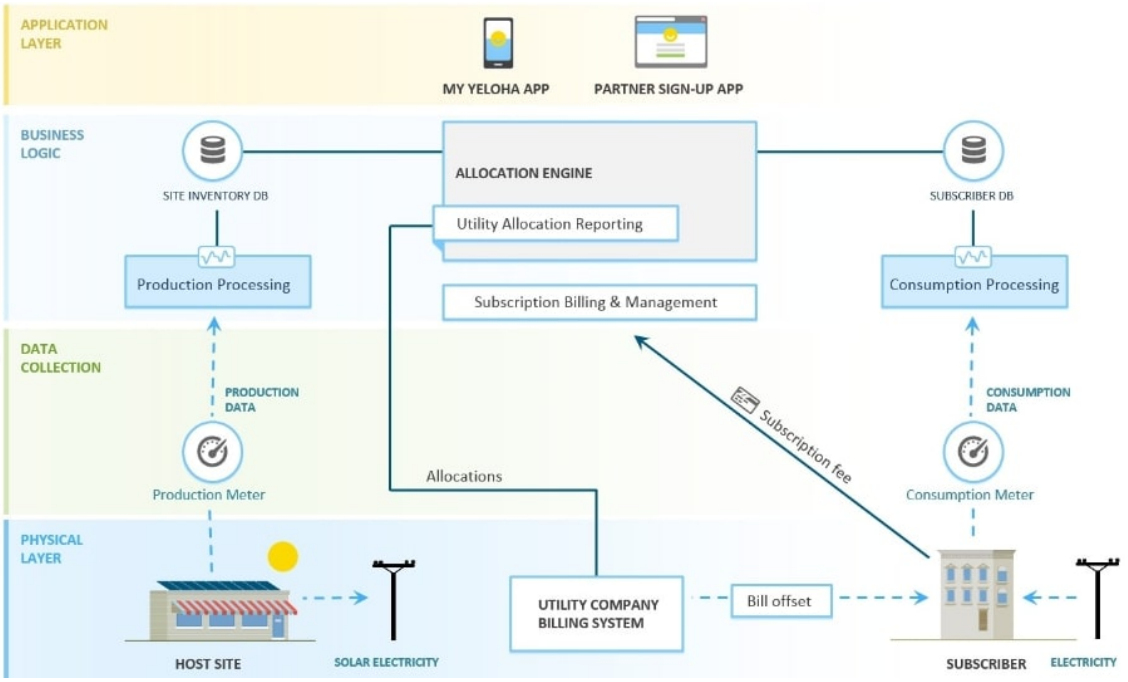

Figure 2.8: Yeloha's business plan.

Sonnenbatterie, a company specialized in battery technology, has established an EC centered around their battery systems. In this case, the consumers pay a fixed tariff of 25 cent per kWh for the energy they consume, Martin [27]. This value is lower than the feed-in tariff paid to the owners of Distributed Generation (DG) for feeding surplus power into the grid making it a preferable option. A software platform is also provided to manage energy supply and demand, Zhang et al. [28]. Additionally, battery owners can network their batteries together becoming part of the Sonnen Virtual Power Plant (VPP).

Micro Grid Sandbox [29] is a local microgrid that allows neighbouring participants to become consumers and/or prosumers. In order to eliminate power companies from

the energy transaction, the Brooklyn microgrid implemented Blockchain technology into their platform.

With Vanderbron, contrary to the SonnennCommunity, producers have the autonomy to set the price energy is sold to the consumers. An agreement is reached between consumers and producers regarding the amount of energy transacted over a specific period of time with a monthly fee established, Martin [27]. Vanderbron functions as a platform that connects independent producers and consumers Vandebron [30].

Reijnders, van der Laan, and Dijkstra [19] studied ECs located in close proximity to one another, all connected to the same coupling point. In this case, the peak shaving is employed to lower the strain on the grid. In one of the communities, GridFlex Heeten, a portion of the houses have PV systems and a percentage of them have a battery systems installed. All members of the community share their smart meter data and PV production and receive their energy consumption information through an APP [31]. It also provides a price forecast for the next 24 hours, enabling the community members to shift their energy usage to different time slots, saving money. The prices are calculated in order to match the cheapest time slots with the time period where the energy traffic on the transformer is low.

Similar to Micro Grid Sandbox, T77 & 077, a local energy community in Thailand, utilizes Blockchain technology to monitor energy generation and transactions within the community alongside with the possibility of invoicing for settlement of the trading position. By using the Powerledger software, the community has a renewable energy penetration of 18% and 2270$ AUD in potential monthly proceeds from P2P transactions, Energy [32].

Peer Energy Cloud, [33], aims to develop a cloud-based platform capable of acting as a virtual marketplace and also incorporates recording and forecasting capabilities. Sensor and actuator technologies are deployed at the end-user level to ensure real-time data availability for accurate forecasting.

The following energy communities are some of the communities present in the European Union (EU) repository, [34].

Sonnenkraftwerk Henstedt-Ulzburg is an energy community located in Germany that utilized the roofs of 6 public buildings such as schools to install PV systems. The energy generated by those systems is then fed into the grid and remunerated according Renewable Energy Sources Act. One of the buildings alone, Alstergymnasium, was able to supply renewable energy to more than 13 families for a year based on the energy produced in the month of May 2015 [35].

The first solar energy community in Galicia is a colaboration between Grupo Vagalume, the company of the warehouses used, and Biowatio Energia. Grupo Vagalume provides the PV panels and a monitoring system allowing the creation of Big Data of customer information. The company of the warehouses manages the finances and Biowatio Energia operates as a demand aggregator managing the purchase and surplus of energy. This system allows a 80% reduction of annual costs for the warehouses [36].

La Citoyenne Solaire is a collective of communities spread across Rilhac-Lastours, France comprising 19 solar plants. Citizens have the opportunity to rent their roofs to La Citoyenne Solaire for PV systems installations reducing the costs and gaining an annual rental fee equivalent of 3% of turnover [37].

The Municipality of Tito, in cooperation with Lucana Energetic Company has implemented three types of PV installations: ground-mounted, multipurpose buildings and school roofs. The current objective of these installations is to help reduce the consumption of public buildings and help meet the needs of other members of the community. A future goal is 100% coverage of energy needed by renewable sources Eroe [38].

Table 2.4 compares the ECs previously referred.

Table 2.4: Comparing existing EC's

	Network Size	Customer	Value Proposition	Plant Type	Capacity
Yeloha (USA)	Local	Yeloha subscribers only Any willing participant latter	Instalation of solar panel and cost free managment	Residental PV	336 kWh/panel
SonnenCommunity (Germany)	International	Costumers with any Sonnen product	Power supply with the addition of batteries and provision of surplus energy	Residental PV	-
Microgrid Sandbox (USA)	Local	Local consumers whether residental or commercial	Blockchain tecknology	Rooftop PV	-
Vanderbron (Netherlands)	National	Indepentent energy supplliers	Establishing local clean energy trading	Wind and PV Farms	200,000 households
GridFlex Heeten (Netherlands)	Local	Costumers with capability of power allocation	Multiple energy communities with the same coupling point and peak load shaving	Wind and PV Farms	49 households
T77 077 (Thailand)	Local	Buildings in the T77 and 077 area	Blockchain tecknology	Residental PV	4.2MWh/daily
PeerEnergyCloud (Germany)	Local	Specific case: Saarlouis	Cloud-based forecasting and marketplace	Residental PV	500 households
Sonnenkraftwerk Henstedt-Ulzburg (Germany)	Local	-	Energy is fed into the grid and renumerated	Public Buildings PV	430-440 MWh/yearly
Santiago Sur Galicia (Spain)	Local	Warehouses and neighbouring houses	Big Data	Commercial Rooftop PV	650 kWp
La citoyenne solaire (France)	Local	-	Rental of rooftops for PV systems instalation	Rooftop PV	1,191,693 kWh
Tito's Renewable Energy Community (Italy)	Local	Schools and sports facilities	Future 100% renewable coverage	PV Systems	ground-mounted PV: 1,340 MWh/year multipurpose building: 26 MWh/year school buildings: 26 MWh/year

2.4 Battery System

When considering the PV generation of a single household without a battery system, it is necessary to recognize that any surplus energy produced by the PV system will be fed into the grid. This assumption is backed by the decision that all systems are connected to the grid to ensure that all households can meet their electricity demands. However, the integration of a battery system provides increased flexibility in managing the electricity load. The presence of a battery system allows the storage of surplus PV generation, enabling the usage of PV generated energy to power the load in a time period when solar radiation would be insufficient to meet the demand. This process contributes to a higher level of PV penetration in household consumption. In sum, the usage of batteries

alongside the PV systems allows for a higher robustness and lower grid dependence when considering a grid-connected system IRENA [39].

2.4.1 Battery Model

Regarding the battery model for hybrid energy systems, Manwell and McGowan [40] created a model known as the Kinetic Battery Model (KiBaM). As depicted in Figure 2.9, the KiBaM divides the total energy stored in the battery into two distinct components: bound energy and available energy. The available energy refers to the portion of energy that is accessible and can be utilized, whereas the bound energy represents the energy that is chemically bound and inaccessible. Prior to converting into electrical energy, the bound energy has to firstly be converted into available energy.

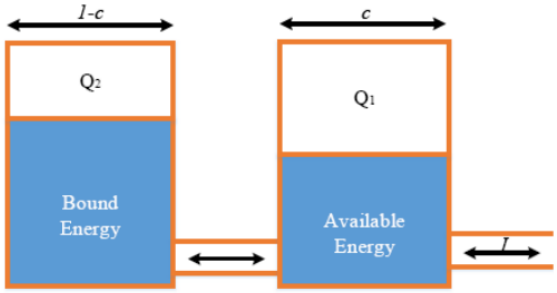

Figure 2.9: KiBaM, taken from Sandhu and Aeidapu [41].

1. Battery model

Equation 2.36 and Equation 2.37 quantify the charge levels of the available and bound energy, respectively, given the current energy levels denoted as Q_1 and Q_2 in Equation 2.35 [41],

$$Q = Q_1 + Q_2 \tag{2.35}$$

$$Q_1^{'} = Q_1 \cdot e^{-k\cdot\Delta t} + \frac{(Q\cdot k\cdot c - P_{bat})\left(1 - e^{-k\cdot\Delta t}\right)}{k} + \frac{c\cdot P_{bat}\left(k\cdot\Delta t - 1 - e^{-k\cdot\Delta t}\right)}{k} \tag{2.36}$$

$$Q_2^{'} = Q_2 \cdot e^{-k\cdot\Delta t} + Q\,(1-c)\left(1 - e^{-k\cdot\Delta t}\right) + \frac{P_{bat}\,(c-1)\left(k\cdot\Delta t - 1 - e^{-k\cdot\Delta t}\right)}{k} \tag{2.37}$$

where P_{bat} is the power charged or discharged into the battery at a given time frame (Δt), c the capacity ratio and k the rate constant.

The charging and discharging constrains are given by Equation 2.38 and Equation 2.39 respectively [41],

$$P_{bat-ch-max} = \frac{k\cdot Q_1\cdot e^{-k\cdot\Delta t} + Q\cdot k\cdot c(1 - e^{-k\cdot\Delta t})}{1 - e^{-k\cdot\Delta t} + c(k\cdot\Delta t - 1 + e^{-k\cdot\Delta t})} \tag{2.38}$$

$$P_{bat-dech-max} = \frac{-k \cdot c \cdot Q_{max} + k \cdot Q_1 \cdot e^{-k \cdot \Delta t} + Q \cdot k \cdot c(1 - e^{-k \cdot \Delta t})}{1 - e^{-k \cdot \Delta t} + c(k \cdot \Delta t - 1 + e^{-k \cdot \Delta t})} \tag{2.39}$$

where Q_{max} refers to the maximum battery capacity.

2. Fluctuation of power injected into the grid

The fluctuation rate of power injected into the grid can be defined by Equation 2.40,

$$D_{gs} = \frac{P_{max} - P_{min}}{\Delta t} \tag{2.40}$$

in which P_{max} and P_{min} are the maximum and minimum power supplied to the grid during the time period (Δt), [41].

3. Constrains for optimization

When considering battery systems it is necessary to ensure various constrains. The battery's State Of Charge (SOC) needs to be maintained between the minimum (SOC_{min}) and maximum (SOC_{max}) values to assure the battery is never completely charged or discharged, as represented in Equation2.41 [41].

$$SOC_{min} \leq SOC \leq SOC_{max} \tag{2.41}$$

Respecting this constrains will lengthen the battery life's time. The battery's charge level needs to be kept within the limits $P_{bat-ch-max}$ and $P_{bat-dech-max}$ to regulate the power flow to the battery, as shown by Equation 2.42 and Equation 2.43 respectively,

$$0 \leq P_{bat-ch} \leq P_{bat-ch-max} \tag{2.42}$$

$$0 \leq P_{bat-dech} \leq P_{bat-dech-max} \tag{2.43}$$

where P_{bat-ch} denotes the power intended for charging, while $P_{bat-dech}$ signifies the power designated for discharging at any specific moment.

The surplus energy that is available in case of a load increase - operating reserve - is given by Equation 2.44, [41],

$$P_{inst} = (1 + \mu\%) \cdot \sum_{i=1}^{N} P_L(t) \tag{2.44}$$

in which P_{inst} represents the total installed energy capacity of the system, P_L is the load and $\mu\%$ denotes the operating reserve percentage. When planning for distributed generation it is usually considered a $\mu\%$ of 10%.

4. Optimizing system size

In the context of a grid-connected system, two operating conditions can occur: the power generated by the PV system is not sufficient to supply the load demand, or the PV system generates surplus energy. In the first case, represented by Equation 2.45, the deficit is sourced from the grid, and in the second case, Equation 2.46, the surplus energy is firstly stored and subsequently sold to the grid, adapted from Sandhu and Aeidapu,

$$P_L(t) = P_{pv}(t) + P_{bat-ch}(t) + P_{from-grid}(t) \tag{2.45}$$

$$P_{to-grid}(t) = P_{pv}(t) - P_{bat-ch}(t) + P_L(t) \tag{2.46}$$

where $P_{pv}(t)$ power output from a PV model and $P_{from-grid}(t)$ is the power purchased form the grid at instance t .

2.4.2 Battery System Optimization

Lüth et al. [42] developed a P2P trading model focused on the flexibility of centralized battery storage versus decentralized as seen in Figure 2.10. To accomplish this, the author developed two market designs: *Pool Hub* and *Flexi User*.

The first market design considers a large battery that is collectively owned by the entire community. The battery can solely be charged by the prosumers of the community with their PV generation who will receive appropriate compensation. However, both prosumers and consumers can discharge the battery.

In contrast, in the *Flexi User* market the batteries are owned individually by the prosumers allowing them to charge the batteries using their PV generation.

In both scenarios prosumers and consumers have the opportunity to engage in local trading using a dynamic P2P price.

In the *Pool Hub* Market, compensations are provided for charging the community battery and discharging is available for everyone at a higher rate than charging. In addition, it assumes that prosumers are unable to feed surplus energy to the distribution system, which can force curtailment in some occasions. While in the *Flexi User* market, grid consumption is reduced by 15% compared to a standard grid consumption. Additionally in the *Pool Hub* market, grid consumption in peak time is transferred to early morning or nighttime hours. In the latter market, throughout the day, the community continuously discharges small amounts of electricity from the conjoined battery with this discharge rate slightly increasing during the evening due to the higher emphasis on P2P trade during daylight hours.

When testing for the different battery characteristics and adjusting the *Pool Hub* market battery to match the *Flexi User* market's battery, the results showed a 0.3% increase in the total cost for *Pool Hub* market, indicating that battery characteristics had an insignificant impact on the model's decisions. In opposition, when testing for battery charge and discharge prices the *Flexi User* market showed a 10% increase in costs. According to the

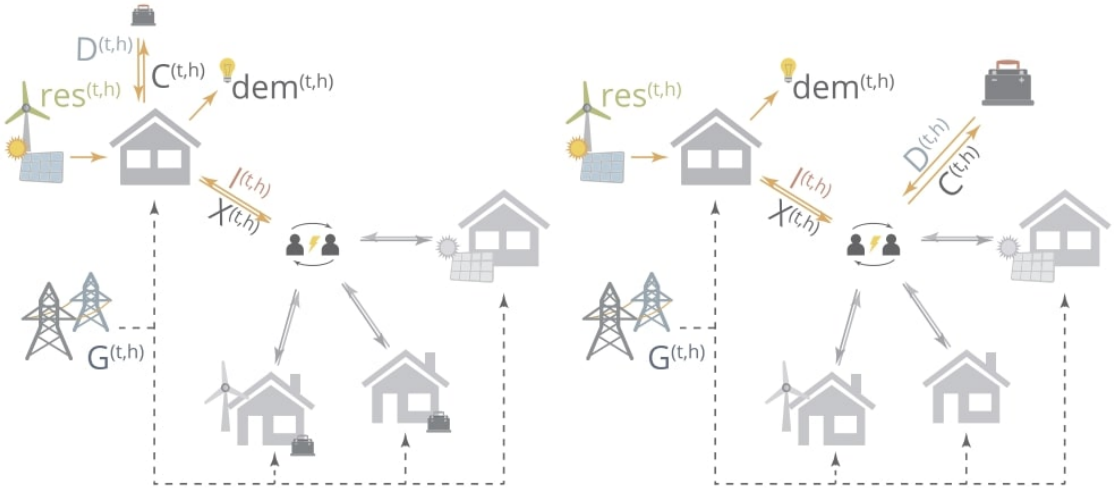

Figure 2.10: Local electricity market designs in different setups: decentralised (a) versus centralised battery (b), taken from Lüth et al. [42].

findings, end customers can save up to 31% on their electrical bill when combining trade and decentralized storage flexibility, and 24% when centralised batteries are considered [42]. The authors demonstrated that a decentralised battery allows flexible utilisation and a higher grid consumption reduction.

Continuing the discussion on centralized and decentralized storage systems, and in order to gain some insight on the optimal level of storage aggregation, Barbour et al. [43] grouped real households into communities of neighbours using real 15 minute consumption values and simulated their PV generation using real PV generation data. The demand profiles, whether for individual households or aggregated communities, were utilized to estimate the optimal level of storage from an economic perspective, using both individual and community batteries.

Misalignment, defined as the difference as between the PV generation and unconsumed energy, was analyzed for the set of houses considering the Pecan Street data as seen in Figure 2.12. Additionally, Figure 2.11 presents the daily load profile for an example home. Both graphs were computed for April. For the specific location and days examined, only 43% of the electricity produced aligned with the demand. While the information present in Figure 2.11 and Figure 2.12 are specific for their location, it is possible to extrapolate a similar behaviour for other locations.

The EC created for this study consist of 4574 households divided into 200 groups. Among these households, 40% have PV systems installed. Thereafter the authors proceeded by locating the center of each cluster and selecting the closest node to serve as the root node for building the community's network. The road network, made available by Open Street Maps, is then connected to corresponding addresses based on geo-location. Lastly, using a method based on the Dijkstra shortest path algorithm, each community is

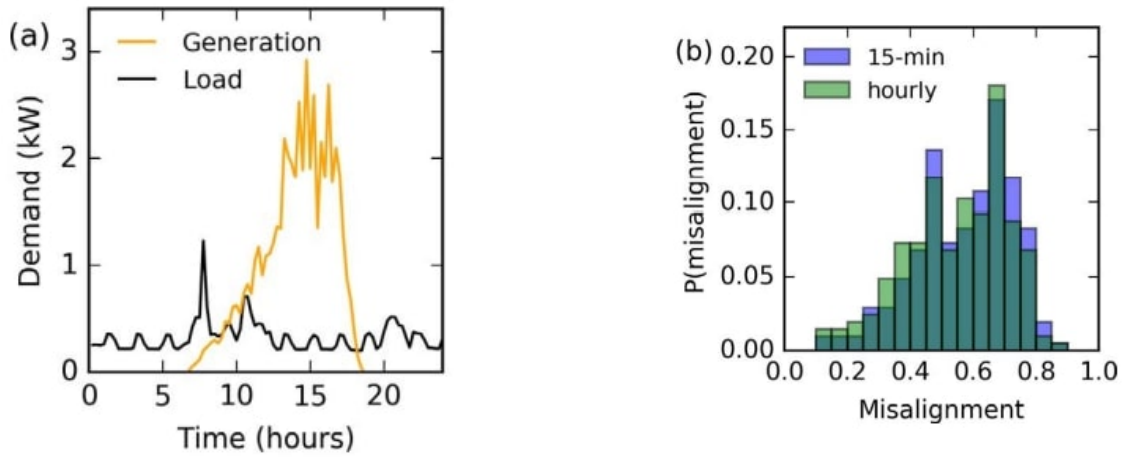

Figure 2.13: (a) daily load and generation profile in April (b) monthly misalignment values between generation and demand for all homes, taken from Barbour et al. [43].

then grown outwards from the root node along the road network creating the distribution presented in Figure 2.14.

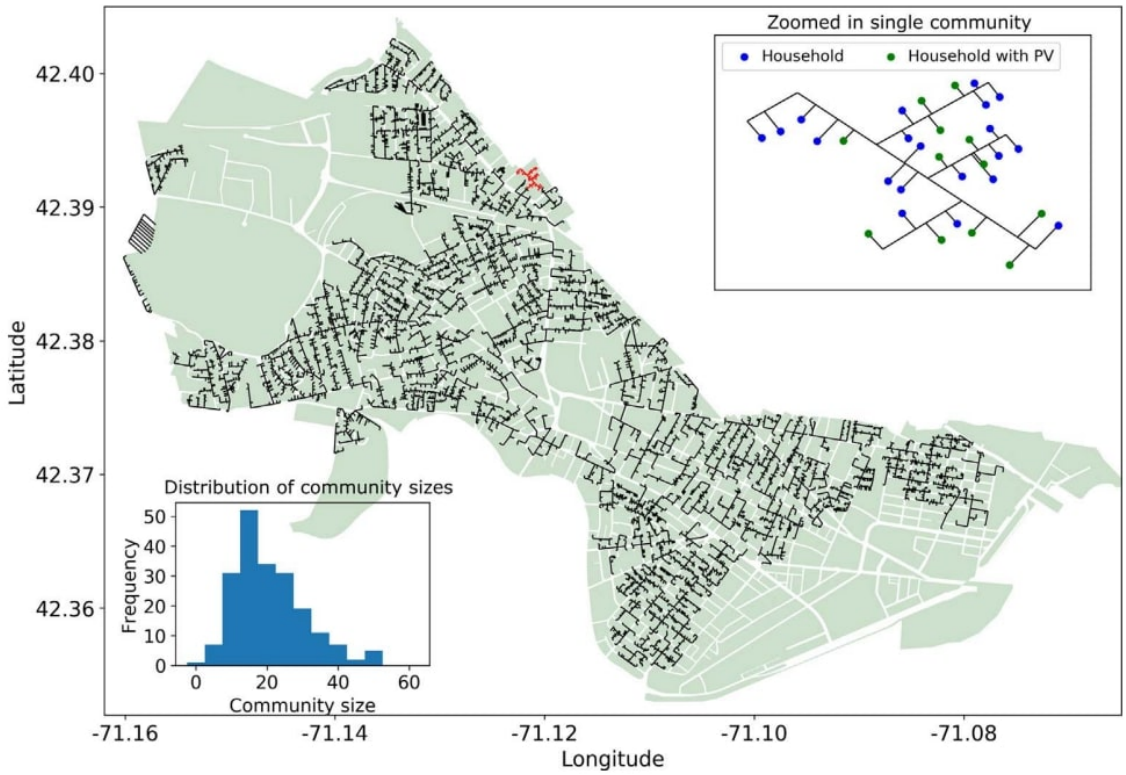

Figure 2.14: Illustration of the community created alongside with the various community sizes and distribution of PVs, taken from Barbour et al. [43].

When establishing the EC behaviour, it was assumed that, when considering a battery for an individual household, surplus energy that isn't stored by the owner is then used

by the community or fed into the national grid in case neighboring households did not require additional energy at that time. In the case of a Community Energy Storage (CES), surplus energy is primarily allocated to neighboring households, and only if there is no immediate demand, it is stored.

After simulating battery usage for a single community, the following statements were observed:

The economic analysis demonstrates that the costs associated with very small batteries outweigh the potential savings. However, as the battery capacity increases, so do the potential savings. The rate of increase in battery savings gradually diminishes and eventually intersects with the comparable yearly cost of the battery, resulting in yearly savings matching the cost. However, storing all surplus PV energy would require over-dimensioning the battery.

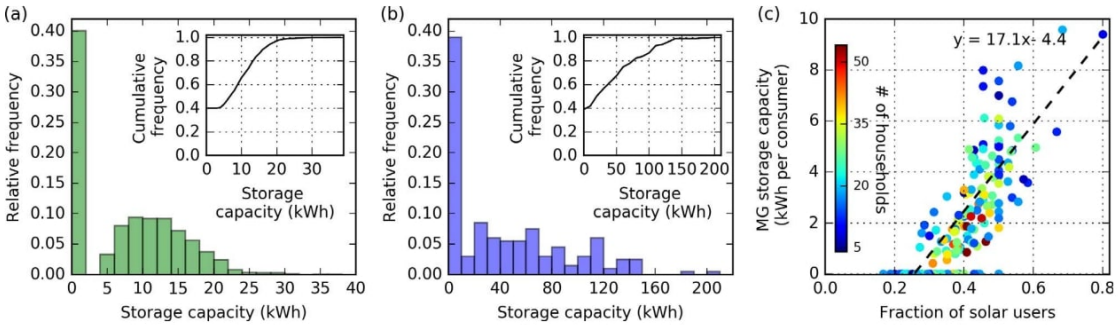

Figure 2.15: Distributions for the optimum battery capacities. (a) For the individual households with PV. (b) For the communities. (c) Optimum battery capacity against the fraction of households with PV, taken from Barbour et al. [43].

Using the same approach when simulating for all the communities and all the individual households and observing Figure 2.15 the following conclusions were drawn.

The study reveals that the total installed storage capacity is higher for individual households compared to communities. Interestingly, 39% of households do not require storage capacity due to the P2P aspect, enabling them to utilize surplus energy from neighboring households. It also is observed that communities with PV penetration below 29% typically do not require battery storage.

Considering the higher costs associated with inverters and maintenance, batteries with capacities below 4kWh are deemed uneconomical. However, in communities where it is viable to install a battery system, the capacity increases by approximately 1.7 kWh per household for a 10% increase in solar adoption.

Furthermore, the adoption of CES leads to a decrease in imports and exports between communities and the grid. Specifically, community batteries exhibit a 70% reduction in imports compared to 46% reduction in batteries installed in individual households.

The results show that the optimum storage for community batteries is 65% of the storage needed for individual households and that community batteries also showed to

be 64%-94% more effective than individual batteries at reducing energy from the group to the wider network [43].

2.5 Performance Indicators

2.5.1 NGE

The absolute Net Grid Exchange (NGE) value is the energy exchanged between the grid and the PV and, when applicable, the battery system and is defined by Equation 2.47,

$$NGE = |E_{grid2load} - E_{surplus}| \tag{2.47}$$

adapted from Liu et al. [44], $E_{grid2load}$ is the load covered by the grid and $E_{surplus}$ the surplus energy from PV to the grid.

2.5.2 SCR

The Self Consumption Rate (SCR) is the percentage of energy produced by the local PV system that is directly consumed, calculated in a year, shown by Equation 2.48,

$$SCR = \frac{\sum_{t=1}^{T} P_t^{\mathrm{PV}} - P_t^{\mathrm{Grid}}}{\sum_{t=1}^{T} P_t^{\mathrm{PV}}} \tag{2.48}$$

taken from Liu et al. [45], P_t^{PV} sum and P_t^{load} sum are the energy generated and consumed respectively.

2.5.3 SSR

The Self Sufficiency Rate (SSR) is the percentage of energy consumed that was produced by the PV system, calculated by Equation 2.49,

$$SSR = \frac{\sum_{t=1}^{T} P_t^{\mathrm{PV}} - P_t^{\mathrm{Grid}}}{\sum_{t=1}^{T} P_t^{\mathrm{Load}}} \tag{2.49}$$

taken from Liu et al. [45], P_t^{export} sum refers to the exported energy.

3

Methodology

Within this chapter, the processes employed for determining the energy potential of a community are expounded upon. This process encompasses various components, including those shared across all scenarios and others that are scenario-specific, such as the complexities associated with battery systems. The discourse within this chapter encompasses the software designed for computing the PV generation, the collection of energy consumption data, the algorithms referent to the battery system calculations, and the topology of P2P energy markets. Figure 3.1 demonstrates the process discussed.

The methodology employed in this study relies on four user-defined inputs within the software framework. These inputs pertain to the buildings under consideration and encompass information regarding their location and orientation, the quantity of buildings to be included, and the approach considered. This is, individual, individual with storage, EC, EC with storage and multiple ECs.

Additionally, the input involves load charts specific to the roles of consumers and prosumers. The data associated with building location and orientation will be elaborated upon in the PV generation section, where it serves as a crucial component for calculating the PV generation for each household.

Furthermore, information related to the user, specifically the client's details, will function as a parameter in the calculations. It is noteworthy that the outcome of the calculations is dependent upon the chosen approach.

Following the completion of the PV calculations, and considering the selected approach, the subsequent step involves initiating the calculation of the performance indicators. Figure 3.1 illustrates a simplified depiction of this process. Two major factors are taken into account: the utilization of battery systems and the incorporation of ECs. Additionally, there exists the potential for these scenarios to overlap. The processes associated with these options will be elaborated upon in greater detail in the subsequent sections.

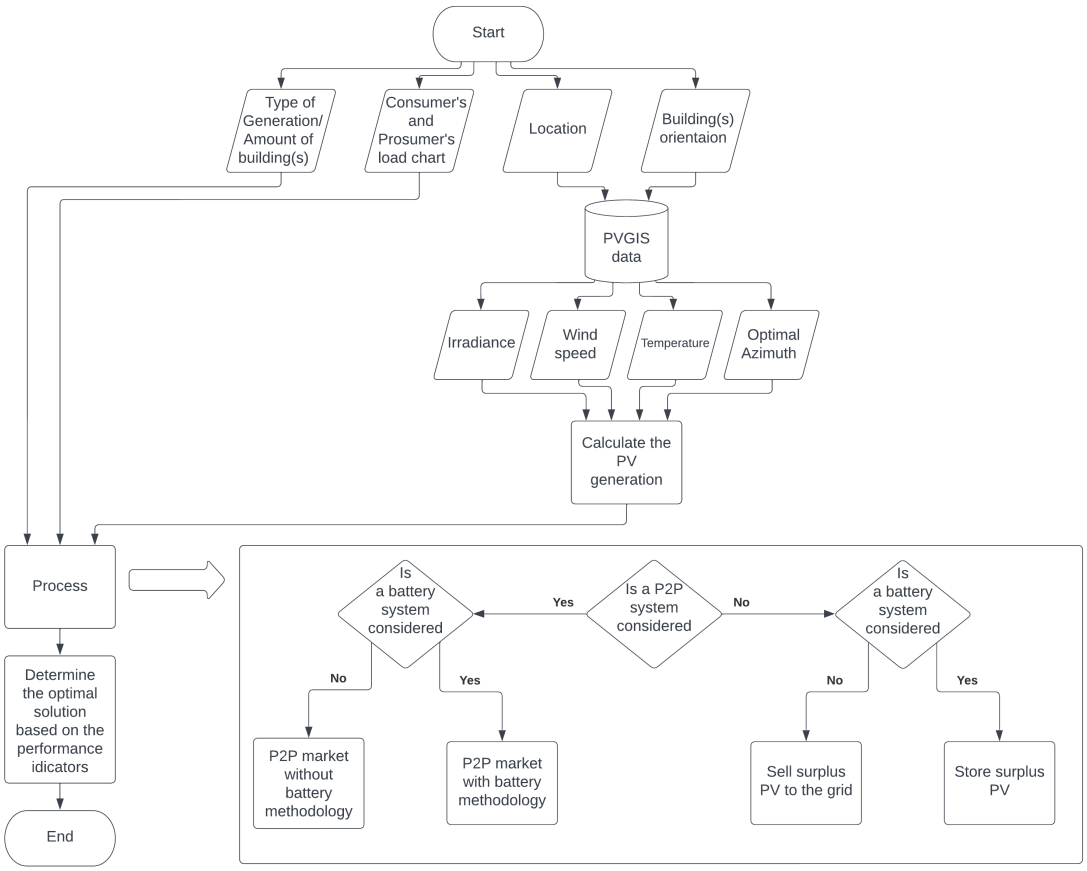

Figure 3.1: Flowchart describing the methodology implemented.

3.1 Client Consumption

Due to the constraints posed by client data privacy, obtaining real consumption data specific to the selected buildings was not feasible. As an alternative, real data consumption datasets were gathered from willing participants who provided their consent. This data collection was made possible through the E-REDES' Balcão Digital [46], a service that grants clients access to their electricity data regardless of their energy company.

Among the various services offered by the E-REDES' Balcão Digital, one of the services provided is the access to the client's energetic history. This dataset encompasses the time period starting from when the consumer adopted a smart meter up until the day the client accesses the service. The consumption data is sorted by months and is represented in 15 minute intervals.

To capture a broader range of consumption patterns and better reflect real-world scenarios, load charts from both single family houses and apartment buildings with a resident count ranging from 1 to 6 were acquired.

3.2 PV Generation

The platform used to retrieve real irradiance data was Photovoltaic Geographical Information System (PVGIS) [47]. "Hourly Radiation Data" was selected as the preferred data type allowing for a more accurate prevision. This data is retrieved by providing the location of the buildings to be considered for the study, the corresponding azimuth and the angle the PV modules will be installed.

Since the dataset selected presents the irradiation hourly and the consumption data is represented in 15 minutes intervals, it is necessary to standardize the datasets for accurate modeling. In cases the client wishes to sell their surplus energy, the sale is made considering a 15 minute interval. Therefore a decision was made to adjust the time intervals of the irradiation dataset by a simple interpolation. This technique ensures that the irradiation dataset aligns with the time intervals of the consumption data.

In the instance the roof had a slope, a 30° inclination was assumed as per Branco et al. [48]. The alignment of the PV modules was done in accordance with the roof inclination to reduce the necessary supporting structure. Installing the modules in this manner forces the azimuth of the modules to be the same as the roofs. In the cases where the building's roof is horizontal, the PV modules were assumed to be at a angle of 35° given it is the optimal inclination for the chosen location and an azimuth of 0° in order to get the maximum generation potential.

This data is then used in a software to later calculate the PV generation. The software user is required to chose from an array of PV modules and once the calculations are completed a second array of compatible inverters are available for choice. These databases were taken from California Energy Commission [49].

3.3 Energy Communities

The initial aspect requiring clarification in this section pertains to the definition of an EC. For the purposes of this study, an EC is characterized as a cluster of nearby households expressing the intention to collaboratively share their surplus PV energy.

Figure 3.2 demonstrates the methodology for the energy community approach.

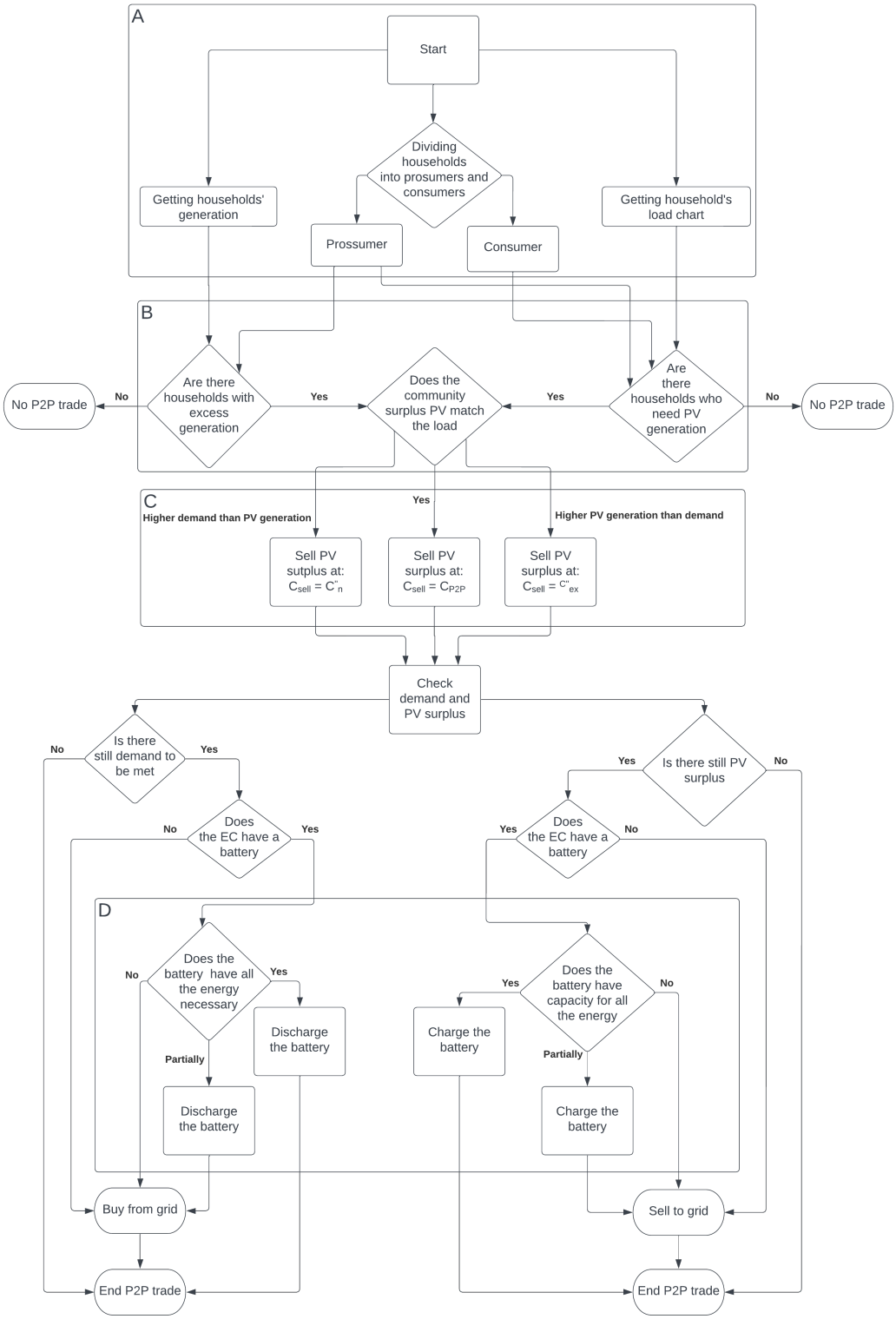

Figure 3.2: Flowchart showing the peer-to-peer market in a energy community.

Block A in Figure 3.2, represents the first step in dimensioning the EC. In order to enhance operational efficiency, the ECs were formed considering a PV penetration higher than 30%. This criteria was chosen since it was stated before that when a PV penetration

lower than 29% is considered, battery systems are not necessary. Firstly the number of households with PV systems are selected and subsequently the number of households to be considered as load is calculated. This calculation enables the establishment of the PV penetration percentage. Subsequently, the generation profiles and load charts, of the prosumer households, are acquired as a preliminary step towards the next stage.

In block, B depicted in Figure 3.2, the setup of transactions within the EC is illustrated. During this stage, the decision is reached regarding whether P2P trading or grid exchange will be implemented.

Block C, shown in Figure 3.2, represents the determination of the P2P energy price. This decision is based on the MMR module. This allows for a more detailed prevision of costs as it considers the three possible cases: (1) the community demand equals the community generation, (2) the community demand is higher than the community generation and (3) the community demand is lower than the community generation.

Despite the MMR module not considering any battery system, this thesis considers a appoach where both P2P markets and battery systems was considered. Block D, illustrated in Figure 3.2, outlines the procedure for situations where energy exchange within the community is not feasible, either due to community surplus or insufficient PV generation. In such cases, it explores options for charging or discharging the battery.

Overall, the households withing the community firstly consider the selling of excess energy and only latter the charging of the battery.

In addition, when considering multi-EC's, a similar concept to the battery system is executed. Firstly the PV generation will be sold between prosumers/consumers of the same EC and the excess sold to a nearing EC.

The flowcharts for the cases where more than one EC is being considered can be accessed in Annex I.

3.4 Battery Systems

In the case of individual households equipped with battery systems, any surplus energy generated is stored locally. However, as previously mentioned in the above section, surplus energy within the EC's is only stored after each consumer within the EC has been given the opportunity to purchase energy from the prosumer. In addition, each EC is equipped with a centralized battery in order to optimize the overall system. Nevertheless, in situations where an EC involves a larger number of households participating, the required battery capacity can become exceedingly high. Figure 3.3 shows the process to determine the price for charging and discharging the community battery.

Throughout the simulations a State of Charge (SoC) between 20% to 80% is considered. The battery capacity is dimensioned in such a way as to enable daily cycling, aiming to maximize the utilization of energy from PV generation and energy stored in the battery. That is, all the energy that is stored in the battery during the production hours is only used when there is no more production accounting for the load peak that occurs during

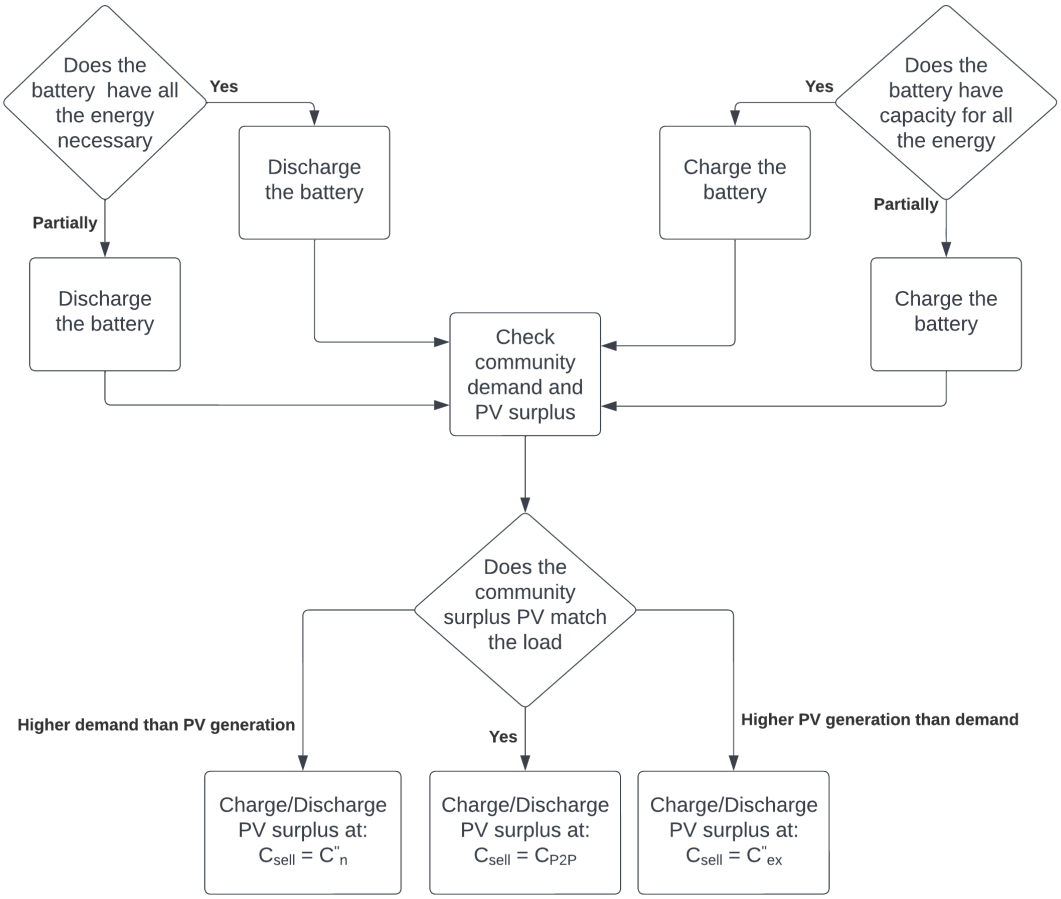

Figure 3.3: Flowchart showing the battery exchanges in an EC

that period. This approach ensures that the battery can be discharged until a SoC of 20% optimizing its usage and effectively managing the energy flow within the system.

3.5 Performance Indicators

his dissertation investigates key performance indicators employed to gauge PV consumption, specifically focusing on Con_{Batt}, Suf_{Batt}, Con_{P2P}, and Suf_{P2P}. Con_{Batt} represents the performance indicator quantifying the consumption of PV energy channeled through the battery, elucidating the efficiency and efficacy of energy storage solutions. Con_{Batt} can be calculated by Equation 3.1

$$Con_{batt} = \frac{\sum_{t0}^{t} P_{batt}}{\sum_{t0}^{t} P_{PV}} \tag{3.1}$$

where P_{batt} is the power the household consumes by discharging the battery and P_{PV} the household PV generation.

Suf_{Batt}, on the other hand, delineates the performance indicator measuring the proportion of the load sustained by PV energy derived from the battery, offering insights into the system's ability to fulfill energy demands autonomously. This performance indicator can be described by Equation 3.2,

$$Suff_{batt} = \frac{\sum_{t0}^{t} P_{batt}}{\sum_{t0} t P_{Load}} \tag{3.2}$$

where P_{Load} is the household load.

Con_{P2P} introduces a novel dimension by assessing the consumption of PV energy facilitated through P2P transactions, examining the intricate dynamics of decentralized energy distribution. Con_{P2P} is calculated by Equation 3.3

$$Con_{P2P} = \frac{\sum_{t0}^{t} P_{P2P}}{\sum_{t0}^{t} P_{PV}} \tag{3.3}$$

where P_{P2P} is the household PV consumption.

Lastly, $Suff_{P2P}$ provides a metric to gauge the extent to which the energy demands are met through PV energy in P2P transactions, thereby contributing to a comprehensive understanding of distributed energy systems. This performance indicator can be described by Equation 3.4.

$$Suff_{P2P} = \frac{\sum_{t0}^{t} P_{P2P}}{\sum_{t0}^{t} P_{Load}} \tag{3.4}$$

When computing for the community, the equations are converted into the equations denoted as Equation 3.6 - 3.8,

$$Con_{batt} = \frac{\sum_{n=1}^{n} \sum_{t0}^{t} P_{batt}}{\sum_{n=1}^{n} \sum_{t0}^{t} P_{PV}} \tag{3.5}$$

$$Suff_{P2P} = \frac{\sum_{n=1}^{n} \sum_{t0}^{t} P_{P2P}}{\sum_{n=1}^{n} \sum_{t0}^{t} P_{Load}} \tag{3.6}$$

$$Con_{P2P} = \frac{\sum_{n=1}^{n} \sum_{t0}^{t} P_{P2P}}{\sum_{n=1}^{n} \sum_{t0}^{t} P_{PV}} \tag{3.7}$$

$$Suff_{P2P} = \frac{\sum_{n=1}^{n} \sum_{t0}^{t} P_{P2P}}{\sum_{n=1}^{n} \sum_{t0}^{t} P_{Load}} \tag{3.8}$$

where n is the number of households considered

4

Implementation

4.1 Client Consumption

In the interest of comparing the client consumption with the generated power provided by the PV system, the client information has to be in the format of a load chart. That information can be provided to the client by E-REDES in case the house is equipped with a smart meter. To ensure that the study results are not influenced by specific environmental conditions during certain months or seasons, it was essential to obtain load charts covering a one-year time frame.

Despite the widespread adoption of smart meters, a significant proportion of households either lack these devices or have recently transitioned from traditional meters to smart meters. Consequently, a number of load charts exhibit missing data for certain months. With the purpose of completing the load charts that lacked information referring to certain months, the complete load charts were analyzed to find which months compared the most to other months.

In the direction of reaching a relation between the existing months, a comparative analysis of the mean monthly consumption for each month compared to the remaining months was conducted as depicted in Equation 4.1. The months chosen to represent the missing months are the ones where x is closer to the unitary value. The equivalent month for each month can be seen in Table 4.1.

The first step in this comparison was finding the consumption's mean value for each month. Subsequently, a comparative analysis was conducted on the monthly average consumption values. This comparison was depicted in Equation 4.1,

$$x = \frac{\mu(month_i)}{\mu(month_j)} \tag{4.1}$$

where $\mu(month_i)$ and $\mu(month_j)$ represent the mean value of their respective months.

The months exhibiting proximate consumption patterns were those in which the variable x approached unity.

The consumption dataset pertains to the year of 2022. However it is important to note that the circumstances during this period were atypical given the impact the Coronavirus

Table 4.1: Equivalent months

Month	Equivalent Month
$L_{January}$	$0.97 \cdot L_{February}$
$L_{February}$	$1.03 \cdot L_{January}$
L_{March}	$1.02 \cdot L_{June}$
L_{April}	$L_{Semptember}$
L_{May}	$1.01 \cdot L_{November}$
L_{June}	$0.98 \cdot L_{March}$
L_{July}	$0.99 \cdot L_{August}$
L_{August}	$1.01 \cdot L_{July}$
$L_{September}$	L_{April}
$L_{October}$	$0.92 \cdot L_{November}$
$L_{November}$	$0.99 \cdot L_{May}$
$L_{December}$	$1.11 \cdot L_{Fev}$

disease (COVID-19) pandemic which resulted in new factors such as telecommute. Consequently, the consumption sample may not represent a typical year and depict higher values of consumption during intervals where normally the values would be significantly lower.

An additional factor to consider when analyzing the months is the rapidly increasing global temperature, Lindsey and Dahlman [50]. The year of 2022 ranked as the sixth warmest year since 1880 [51]. which can potentially introduce a discrepancy between the expected values for the Winter months since utilization of heating devices may have comparatively reduced in comparison to other years.

For further information regarding the relation of the existing months, one may refer to Annex II, which presents a comprehensive table encompassing the values for all the months.

4.2 PV Generation

4.2.1 Building Data

Using Google Engine [52], it is possible to extricate the roof area of the buildings under consideration. This feature makes it possible to exclude non-usable portions of the roofs. This information is then transformed into a GeoJson file where the coordinates of each house are represented in a polygonal format.

As stated before, a distinction between apartment buildings and single family houses is considered given the inherent disparities. Accordingly, different files were produced depending on their type: apartment building or single family house.

To automate the process of calculating the PV production, the houses coordinates were were further categorized into five different files depending on their roofs orientations : North, South, East, West or Horizontal.

In addition to the location and azimuth, the buildings height is crucial to adjust the wind speed in view of calculating the PV generation. To determine the building height Google Earth's Three Dimensions (3D) [53] functionality was used.

Lastly, each building will then be given an Identification (ID) number. This ID will be referent to the entire building dataset and not particular to any EC. This way it will be possible to identify the buildings selected when doing any calculations.

The final GeoJson file encompasses the roof area coordinates and incorporates 4 essential properties: ID, orientation, type and height.

4.2.2 Dimensioning the PV System

During the dimensioning process of PV system, the primary objective of this study was to maximize self-sufficiency and self-consumption. This decision was made to align with the overarching goal of incorporating a greater share of renewable energy into the total energy consumption. Consequently, a preference for a self-consumption approach was adopted over an economic one. Therefore to achieve this objective, the number of modules to be implemented was determined based on covering the "worst-case scenario". This scenario encompasses the situation where consumption reaches its highest value coinciding with the lowest irradiation value.

In order to avoid the consideration of unrealistic scenarios, such as experiencing a peak load during times of negligible irradiation (e.g., between 8-9 am and 4-5 pm), a precautionary approach is adopted. When evaluating this time frame, the calculated required number of modules tends to significantly exceed the actual necessity, resulting in an overestimation. To address this concern while still incorporating a "worst-case scenario" perspective and guarding against overestimation, a specific threshold has been defined. This threshold establishes the relationship between the load and the anticipated PV generation assuming the installation of a single solar module. Through multiple simulations conducted with a single household, which had previously sought input from a power company for simulating the required PV modules, an acceptable threshold was determined. The identified threshold value was set at 30%. This criterion aims to eliminate extreme scenarios that may not accurately reflect real-world conditions and, instead, focuses on more realistic scenarios where PV generation can significantly contribute to fulfilling the energy demand.

The final step into dimensioning the PV system is adapting the optimal number of modules to the practical case. This step takes into account factors such as the type of modules selected and the available area on the roof. By applying Equation 4.5, it becomes possible to accurately calculate the optimal number of PV modules that can be installed on the given roof area. It is important to consider that in certain situations, the number of modules required to fully meet the energy demand during the "worst-case" scenario may exceed the available space on the roof. In such cases, the maximum possible number of modules that can be accommodated on the roof is chosen. To establish the necessary

spacing between rows to avoid potential shading, Equation 4.2 serves to compute the corrected module spacing, D, for a solar panel mounting system. The application of this equation requires knowledge of the mounting system's relative height, denoted as Height. By using the value of Height, the formula for D′ is derived, accounting for the solar elevation angle. The solar elevation angle is determined through the tangent of the sun's angle above the horizon.

$$D' = \frac{Height}{tan(SolarElevation)} \tag{4.2}$$

After obtaining D′, a correction factor is applied due to the non-perpendicular alignment of sun rays with an imaginary plane aligned with the mounting structure's orientation. The final corrected module spacing, D, is achieved by multiplying D′ by the sine of the azimuth correction angle as seen in Equation 4.3.

$$D = D' \cdot sin(AzimuthCorrection) \tag{4.3}$$

It is necessary to compute the panel capacity of a roof in accordance with the calculated distance, denoted as D. This is shown by Equation 4.4,

$$n_{roof} = \frac{a_{roof}}{D \cdot l_{module}} \tag{4.4}$$

where l_module is the length of the module considered.

Conversely, if the available space is sufficient, the number of modules needed to achieve self-sufficiency is selected as shown by Equation 4.6.

$$n_{roof} = \frac{a_{roof}}{a_{mod}} \tag{4.5}$$

$$n_{mod} = min(n_{ss}, n_{roof}, n_{dist}) \tag{4.6}$$

4.2.3 PV Module Production Calculations

To accurately estimate the energy output generated by the PV system, it is essential to employ a modeling approach that incorporates not only the PV generation itself but also accounts for the effects of an inverter.

4.2.3.1 PV Modules

Upon the selection of the module and determination of the appropriate quantity of module, it is necessary to consider the influence of various factors such as wind speed and the temperature of cells of the module.

A dataframe is created with the necessary factors to calculate the PV generation for each building: irradiation, wind speed and cell temperature.

Irradiation

PVGIS provides comprehensive data on beam, diffuse and reflected irradiation for the designated location. In order to model the system accurately, a decision was made to incorporate all types of radiation due to their respective contributions to PV power generation. As previously indicated, the selected irradiation format presents its values in hourly intervals, necessitating the implementation of an interpolation technique to convert them into 15 minute intervals.

Considering one of the dissertation's focus on roof orientation, the irradiation data will be treated separately based on the azimuth corresponding to each roof's orientation. This approach allows for the incorporation of irradiance variations from different orientations, and enabling more accurate calculations of PV generation.

Cell Temperature

One of the influential factors impacting the energy output of the PV system is the cell temperature, wherein an elevated value inversely correlates with the module's efficiency. Consequently, it becomes necessary to compute the cell temperature for every irradiation value, corresponding to intervals of 15 minutes.

Equation 4.7, as presented, provides the method to calculate the cell temperature.

$$T_{cell} = T_{amb} + G \cdot e^{(-3.56+0.0750 \cdot W_{speed})} \tag{4.7}$$

For the purpose of this dissertation an open rack mounting configuration was considered and a and b were replaced by the corresponding values.

Additionally, the ambient temperature referenced in the Equation 4.7 is derived from PVGIS data and subsequently interpolated to align with 15-minute intervals. Nonetheless, it remains necessary to adjust the wind speed to suit the specific height of each building.

Wind Speed

Once again, PVGIS provides the wind speed for a height of 10 meters. To account for the specific height of the buildings under consideration, Equation 4.8 outlines the requisite calculation to convert the wind speed from 10 meters to the precise height of the buildings. The necessary building height information can be extracted from the GeoJson file that contains the building data as referenced in the initial section of this chapter.

$$W_{speed} = W_{10} \cdot \left[\frac{h}{10}\right]^{0.22} \tag{4.8}$$

Since this study focus on residential buildings the variable $alpha$ was replaced by the value corresponding to the urban category.

PV Systems Output

The relationship between the contributing factors and the power output can now be described by Equation 4.9.

$$P_{out} = \frac{G}{1000} \cdot P_{max} \cdot [1 + \Upsilon \cdot (T_{cell} - 25)] \tag{4.9}$$

DC Losses

However it is necessary to take into account the Direct Current (DC) losses. These can be attributed to cable losses, dust accumulation and various other factors that affect the module production.

$$\psi_{cables} = 1\% \tag{4.10}$$

$$\psi_{dust} = 5\% \tag{4.11}$$

$$P_{PV} = P_{out} \cdot (1 - (\psi_{cables} + \psi_{dust})) \tag{4.12}$$

$$P_{PV} = P_{out} \cdot (1 - (0.01 + 0.05)) \tag{4.13}$$

Equation 4.13 can now be used to calculate the DC power to be injected into the inverter.

4.2.3.2 Inverters

The inverter plays a crucial role in converting the DC electricity produced by the PV modules into Alternate Current (AC) power. By including the inverter in the modeling process, the overall performance and efficiency of the PV system can be evaluated, taking into consideration factors such as inverter efficiency, power losses, and compatibility with the specific system configuration.

Inverter Selection

A selection of inverters was made from the catalog California Energy Commission [49], and the designated inverter was chosen from a comprehensive list comprising a total of 1508 distinct inverters.

In order to select the correct inverter it is necessary to verify the compatibility of the PV system's open circuit voltage, short circuit current and maximum power with the inverter. Given the relatively small scale of the modeled PV systems, the analysis focuses on a single string of modules. As a result, the consideration of string intake does not emerge as a relevant parameter.

Furthermore, it is necessary to select the appropriate inverter in accordance with the specific configuration of the system, whether it is grid-connected or battery-connected.

With that purpose, the following parameters have to be assured.

$$P_{PV} \cdot 0.7 \leq P_{in} \leq P_{PV} \cdot 1.2 \tag{4.14}$$

$$ISC_{PV} < ISC_{inv} \tag{4.15}$$

$$VOC_{PV} < MAXV_{inv} \tag{4.16}$$

$$Umpp_{PV} < Umpp[MAX]_{inv} \tag{4.17}$$

$$Umpp_{PV} > Umpp[MIN]_{inv} \tag{4.18}$$

Where P_{in} is the power fed into the inverter, ISC_{PV} is the PV model current, ISC_{inv} is the current accepted by the inverter, VOC_{PV} is the PV model voltage, $MAXV_{inv}$ is the maximum voltage accepted by the inverter, $Umpp_{PV}$ is the module's voltage maximum power point and $U_{mpp_{inv}}$ is the inverters' voltage maximum power point.

Inverter Efficiency

Inverter efficiency can be evaluated through a weighted efficiency metric commonly provided in the datasheet. While this metric is generally accurate, it may prove misleading under sub-optimal conditions, particularly during periods of low irradiance. To address this, a more comprehensive approach involves assessing the efficiency of a specific inverter by subjecting it to multiple loads and measuring the efficiency for each load condition. The California Energy Commission database offers testing results for inverters at various load levels (10%, 20%, 50%, 75%, and 100% of maximum load) across the minimum, nominal, and maximum voltage ranges supported by the inverter.

By employing a Python function, it becomes feasible to generate a curve based on the before mentioned tests, making it possible to later verify the inverter efficiency depending on the power being injected into the system.

AC Losses

To determine the AC losses attributed to cables, the initial step involves calculating the cable resistance. The mathematical formulation for these computations, can be illustrated by Equation 4.19 [54],

$$R_{cables} = \rho \cdot \frac{L}{A} \tag{4.19}$$

where the value of ρ correspond to the specific material properties associated with the selected cables as it can be seen in Table 4.2, L is the cable length and A is the conductor area.

Copper is a frequently used material for cables and is therefore chosen as the applicable value making the cable resistance possible to calculate by applying Equation 4.20.

$$R_{cables} = 1.7 \cdot 10^{-}8 \cdot \frac{L}{A} \tag{4.20}$$

Table 4.2: Electrical resistivity for certain materials used in cables, taken from [55]

Material	Electrical Resistivity At 20°C
Aluminium	$2.8 \cdot 10^{-}8$
Copper	$1.7 \cdot 10^{-}8$

In this dissertation, the AC losses were computed up to the main electrical panel, with energy transport facilitated by a standard copper cable.By employing such a cable, and due to its small distance from the inverter to the main switchboard and its wide section the power factor can be confidently regarded as unity. In this manner, the cable losses can subsequently be computed using Equation 4.21,

$$p_{cables} = R_{cables} \cdot I^2_{DC_{System}} \tag{4.21}$$

where $I_{DC_{System}}$ is the system current.

Having determined the cable losses, it is now possible to compute the AC power generated by the inverter shown by Equation 4.22,

$$P_{AC_{System}} = P_{DC_{System}} \cdot \eta_{inv} \cdot (1 - p_{cables}) \tag{4.22}$$

where η_{inv} is the inverter's efficiency.

4.3 Energy Markets

Energy markets are fundamental to efficient production, distribution, and consumption of energy. Time bands and energy pricing are crucial concepts in the dimensioning of energy markets. The selection of an appropriate time band schedule holds the potential to improve the advantages derived from PV generation.

The time band scheme employed in this study was Portugal's three-time-band system, as illustrated in Table 4.3. These time bands are categorized based on the demand patterns, and their associated energy pricing is determined accordingly, with the highest prices allocated to the time band characterized by the higher demand. Nevertheless, this particular time band structure was chosen due to its alignment with the solar path. The PV generation is maximized during the time bands associated with both higher and lower energy prices, respectively intermediate and off-peak time bands. Among these, the off-peak time band stands out as the primary period. Consequently, the intermediate time band coincides with a decrease in solar irradiation, no longer sufficient to generate energy from PV sources. However, households can rely on their battery systems during

this period, thereby avoiding the need to purchase electricity from the grid. Lastly, the cheapest time band, off-peak, occurs when there is no PV generated energy available stored. Making this a cost-saving approach.

Table 4.3: Time bands regarding energy sale, taken from ERSE.

		Time Bands		
		Peak	Off-Peak	Intermediate
Winter	Week Days	00:00 - 07:00	07:00 - 09:30 12:00 - 18:30 21:00 - 24:00	09:30 - 12:00 18:30 - 21:00
	Saturday	00:00 - 09:30 13:00 - 18:30 22:00 - 23:00	09:30 - 13:00 18:30 - 22:00	-
	Sunday	00:00 - 24:00	-	-
Summer	Week Days	00:00 - 07:00	07:00 - 09:15 12:15 - 24:00	09:15 - 12:15
	Saturday	00:00 - 09:00 14:00 - 20:00 22:00 - 23:00	09:00 - 14:00 20:00 - 22:00	-
	Sunday	00:00 - 24:00	-	-

Energy prices for the above mention time bands were taken from Energia [57] and are described by Equation 4.23 - 4.23.

$$p_{intermediate}(€/kWh) = 0.1145 \tag{4.23}$$

$$p_{off-peak}(€/kWh) = 0.1261 \tag{4.24}$$

$$p_{peak}(€/kWh) = 0.2312 \tag{4.25}$$

$$p_{surplus}(€/kWh) = 0.07 \tag{4.26}$$

4.4 Distribution Transformer

The calculation of the aging process in a distribution transformer is unaffected by the type of PV plant, whether an EC is considered or not. The data required for this calculation are regarding the transformer itself and the surrounding environmental conditions.

The majority of the required information to calculate the hot-spot temperature can be obtained from the IEC 60076-7 norm and is presented in Table4.4.

The IEC 60076-7 norm presents values for the parameters used in distribution transformer model previously shown that can used to calculate the hot spot temperature. Table 4.4 shows the values used for these parameters.

Nevertheless, the transformer's capacity and operating conditions are subject to variation depending on the specific case. All the methodologies employed in this study share a consistent feature—the utilization of a standardized time frame for simulating the model. As discussed in preceding sections of this dissertation, the comprehensive computations are conducted within a 15-minute time frame. To ensure coherence across the thesis and facilitate calculations, this temporal parameter is also applied in the assessments of transformer aging.

Table 4.4: Parameters used in this dissertation and their values, as in the IEC 60076-7 norm.

Parameter	Value	Unit
$\Delta\theta_o r$	45	K
$\Delta\theta_h r$	35	K
τ_o	150	min
τ_w	7	min
x	0.8	–
y	1.3	–
R	8	–
$k_1 1$	0.5	–
$k_2 1$	2.0	–
$k_2 2$	2.0	–
L_r	1	kVA

Information regarding distribution transformers can be obtained from ERSE [56]. This platform allows access to data pertaining to the available distribution transformers and their respective capacity and the percentage of usage. However, it does not provide insights into the specific allocation of transformers to individual buildings. Consequently, it was decided to evenly distribute households across the transformers.

Subsequently, it is necessary to calculate the power output of transformers during each designated time interval. Given the known transformer capacity and utilization levels, an initial assumption was made, considering a constant value for power exchange in each time slot. The next step involves recalculating the power exchange while incorporating PV generation. Given that the initial value does not account for the PV generation, the entirety of energy stemming from PV generation has to be subtracted. This revised calculation is illustrated by Equation 4.27,

$$P_{transformer} = P_{previous-transformer} - P_{PV} \tag{4.27}$$

where P_{PV} is the power originated from the PV generation in the community and $P_{previous-transformer}$ is before the introduction of PV generation in the community and can be calculated by Equation4.28,

$$P_{transformer} = P_{transformer} \cdot OperationalUtilization(\%) \tag{4.28}$$

where $P_{transformer}$ is the transformer capacity and $OperationalUtilization(\%)$ is the percentage of the capacity that is being used by the community.

In this context, the energy deducted from the initial transformer input can be categorized into two groups: the energy that the household did not require from the transformer, as it was supplied by their PV generation, and the surplus PV-generated energy that is fed back to the transformer. It is presumed in this scenario that the surplus energy flows through the transformer rather than being directly transferred to another household. This assumption is made to account for a worst-case scenario.

When considering the individual approach, the PV generated power can be divided into two different categories as shown by Equation 4.29,

$$P_{PV} = P_{sell} + P_{LM} \tag{4.29}$$

where P_{sell} is the surplus PV generated power the households were not able to consume and sold to the grid and P_{LM} is the PV energy the households consumed directly, the load match.

In the case of the individual with storage approach, Equation 4.29 can also be applied taking in consideration the definition applied by Equation 4.30,

$$P_{sell} = P_{surplus} - P_{store-batt} \tag{4.30}$$

where $P_{surplus}$ is the PV surplus after consumption and P_{store_batt} is the PV generated power stored in the batteries and later consumed by the households.

When any of the three approaches regarding ECs is considered, the power generated and consumed from the PV and P2P system can be characterized by Equation 4.31,

$$P_{PV} = P_{sell} + P_{house-buy} + P_{LM} \tag{4.31}$$

where P_{house_buy} is the PV generated power that was exchanged between members of the community or adjacent communities.

When considering EC with storage, Equation 4.30 can be used once again.

With all the acquired data, it is now possible to calculate the hot-spot temperature using the block diagram function in MATLAB with the equations presented in the section pertaining to the transformer aging in the methodology Chapter. This process can be seen in Figure 4.1.

The above decision diagram was implemented in the Python program. This way, the hot spot temperature can be calculated at any instance.

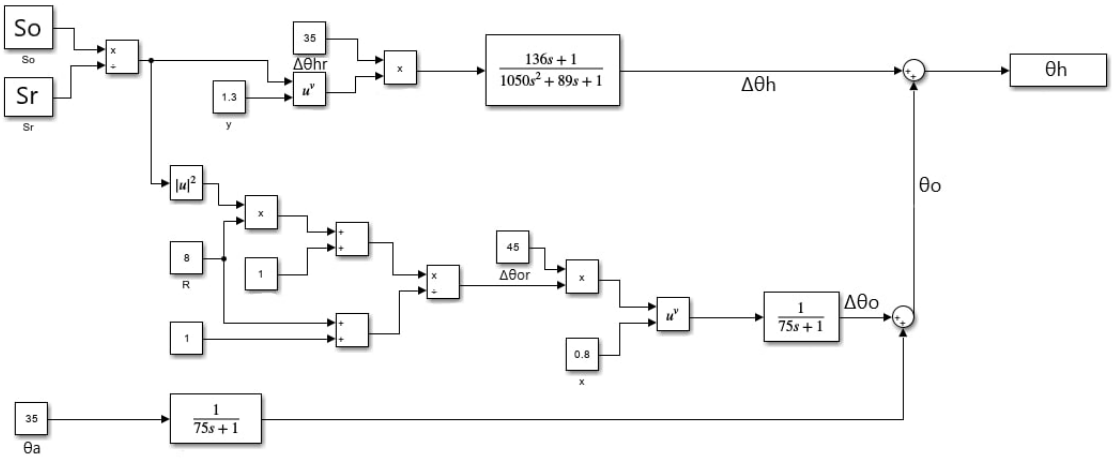

Figure 4.1: Matlab implementation of the block diagram for the hot spot temperature of the distribution transformer.

4.5 Battery System

The batteries employed in the study were sourced from the same database as the PV modules and inverters. In order to optimize the consumption of energy generated through the PV systems, a daily cycling approach was implemented. In the following subsections, the selection process for the batteries and the parameters taken into account during this process are shown.

All computations in this section were performed based on a standard day divided into 15-minute time intervals. A mean value was derived for each parameter within every 15-minute time slot, which was then extrapolated to represent a full day. This methodology was adopted to align with the daily cycling approach.

4.5.1 Daily Cycling

The adoption of a daily cycling approach allows a higher penetration of PV generated energy, increasing the utilization of renewable resources. Additionally, it provides an easier computation of the battery's current state, making it easier to assess the level of charge or discharge. However, it is necessary to incorporate this approach with the monitorization of the SoC and adhering to the maximum charging and discharging restrictions.

The daily cycling approach was implemented as follows. Throughout the daytime period, any surplus energy that is not used by the individual household, or in case of an EC, the collective households, is designated for storage within the battery system. In instances where there is an insufficient energy supply, such energy is to procured from the grid. Subsequently, when the solar irradiation reaches a value where energy generation is no longer viable, the battery will be discharged by the household(s).

In the context of this thesis, it is necessary to distinguish between the individual and the EC approach. Under the individual approach, a household is responsible for charging

the battery during surplus periods and discharging it as needed. In contrast, the EC approach allows one household to charge the community battery, with another household discharging the battery in subsequent periods. This transaction is subject to taxation, treating it as if the household that charged the battery is selling surplus energy to the household that discharged the battery.

This process allows for a daily cycle making sure the battery is dimensioned for each household needs and diminished the possibility of over dimensioning the battery leading to a higher cost.

To determine the battery capacity that aligns with the daily cycling approach, a method was utilized based on the daily SoC value.

With a typical day it becomes feasible to assess the excess PV generated power that can be directed to the battery. Once more, it is crucial to distinguish between the individual and EC approach. In the individual approach, the surplus PV is calculated solely with the household consumption and PV generation, the load match. Conversely in the EC approach, surplus PV was calculated only after the P2P energy exchanges. Consequently, for the EC approach, takes into consideration both load matching and P2P energy exchanges.

4.5.2 SoC

The advised SoC range for battery systems can vary depending on the specific battery technology and manufacturer's recommendations. However, as a general guideline, it is often recommended to maintain the SoC within the range of 20% to 80% which shows significantly improved capacity retention, Jiang et al. [58] . Keeping the SoC above 20% helps to prevent deep discharge and minimize the risk of damaging the battery. On the other hand, limiting the SoC to 80% helps to avoid overcharging and extends the overall lifespan of the battery.

The following equations enable the estimation of SoC at any given moment by considering the charging and discharging power levels, time intervals, and the battery's capacity. The battery's capacity was calculated through a test battery capacity value. This capacity value represents the state of charge of the battery in kWh instead of a percentage. This value is reached by simply adding all the surplus PV energy that would be feed into the grid in a typical day. The calculation for the test capacity can be seen in Equation 4.32,

$$Cap_{def}(\Delta t) = Cap_{test}(\Delta t) - P_{grid}(\Delta t) \tag{4.32}$$

where $Cap_{test}(\Delta t - 1)$ is the previous test SoC value and $P_grid(\Delta t)$ is the energy that is being traded with the grid.

To determine the SoC value it is first necessary to understand what is the energy that is being traded with the grid. Equation 4.33 quantifies the energy transaction $P_{grid/bat}$,

$$P_{grid}(\Delta t) = P_{cons}(\Delta t) - P_{PV}(\Delta t) \tag{4.33}$$

where P_{cons} is the consumption, and P_{PV} the PV generation, at each specific moment Δt.

With this intermediate value for the test SoC, it is now possible the create constrains for the theoretical charge of the battery. These constrains are shown in Equation 4.34,

$$\begin{cases} SoC_{test}(\Delta t) = 0, if\, SoC_{def}(\Delta t) < 0 \\ SoC_{test}(\Delta t) = SoC_{def}(\Delta t), if\, SoC_{def}(\Delta t) > 0 \end{cases} \tag{4.34}$$

where $SoC_{test}(\Delta t)$ is the SoC value for the various time intervals , Δt.

The battery capacity can be defined as the maximum $SoC_{test}(\Delta t)$ since this value is measured in kWh. As stated before, a 15 minute time interval is being considered, and since the battery capacity is stated in kWh, a correcting factor was applied when considering the transactions, shown in Equation 4.35,

$$P_{bat} = max(SoC_{test}) \cdot 4 \tag{4.35}$$

where $max(SoC_{test})$ is the maximum $SoC_{test}(\Delta t)$.

4.5.3 Battery Capacity Dimensioning

In order to accurately determine the capacity of the battery, it is necessary consider various factors: the Depth of Discharge (DoD), the household energy consumption and the losses aggregated with the battery.

Given the decision to utilize SoC between the values of 20% and 80% as a criterion, the DoD can be replaced by the SoC as the latter consistently assumes lower values. The capacity of the battery can be calculated by Equation 4.36,

$$E_{bat} = \frac{E_{surplus} \cdot n_{days}}{\eta_{bat} \cdot SoC_{thr}} \tag{4.36}$$

with $E_{surplus}$ representing the household's average daily surplus energy, η_{bat} denoting the battery's efficiency, SoC_{thr} indicating the threshold in which the SoC needs to be maintained - 20% to 80% - and n_{days} being the days of autonomy for which the battery is dimensioned. Since the daily cycle approach was implemented, the requirement is limited to a single day of autonomy. Considering that the batteries in this study are of the lithium-ion type, an efficiency value of 95% will be assumed.

$$E_{bat} = \frac{E_{surplus}}{0.95 \cdot 0.60} \tag{4.37}$$

Equation 4.37 represents the theoretical value of the capacity of the battery where $E_{surplus}$ in this case, can be replaced by the previously calculated P_{bat}.

Differing from the approach implemented for the PV modules, P_{bat} is achieved by considering the average daily surplus energy. This deviation in approach was due to the higher cost associated with battery systems, which rendered the application of a worst-case scenario impractical during the battery sizing process. In the context of battery

dimensioning, a worst-case scenario would entail low household energy consumption coupled with high PV generation, resulting in a significant demand for energy storage. However, such a scenario is more likely to occur during independent cases, such as vacations, and does not represent the regular household functioning. Hence, it was deemed more appropriate to base the battery dimensioning calculations on average daily surplus energy instead of a worst-case scenario.

A method was created determine the optimal capacity value for the battery. By utilizing a trial and error approach, the algorithm takes the theoretical battery capacity as an input and iteratively searches for the battery configuration that best adheres to the constraints the SoC and daily cycling approach. Specifically, the method aims to identify the battery configuration that completes its cycling with a lower capacity, aiming to reach SoC peak value closer to the 80% mark while ensuring it remains closer to 20% before the end of the day. The batteries used for this method were taken from California Energy Commission [49]. The database also offers the maximum discharge rate, which was subsequently utilized instead of the calculated value.

4.5.4 Battery's Energy Transactions

The energy transaction, as determined by the preceding equations, enables the calculation of the current state of charge of the battery, utilizing the battery's capacity as a parameter. This is shown by Equation 4.38,

$$SoC(t)_c = SoC(t - \Delta t) + \frac{P_{grid}(\Delta t)}{P_{bat}} \tag{4.38}$$

where $SoC(t)_c$ is the calculated state of charge, P_{bat} is the battery's capacity and $SoC(t - \Delta t)$ is the previous state of charge.

The final step in defining the SoC is the batteries function at the time specified. Depending on the task, charging or discharging, and the previous SoC, the current SoC is calculated differently. In the case that the previous SoC is 0% or 100% no discharging or charging respectively is possible. When the previous SoC presents a value that allows charging or discharging, the current SoC is calculated as stated in Equation 4.38. This process is depicted in Equation 4.39.

$$\begin{cases} SoC(t) = SoC(t - \Delta t), \text{if } P_{grid}(\Delta t) > 0 \cap SoC(t - \Delta t) = 0\% \\ SoC(t) = SoC(t - \Delta t), \text{if } P_{grid}(\Delta t) < 0 \cap SoC(t - \Delta t) = 100\% \\ SoC(t) = SoC(t)_c, \text{if } P_{grid}(\Delta t) > 0 \cap SoC(t - \Delta t) \neq 0\% \\ SoC(t) = SoC(t)_c, \text{if } P_{grid}(\Delta t) < 0 \cap SoC(t - \Delta t) \neq 100\% \end{cases} \tag{4.39}$$

These equations serve as mathematical representations of the energy transaction, SoC calculations, and the adjustment of SoC based on energy sourcing, allowing for a quantitative analysis of the battery system's behavior within the overall PV system operation.

It is important to note that these equations provide a simplified representation of the SoC calculation and may not consider certain factors such as temperature effects and self-discharge.

4.6 Dimensioning Energy Communities

In this dissertation, the definition of ECs diverges from that outlined in Portuguese legislation, particularly in the context of Decreto-Lei n.º 15/2022 dated January 14. The EC examined in this study consists of individual households located in close proximity to one another, aiming to collaboratively distribute surplus energy generated from PV sources among its members, be they consumers or prosumers. Hence, the subsequent sections are grounded in this specific definition.

To achieve a favorable outcome from the development of an EC, various factors are essential. These factors include the selection of a appropriate renewable energy and the corresponding implementation of suitable energy plant. The active engagement and participation from community members must be ensured. Furthermore, an efficient distribution infrastructure must be established to facilitate the smooth transmission of energy within the community, or communities, alongside the establishment of a robust energy transfer market, complemented by effective pricing mechanisms and regulatory frameworks, such as the ones defined previously. Lastly, the integration of an energy storage system can be integrated to enhance the resilience and flexibility of the EC, enabling utilization of surplus energy.

4.6.1 Modeling Energy Communities

The ECs created for this study rely exclusively on PV generation as the primary energy source, considering rooftop PV plants. The initial step involved categorizing each household based on their role within the EC, distinguishing between consumers and prosumers.

Multiple scenarios were examined, to evaluate the impact on various factors, such as transformer aging. Consequently, it was determined that all households should be served by the same distribution transformer. The exception to this rule would be in the case of multiple EC, where different transformers could be considered. The decision was based on the proximity of households, as distribution transformers typically serve households in close proximity to each other. This allows for a lower energy loss.

To establish the ECs grid, the number of participants must first be determined. This enables the selection of households to join the EC while maintaining the minimum ratio specified between prosumers and consumers. The initial household is chosen as the node, and subsequent participants are selected from households located within the radius of households already served by the transformer connected to the node.

4.6.2 Markets

As mentioned before, the market model chosen for this dissertation is the MMR method [23]. As this method allows to determine the value of energy based on the current market rather than relying on auctions. Therefore it becomes necessary to establish an alternative allocation method. To minimize energy losses, the decision was made to implement an energy allocation strategy that takes into account the distance between the prosumer and consumer. This was made possible by the building's coordinates presented in the GeoJson. Additionally, it was also determined that households capable of satisfying the complete energy requirements of the purchasing household were preferred over those that could only supply partial if the energy necessary.

The P2P energy price will be calculated by Equation 4.40,

$$p_{P2P} = \frac{p_{BFG} + p_{surplus}}{2} \tag{4.40}$$

where, p_{P2P} is the P2P energy price, $p_{surplus}$ is the price at which any surplus PV will be sold, further referenced as $p_{ex}(t)$ or p_{im} depending on the community's overall deficit and, depending on the time band considered, p_{BFG} is the energy markets price and can be substituted by $p_{intermediate}$, $p_{off-peak}$ or p_{peak} and their respective values were defined in the energy market section.

In cases where energy demand within the community equals the energy production, the selling and buying price will be equal to the P2P price, Equation 4.41.

$$p_{ex}(t) = p_{im}(t) = p_{P2P} \tag{4.41}$$

When PV generation is higher than demand, the selling energy price will be calculated by Equation 4.42.

$$p_{ex}(t) = \frac{\sum_{n=1}^{N} L^n(t) \cdot p_{P2P} + \left(\sum_{n=1}^{N} P^n_{PV}(t) - \sum_{n=1}^{N} L^n(t)\right) \cdot p_{surplus}}{\sum_{n=1}^{N} P^n_{PV}(t)} \tag{4.42}$$

In this scenario, when considering an EC equipped with a battery system, each prosumer who charges the battery receives compensation equal to the value they would have received if they had sold the energy to another member within the community, calculated by Equation 4.42. This equation is also valid when considering the energy transaction between various ECs.

Lastly, considering lower generation than demand, the buying price is given by Equation 4.43

$$p_{ex}(t) = \frac{\sum_{n=1}^{N} P^n_{PV}(t) \cdot p_{P2P} + \left(\sum_{n=1}^{N} L^n(t) - \sum_{n=1}^{N} P^n_{PV}(t)\right) \cdot p_{BFG}}{\sum_{n=1}^{N} L^n(t)} \tag{4.43}$$

When a community member needs to discharge the battery, regardless of whether the overall community has surplus PV energy or not, Equation 4.43 can also be utilized as the cost for discharging the battery.

Lastly, the electricity bill for each individual household can be calculated by Equation 4.44.

$$p_n = \sum_{t=0}^{T} \left(P_{im}^{n}(t) \cdot t \cdot p_{im}^{''}(t) \right) - \sum_{t=0}^{T} \left(P_{ex}^{n}(t) \cdot t \cdot p_{ex}^{''}(t) \right) \tag{4.44}$$

4.7 Software

This section will explore the software's development designed for simulating different scenarios. The software comprises five main components: household generation, battery capacity dimensioning, P2P market simulation, transformer aging calculation, and performance indicator calculation. This section will also discuss the user input requirements and the necessary parameters for operating this software.

4.7.1 PV Generation

4.7.1.1 Households Information

Given the absence of a standardized format for providing the households necessary information to the software, a decision was made to use a GeoJSON file. Each household in the GeoJSON file is divided into 3 sections: 'id', 'geometry' and 'properties'.

To calculate the PV generation for each household, it is necessary to obtain the irradiation data specific to the household's location. As previously mentioned, these locations are determined using geographical coordinates sourced from Google Earth Engine [52], and these coordinates are inputted by the user, Figure 4.3. These coordinates are under 'geometry'. These coordinates are also used in order to calculate the rooftops areas using a polygon function.

As previously mentioned, irradiation data is sourced from PVGIS [47]. To obtain the irradiation values, it is necessary to specify both the azimuth and tilt angle. This information can also be extracted from the GeoJSON data, provided in the format of building orientation. Depending on the orientation indicated, 'Dir', the azimuth angle is determined accordingly. As described in Chapter 3, the tilt angle is usually equivalent to the roof tilt, except in cases where the roof has no angle, 'Horizontal', in which case the optimal angle is used. As most households have roofs facing different orientations, an property is added to the GeoJSON file, 'Building ID', in order to match rooftops that belong to the same building.

Furthermore, to calculate the temperature of the PV module cells and to adjust the wind speed to various heights, the height of the buildings, obtained from Google Earth [53], is specified within the 'Height' attribute.

Finally, it's important to note that buildings can be categorized as either single family houses or apartment buildings, and this differentiation is made in the 'Type' attribute.

```
{"type": "FeatureCollection",
  "features": [
    {
    "geometry": {
        "coordinates": [ ],
        "type": "Polygon"
      },
    "id": " ",
    "properties": {
        "Dir": " ",
        "Height": " ",
        "Type": " ",
        "Building ID": " "
      },
      "type": "Feature"
    } ] }
```

An attribute that is not presented in the GeoJSON but is inputted by the user is the type of location, Figure4.2.

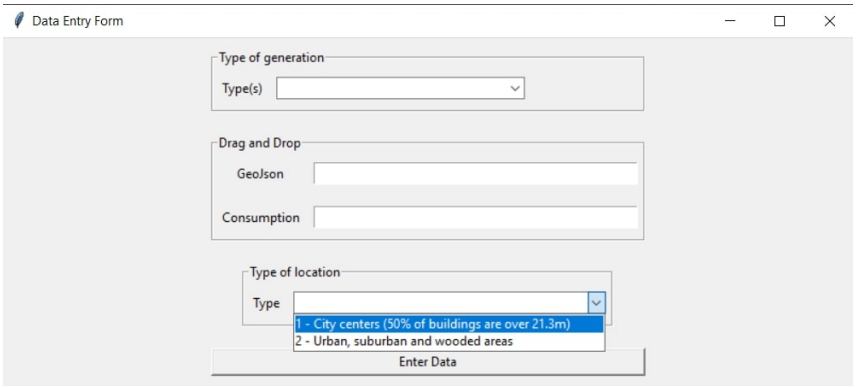

Figure 4.2: User's interface - Type of terrain

4.7.1.2 PVGIS

For the correlation between the software developed and the PVGIS [47] platform, an API was used.

4.7.1.3 Household consumption

When it comes to household consumption and related information, the user provides the necessary data in a JSON file, Figure 4.3.

In the case of apartment buildings, where a single rooftop serves multiple households, there is a need to establish a connection between the building's information and the household data. This linkage is achieved by duplicating the 'Building ID' attribute from the building GeoJSON and incorporating it into the households' JSON.

Depending on the user's chosen PV approach, it may be necessary to determine whether a household functions as a prosumer or a consumer. This classification is indicated by the 'Role' attribute. Furthermore, if the chosen approach involves ECs, it is also crucial to specify which houses are affiliated with particular EC, which can be identified through the 'EC' attribute, Figure 4.4.

```
{ "Households": [
    {
        "Household ID": " ",
        "Building ID": " ",
        "Load Chart": " ",
        "Role": " ",
        "EC": " "
    } ]
```

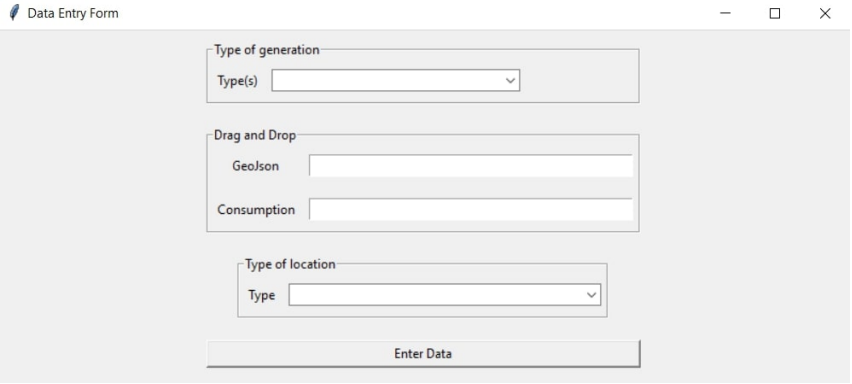

Figure 4.3: User's interface

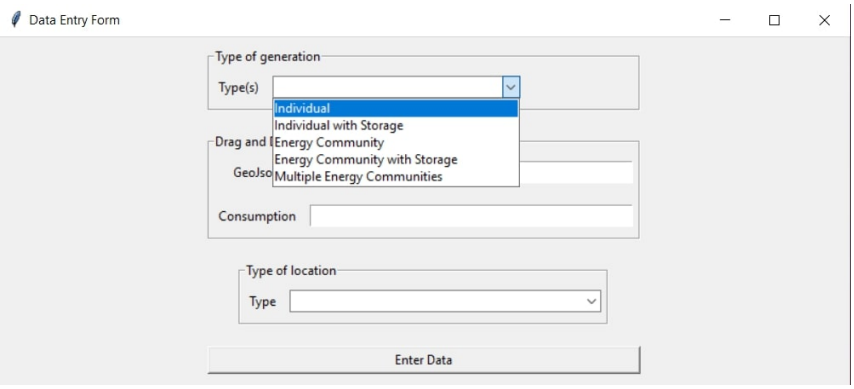

Figure 4.4: User's interface - PV approach

4.7.1.4 PV modules, inverters and batteries

As mentioned in Chapter 3, the PV modules, inverter and batteries are taken from the California Energy Commission [49].

The PV module is presented as a selection to the user. Firstly, the user is able to choose the module brand, Figure 4.5. Secondly, only the power range the chosen brand offers are present, Figure 4.6, and lastly the modules that respect both previous constrains are presented to be selected, Figure 4.7.

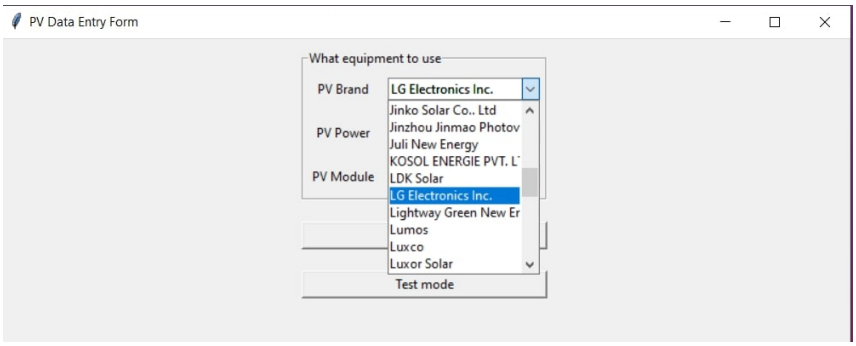

Figure 4.5: User's interface - PV modules brands

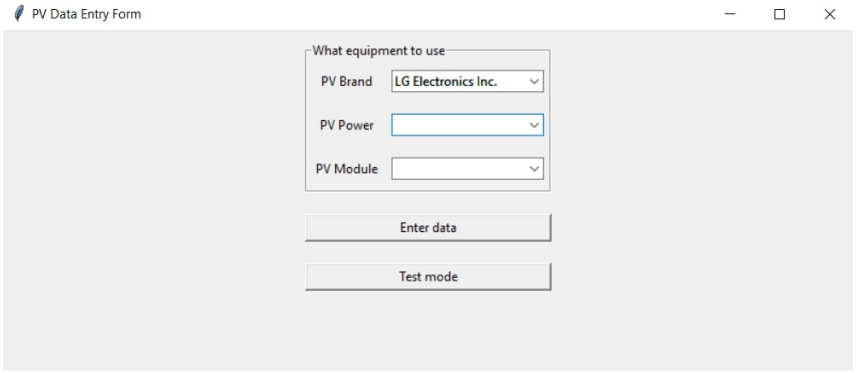

Figure 4.6: User's interface - PV power

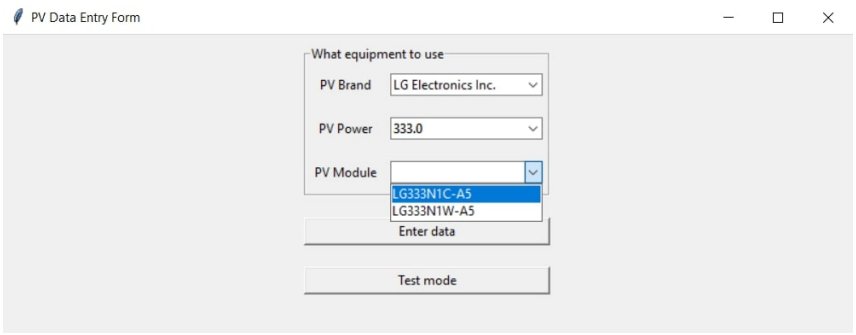

Figure 4.7: User's interface - PV module

The selection of the inverter is based on the current and voltage specifications of the PV module array. Similarly, the choice of batteries aligns with the daily median, with the

selected battery being the one from the database that most closely matches the calculated value. A more detailed explanation of these calculations can be found earlier in this Chapter.

4.7.1.5 Distribution transformers

As mentioned before, the transformer information is taken from E-REDES Open Data platform [59]. This information can be obtain via a GeoJSON the platform provides with the transformers information by using the households geographical coordinates as a parameter. This allows to filter the closest transformer to the household.

Despite the fact that all calculations are performed within the Python software, the transformer aging calculations are conducted in MATLAB. Using the 'matlab.engine' package, the Python environment can load the MATLAB module and configure the simulation parameters. By instantiating a SimulinkPlant object within the Python software, a connection to MATLAB is established, allowing the simulation to start. Upon completion of the simulation, the Python software retrieves the output data and subsequently closes the connection to MATLAB.

4.7.1.6 Output

The software developed gives the performance indicators presented in Chapter 2 and the transformer aging. These indicators are presented for the community as a whole.

All the calculations within the software were conducted as outlined in earlier in this Chapter.

5

Study Case: Oeiras

5.1 Location

Oeiras provides a multitude of buildings with various characteristics. Being mostly a residential area, households rage from single family houses to seven plus apartment buildings. In spite of the fact that it is a residential area, a large percentage of the buildings have a significant distance between each other and the ones that are close together, or are geminated houses, are the same height making it so the shading a building will cast on it's neighbour is minimum. Lastly, Oeiras is a coastal municipality therefore the ambient temperature will have lower values and stronger winds which will have a positive impact on the power production of the PV systems. The mentioned characteristics make Oeiras an ideal location to simulate the various cases presented in this thesis, in residential PV production.

As mentioned before, a distinction between single family houses and apartment buildings was made. The locations chosen for apartment buildings and single family houses are shown in Figure 5.1 and Figure 5.2 respectively.

In the cases where both typologies are used it was considered that the locations were adjacent making the distance between them minimal.

5.2 Consumption

The consumption charts for each household can be seen in Annex III.

5.3 PV Module

For the purpose of achieving uniform and consistent results, the PV module JKM575M-7RL4-V from JinkoSolar was selected. It is a mono-crystalline module with 2 series of 78 cells providing a maximum power of 540 Watt peek (Wp). The selected module occupies an area of 2,48 square meters where the long and short side are 2.206 and 1.122 meters respectively.

Figure 5.1: Chosen location for the study case apartment buildings

Table 5.1: PV module characteristics

Manufacturer	Model Number	Family	Efficiency (%)	N cell	Nameplate Isc (A)	Nameplate Voc (V)	Nameplate Ipmax (A)	Nameplate Vpmax (C)	Average NOCT	Pmax (%/°C)	Isc (%/°C)	Voc (%/°C)	Mounting	Long Side (m)
Jinksolar	JKM510M-72HL4-TV	Monocrystalline	20.60	72	13.05	48.94	12.32	41.40	45	-0.35	0.048	-0.28	Rack	2.206

5.3.1 Module Shading

As previously stated, in order to mitigate the PV module's shading, it is necessary to calculate the appropriate inter-row distancing. The method sun path method offers a means to calculate the distance considering the worse case scenario, the month of December. Figure 5.3 shows the sun path for the location of Oeiras alongside the solar elevation.

Considering that the PVGIS datasets start presenting irradiation values as soon as 8AM, the solar elevation and azimuth were obtained for the corresponding time period, 8AM-4PM.

The value for the azimuth correction can be obtained by Equation 5.1.

Figure 5.2: Chosen location for the study case single family houses

$$A = 180 - A^{'} \tag{5.1}$$

Given the fact that it is only necessary to calculate the inter-row distance when considering buildings with horizontal roofs, it was asserted that all modules would be installed with an inclination of 35º since that is the optimal value for the selected location, depicted in Figure 5.4.

With Figure 5.2 it is possible to calculate the module height relative it's inclination, where α is the 35º and h' is the 2.48 meters mentioned above.

$$sin(\alpha) = \frac{H}{h'} \tag{5.2}$$

It is now possible to calculate the inter-row distance applicable in this case by applying Equation 5.3 and Equation 5.5, with the values present in Table 5.3.

$$D^{'} = \frac{1.383}{tan(7.5)} \tag{5.3}$$

$$D^{'} = 10.5m \tag{5.4}$$

$$D = 10.5 \times cos(52.5) \tag{5.5}$$

Table 5.2: Individual with Storage approach

Manufacturer	Jinksolar
Model Number	JKM510M-72HL4-TV
Family	Monocrystalline
Efficiency (%)	20.60
N Cell	72
Nameplate Isc (A)	13.05
Nameplate Voc (V)	48.94
Nameplate Ipmax (A)	12.23
Nameplate Vpmax (C)	41.40
Average NOCT	45
Pmax (%/°C)	-0.35
Isc (%/°C)	0.048
Voc (%/°C)	-0.28
Mounting	Rack
Long Side (m)	2.206
Short Side (m)	1.122

Table 5.3: Values for calculation inter-row spacing

Solar Elevation (S)	Solar Azimuth (A')	Solar Azimuth Correction (A)	Height (H)
7.5º	127.5º	52.5º	1.383 m

$$D = 6.39m \tag{5.6}$$

After the calculations, the resulting value for the inter-row spacing is approximately 6.39 meters which will be rounded up to 6.40 meters to facilitate the calculations and possible implementation.

5.3.2 Number of PV Modules

The final number of PV modules simulated for each household, calculated as described in Chapter 4, can be found in Annex IV.

5.3.3 Communities Dimensioning

According to Lopes et al. [24], the impact on transformers became noticeable at 16 households and pronounced at 19 households. As a result, it was decided to investigate each scenario within the range of 16 to 20 households.

In the context of scenarios involving multiple energy communities, two distinct communities were defined. This approach facilitated the representation of transactions between these communities without depleting the surplus of PV and coming back to a scenario where the communities did not engage in trade with each other. Additionally, one of the communities consisted of apartment buildings, while the other comprised single-family

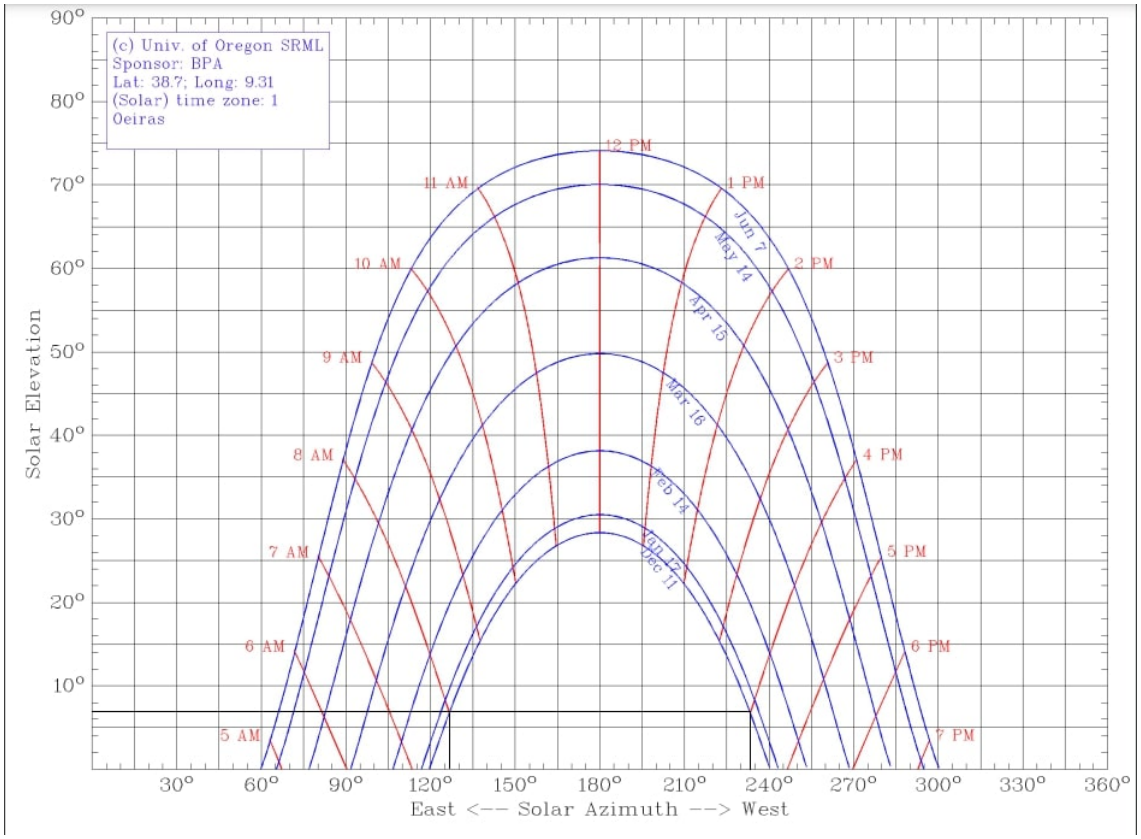

Figure 5.3: Sun's path and elevation for the months of June to December in Oeiras

houses, enabling an examination of whether one building type was preferred over the other.

5.4 Inverter

In scenarios without a battery system, a micro inverter was selected for each individual PV module to simplify the calculations. However, when a battery system was present, the software opted for a inverter for the entire system. This choice was motivated by situations in which a household might require an inverter not found in the selected database. Table 5.4 presents the micro inverter's characteristics.

Table 5.4: Micro inverter datasheet

Micro Inverter Model	APsystems DS3-H
Output Power (VA)	960
Output Current (A)	4.2
Output Voltage Range (V)	184-253
Maximum Input Current (A)	20 x 2
Maximum Input Voltage (V)	60V
Weighted Efficiency (%)	97.3

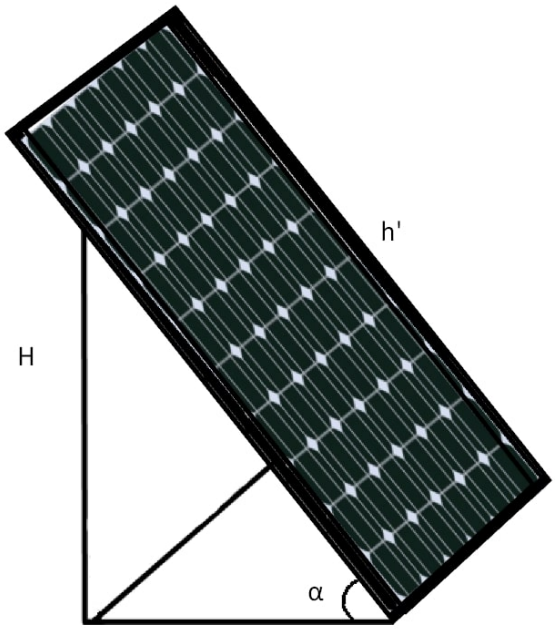

Figure 5.4: PV module disposition

5.5 Battery System

Using the software explained in Chapter 4, it was possible to dimension the battery capacity for each household and for each energy community. As mentioned before, this dimensioning was based on a daily cycling approach. Table 5.5 and Table 5.6 present the battery capacity of the battery for each case. In brackets are the calculated values. As evident, it was not always possible to find the most adequate battery.

If the datasheet did not specify, the depth of charge considered was of 90%.

5.6 Distribution Transformers

As mentioned before, the capacity and usage level of distribution transformers in the Portuguese grid can be acquired from the E-REDES Balcão Digital platform [46]. In the area under simulation, two transformers were identified as the most likely ones to serve the selected buildings. These transformers can be seen in Figure 5.5 and Figure 5.6.

As it is possible to see in Equation 5.7, the usage level is presented as a range. To simplify calculations, the midpoint of this range was adopted as the constant usage level throughout the simulation period.

5.7 Results

During the simulations, each household underwent individual simulation. Consequently, performance indicators were computed separately for each household and

Table 5.5: Battery capacity for each household

Household	Battery Capacity (kWh)
1	2.56 (3)
2	2.56 (3)
3	2.56 (3)
4	2.56 (3)
5	3.8 (4)
6	3.8 (4)
7	3.8 (4)
8	5
9	5
10	2.56 (3)
11	2.56 (3)
12	2.56 (3)
13	7.2 (7)
14	7.2 (7)
15	7.2 (7)
16	7.2 (7)
17	15
18	15
19	15
20	15

Table 5.6: Battery capacity for each energy community

	Households				
	16	17	18	19	20
Battery Capacity (kWh)	12 (11)	10	16	24	24(26)

Table 5.7: Transformers and their installed power and usage level

Transformer	Capacity (kVA)	Usage level (%)
1	500	20-39
2	400	40-59

attribute within every scenario. To obtain a more comprehensive insight, two of the performance indicators, SSR and SCR, were further subdivided into more detailed components based on the simulated approach.

In order to examine the community within each approach, the performance indicators were also computed by considering the collective sum of households for each scenario. In other words, these performance indicators were calculated by aggregating the total PV generation, energy consumption, and energy exchanged with the grid across all households. These values exclusively pertain to households equipped with PV systems, or those utilizing energy generated by PV systems, facilitated by ECs. This are the values presented in the following tables.

The results presented in this section are derived from the methods presented earlier. The computations for the transformer aging were described in the Transformer Aging

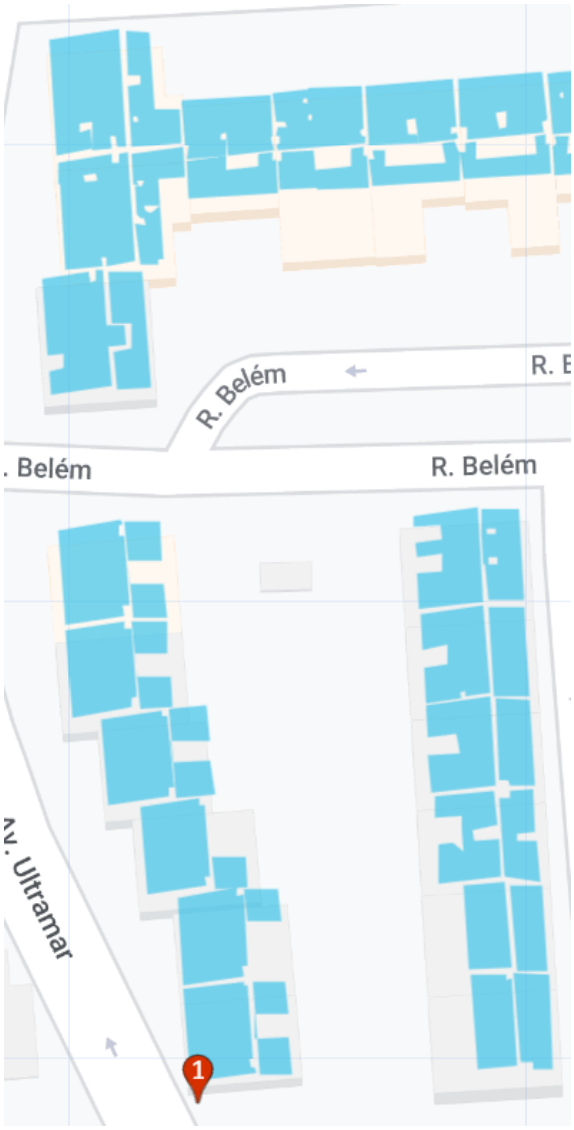

Figure 5.5: Distribution transformers

section in Chapter 4, while the computations for the remaining performance indicators were discussed in the Performance Indicators section in Chapter 2.

In Annex V and VI it is possible to see the performance indicators and electrical bill for each household. As the aim of this thesis is to assess the impact of different methods on the overall community, the presented results serve as intermediate calculations utilized for determining the community values.

5.7.1 Individual

In the individual approach, since there are no P2P markets or storage systems, the performance indicators and transformer aging are only referent to direct PV consumption and grid exchanges, shown in Table 5.8 and Table 5.9 respectively.

The electricity bill, shown in Table VI.1 both scenarios, without PV implementation and

Figure 5.6: Distribution transformers

Table 5.8: Performance indicators for the individual approach

	Households				
	16	17	18	19	20
NGE (kWh / year)	94933.8	115796.1	136406.7	157029.1	177634.8
SSR	0.29	0.31	0.32	0.33	0.34
SCR	0.37	0.37	0.36	0.35	0.35

Table 5.9: Transformer aging for the individual approach

Households	Minimum Power (kVA)	Hot Spot Temperature (°C)	Aging (days/year)
16	141.23	47.91	0.02
17	139.27	47.91	0.02
18	137.29	47.91	0.02
19	135.28	47.91	0.02
20	133.26	47.91	0.02

with the individual approach, was determined using the standard energy price specified in Chapter 4.

Table 5.10: Energy bill for the community for the individual approach

Household	No PV (€)	Individual (€)
16	10 721.86	4 826.42
17	12 894.44	5 370.20
18	14 957.84	5 823.08
19	17 022.05	6 276.98
20	19 085.30	6 729.58

5.7.2 Individual with Storage

In this approach, since battery systems are present, the SSR and SCR were divided into the percentage of PV that is directly consumed by the household, $SSRLM$ and $SCRLM$, and the the percentage of PV that is consumed by discharging the battery later on, $Suff_{batt}$ and Con_{batt}. $SSRTotal$ and $SCRTotal$ are the total percentage of PV consumed by each

household. These values can be seen in Table 5.11.

Table 5.11: Performance indicators for the individual with storage approach

	Households				
	16	17	18	119	20
NGE (kWh / year)	12829.94	16098.00	19272.42	22437.44	25607.96
SSR LM	0.29	0.31	0.32	0.33	0.34
SCR LM	0.37	0.36	0.36	0.36	0.35
$Suff_{batt}$	0.32	0.35	0.37	0.4	0.41
Con_{batt}	0.39	0.41	0.42	0.43	0.44
SSR Total	0.61	0.66	0.69	0.73	0.75
SCR Total	0.76	0.77	0.78	0.79	0.79

Table 5.12 presents the values used to calculate the transformer aging and the respective transformer aging for each scenario.

Table 5.12: Transformer aging for the individual with storage approach

Households	Minimum Power (kVA)	Hot Spot Temperature (°C)	Aging (days/year)
16	145.73	47.91	0.02
17	144.67	47.91	0.02
18	143.59	47.91	0.02
19	142.58	47.91	0.02
20	141.56	47.91	0.02

As computed in the earlier approach, the electricity bill was determined using the standard electricity rate. It was assumed that charging and discharging had no monetary value, as the battery was considered to be owned by the household. Consequently, only grid electricity exchanges translated into charges resulting in the electricity bill shown in Table VI.2.

Table 5.13: Energy bill for the community for the individual with storage approach

Household	No PV (€)	Individual with Storage (€)
16	10 721.86	3 320.01
17	12 894.44	3 331.45
18	14 957.84	3 227.42
19	17 022.05	3 123.57
20	19 085.30	3 019.13

5.7.3 Energy Community

Similar to the previous approach, the SSR and SCR were subdivided into more detail. In this instance, $Suff_{P2P}$ and Con_{P2P} are referent to the PV generated energy that is exchanged between households. It's important to note that while individual households may exhibit SCR values greater than 1, the community as a whole can never surpass this threshold in this context. These values are presented in Table **??**.

Table 5.14: Performance indicators for the multiple energy communities approach

	Households									
	16		17		18		19		20	
	EC 1	EC 2	EC 1	EC 2	EC 1	EC 2	EC 1	EC 2	EC 1	EC 2
NGE (kWh / year)	66395.71	154596.69	77298.8	166095.86	87984.31	171200.42	99872.54	197773.17	111384.94	211521.37
SSR LM	0.16	0.21	0.17	0.20	0.17	0.20	0.20	0.20	0.19	0.21
SCR LM	0.34	0.49	0.38	0.49	0.35	0.50	0.34	0.49	0.36	0.50
$Suff_P2P$	0.16	0.20	0.15	0.09	0.17	0.10	0.16	0.11	0.17	0.09
Con_P2P	0.33	0.20	0.34	0.22	0.35	0.24	0.27	0.29	0.36	0.50
SSR Total	0.32	0.29	0.33	0.29	0.34	0.29	0.36	0.29	0.36	0.30
SCR Total	0.67	0.69	0.72	0.70	0.69	0.74	0.61	0.78	0.69	0.72

In this approach, both transformers were taken into account. Due to their varying levels of usage, the aging process resulted in different values, which are detailed in Table 5.15.

Table 5.15: Transformer aging for the energy community approach

	Minimum Power (KVA)		Hot Spot Temperature (°C)		Aging (days/year)	
Households	EC 1	EC 2	EC 1	EC 2	EC 1	EC 2
16	144.72	188.50	47.91	91.07	0.02	0.55
17	144.72	186.63	47.91	91.07	0.02	0.55
18	142.76	186.63	47.91	91.07	0.02	0.55
19	142.76	184.32	47.91	91.07	0.02	0.55
20	140.75	184.32	47.91	91.07	0.02	0.55

In contrast to the two preceding approaches, the electricity cost is not based on the standard rate but is determined by the community, dependent upon the PV generation ratio relative to consumption. Because the electricity price is community-specific, EC1 and EC2 feature distinct rates for the same time intervals. The outcomes are presented in Table VI.5.

Table 5.16: Energy bill for the community for the energy community approach

Household	No PV (€)		EC (€)	
	EC1	EC2	EC1	EC2
16	10 721.86	25 472.08	4 164.59	10 371.7
17	12 894.44	27 536.39	4 437.77	11 496.46
18	14 957.84	29 602.42	5 713.90	12 073.93
19	17 022.05	32 538.60	4 609.29	14 804.42
20	19085.30	35 329.02	6 071.66	14 606.11

5.7.4 Energy Community with Storage

This approach integrates the performance indicators discussed in the earlier approaches, enabling a distinction between three sources of PV utilization: direct consumption within the generating household, PV obtained through P2P transactions, and PV acquired via battery discharging. As in the previous scenario, individual households may exhibit SCR values greater than 1, as they draw on PV from multiple sources. These values are presented in Table 5.17

Table 5.17: Performance indicators for the energy community with storage approach

	Households				
	16	17	18	119	20
NGE (kWh / year)	38740.35	47967.7	51154.70	48714.63	49182.61657
SSR LM	0.16	0.17	0.17	0.21	0.17
SCR LM	0.34	0.38	0.35	0.36	0.36
$Suff_{P2P}$	0.11	0.11	0.14	0.13	0.14
Con_{P2P}	0.23	0.24	0.28	0.23	0.27
$Suff_{batt}$	0.20	0.17	0.18	0.24	0.18
Con_{batt}	0.41	0.38	0.37	0.41	0.30
SSR Total	0.47	0.45	0.49	0.58	0.49
SCR Total	0.98	1	1	1	0.93

As well as in the previous approach, both transformers are considered, independently, in the aging process. The calculations to define the power exchanged with the transformer are outlined in Chapter 4 and the results are available in Table 5.18.

Table 5.18: Transformer aging for the energy community with storage approach

Households	Minimum Power (kVA)	Hot Spot Temperature (°C)	Aging (days/year)
16	146.38	47.91	0.02
17	145.47	47.91	0.02
18	144.92	47.91	0.02
19	143.52	47.91	0.02
20	142.24	47.91	0.02

Similarly to the previous approach, the energy price is determined by the communities and their transactions. In this instance, it is important to note that both the charging and discharging of the battery are monetized. There is no difference in the pricing for charging and discharging and are the same as the electricity price in their time interval. The energy bill can be seen in Table 5.19.

Table 5.19: Energy bill for the community for the energy community with storage approach

Household	No PV (€)	EC with Storage (€)
16	10 721.86	3 378.37
17	12 894.44	3 605.97
18	14 957.84	3 920.51
19	17 022.05	3 910.46
20	19 085.30	4 531.61

5.7.5 Multiple Energy Communities

Similarly to how it was done in both energy community approaches, the SSR and SCR are differentiated based on whether the PV is used directly or exchanged through P2P transactions. It's worth noting that these indicators do not specify which energy

Table 5.20: Performance indicators for the multiple energy communities approach

	Households									
	16		17		18		19		20	
	EC 1	EC 2	EC 1	EC 2	EC 1	EC 2	EC 1	EC 2	EC 1	EC 2
NGE (kWh / year)	66395.71	154596.69	77298.8	166095.86	87984.31	171200.42	99872.54	197773.17	111384.94	211521.37
SSR LM	0.16	0.21	0.17	0.20	0.17	0.20	0.20	0.20	0.19	0.21
SCR LM	0.34	0.49	0.38	0.49	0.35	0.50	0.34	0.49	0.36	0.50
$Suf_{fp}2P$	0.16	0.20	0.15	0.09	0.17	0.10	0.16	0.11	0.17	0.09
Con_p2P	0.33	0.20	0.34	0.22	0.35	0.24	0.27	0.29	0.36	0.50
SSR Total	0.32	0.29	0.33	0.29	0.34	0.29	0.36	0.29	0.36	0.30
SCR Total	0.67	0.69	0.72	0.70	0.69	0.74	0.61	0.78	0.69	0.72

community engaged in the exchanges. However, this information can be inferred from the indicators in the energy community approach, given that the households considered are consistent in both cases. These indicators are seen in Table 5.20.

As detailed in Chapter 4, the additional power exchanged by each household with the transformer is computed based on a scenario where no PV generation occurs. This approach accounts for both surplus PV power that the transformer must purchase and the PV generated power that a household does not need to acquire from the transformer. With exchanges occurring between the communities, it's important to note that any surplus or deficit power is allocated to the transformer it would have originally been associated with. In other words, if a household from EC1 purchases PV-generated energy from a household in EC2, the power deficit is attributed to the transformer in EC1, as this transformer was initially responsible for supplying the required power.

Table 5.21: Transformer aging for the multiple energy communities approach

	Minimum Power (kVA)		Hot Spot Temperature (°C)		Aging (days/year)	
Households	EC 1	EC 2	EC 1	EC 2	EC 1	EC 2
16	142.38	190.84	47.91	91.07	0.02	0.55
17	142.38	188.97	47.91	91.07	0.02	0.55
18	140.52	188.87	47.91	91.07	0.02	0.55
19	140.52	186.56	47.91	91.07	0.02	0.55
20	148.24	183.73	47.91	91.07	0.02	0.55

Lastly, the energy bill was determined by using the electricity prices set by each community, with the selling community dictating the price. The results can be seen in Table 5.22.

Table 5.22: Energy bill for the community for the multiple energy communities approach

Household	No PV (€)		Multiple EC (€)	
	EC1	EC2	EC1	EC2
16	10 721.86	25 472.08	3 336.19	10 170.64
17	12 894.44	27 536.39	4 247.04	11 574.41
18	14 957.84	29 602.42	4 469.51	12 936.35
19	17 022.05	32 538.60	4 521.42	13 730.32
20	19085.30	35 329.02	6 350.35	14 135.82

5.8 Discussion

As anticipated, the individual approach yielded the least favorable outcomes concerning SSR and SCR. The absence of supporting systems, such as P2P trading or a storage system, results in a substantial percentage of unutilized PV generated power. The introduction of a battery system enables greater savings on the electrical bill, yet this advantage is offset by the considerable costs associated with the battery. On the other hand, the energy community with storage approach demonstrates superior performance indicators and achieves an electrical bill value comparable to that of the individual with storage approach.

The financial distinction between the EC approach and the EC with storage approach exhibits minimal variance, as the costs associated with charging and discharging the battery align with those of P2P trading. Consequently, neither approach emerges as superior when excluding the initial investment in the community battery. Nevertheless, as evident in the preceding sections, the required battery capacity for an individual household far exceeds that needed for a community. This disparity arises from the calculation of the community's battery capacity, which took into account the P2P trading dynamics.

Upon examining the multi-EC approaches, it becomes apparent that the maximum power capacity managed by the EC1 transformer has diminished in contrast to the EC method, while the maximum power capacity handled by the EC12 has increased. This shift is attributed to the occurrence of P2P exchanges at low voltage levels. Consequently, the transformer of the EC2 did not necessitate feeding all of the surplus power back into the grid.

The instances of repeated values in the EC transformer aging are observed when a household added from the preceding scenario is classified as a consumer rather than a prosumer. Given that a consumer household lacks power generation capability, there is no contribution of power fed back to the transformer. Consequently, the power input to the transformer remains constant in such cases. This suggests that adopting an EC approach is more advantageous than an individual one, given that the inclusion of consumer households positively influences the transformer.

Another crucial aspect not explicitly depicted in the presented results involves the distinction between the power fed into the grid and the power not drawn from the grid, in contrast to the no-PV approach. In this dissertation, the incorporation of both power fed back into the transformer and the power consumed by each household, whether from their own PV generation or that of their neighbors, is examined as deductions from the transformer power in the absence of PV. Consequently, the results do not allow for a clear differentiation between the two. It is noteworthy, however, that the power deducted from the transformer due to PV consumption cannot fall below zero, while the power fed into the grid can reach negative values. Hence, a reduction in power in the multi-EC approach compared to the EC approach does not signify an increase in power fed into the grid due to the P2P trading. Instead, it denotes a decrease in power drawn from the grid. This

differentiation serves to underscore the viability of both EC and batteries approaches.

Figure 5.7 and Figure 5.8 show the transformers available in the study case area and the amount of apartment buildings in each building. The area studied presented 7 transformers and a total of 1616 households. If an average of 230 houses per distribution transformer is considered, even in the worst-case scenario, it was observed a maximum load decrease of 16.74 kVA. Extrapolating this behavior to other houses would result in a maximum cumulative decrease of 193 kVA, which still remains well below the standard transformer capacity. This deduction is based on the optimal performance range of a transformer being within 1.5 times its rated power. In the specific instance of the EC1 transformer with a rated power of 500KVA, its critical operational range falls below -750KVA and above 750KVA. This suggests that ECs can be integrated seamlessly into this existing power infrastructure without overburdening transformers.

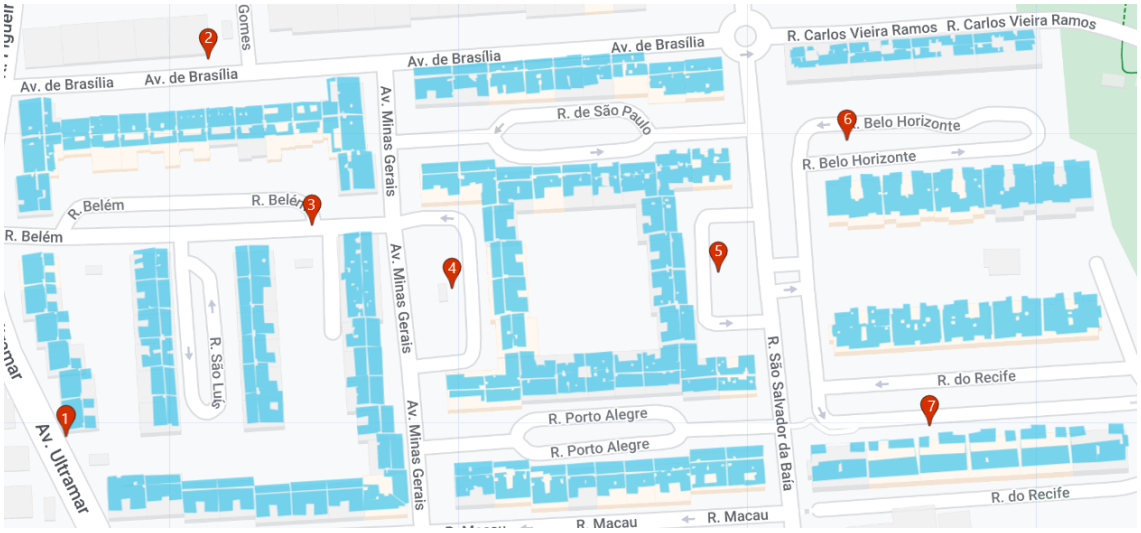

Figure 5.7: Transformer in the study case area

Figure 5.8: Apartment per buildings

6

Conclusions

In conclusion, the results confirm the expected advantages of ECs with storage in optimizing PV consumption. The individual approach, although valuable, consistently yielded lower values in comparison. This outcome underscores the effectiveness of ECs in harnessing surplus PV energy to benefit the entire community.

The utilization of the median day approach for battery dimensioning, in the individual with storage approach, while initially promising, has not yielded the anticipated results. This approach has the potential to lead to suboptimal battery usage and increased costs, particularly in the current market scenario where battery prices remain high. In instances where batteries were not optimally dimensioned, the SSR and SCR results, closely resembled those of the multiple ECs, highlighting the significance of precise battery dimensioning.

Energy community batteries prove to be a more lucrative option due to their lower capacity requirements to maintain a 20%-80% SOC and daily cycling, making them a cost-effective choice. Conversely, individual batteries do not exhibit the expected SCR levels, as they were initially calculated based on a median day. This deviation could be rooted in the fact that individual households have distinct daily energy consumption patterns, rendering the median day approach less effective compared to community scenarios. In the latter approach, the distinct energy usage patterns among individual households can sometimes offset each other making P2P trading and battery systems more viable. However, the individual-with-storage approach stands out by showcasing minimal fluctuations in the power supplied to the transformer, offering a stable and reliable solution.

One notable aspect of ECs is their high SCR. This is primarily attributed to houses without PV generation benefiting from the surplus PV energy generated by others within the community. This cooperative approach enhances overall energy efficiency.

Moreover, the study revealed that there is no significant negative impact on distribution transformers within these communities. Figure 5.7 and Figure 5.8 show the transformers available in the study case area and the amount of apartment buildings in each building.

Additionally, the analysis found that there was no significant difference in PV module

dimensioning between single family houses and apartment buildings. Both types of structures were capable of accommodating the necessary PV modules, though single-family houses typically required more due to their higher energy consumption. However, this increased investment in PV modules for houses with greater consumption resulted in more substantial savings on electricity bills. Due to the greater number of PV modules on single family houses, their influence becomes more pronounced when evaluating multi EC scenarios.

Comparing various approaches to manage energy costs, it becomes evident that the EC approach stands out as the most effective in reducing prices while factoring in battery expenses. Although the individual with storage approach may initially appear to have the lowest prices, the significant upfront investment required for batteries ultimately raises the overall cost. On the contrary, the EC approach optimizes battery usage within the community, spreading the expense more efficiently, resulting in a more cost effective energy solution for all community members.

In summary, ECs with storage offer an efficient and sustainable approach to optimizing PV consumption, with a high SCR and minimal impact on infrastructure. Whether in single family houses or apartment buildings, the benefits of PV adoption within ECs are evident, contributing to a greener and more cost-effective energy future.

Bibliography

[1] University, Harvard. *Commons-based Peer Production (CBPP)*. URL: https://rcc.harvard.edu/commons-based-peer-production (cit. on p. xvii).

[2] E. Commission. *Energy communities*. URL: https://energy.ec.europa.eu/topics/markets-and-consumers/energy-communities_en (cit. on p. xvii).

[3] *Decreto-Lei n.º 15/2022, de 14 de janeiro*. 2022-01. URL: https://dre.pt/dre/detalhe/decreto-lei/15-2022-177634016 (cit. on p. 1).

[4] *Low carbon green growth roadmap for Asia and the Pacific Fact Sheet - ESCAP*. URL: https://www.unescap.org/sites/default/files/14.%5C%20FS-Decentralized-energy-system.pdf (cit. on p. 1).

[5] D. Ritter, D. Bauknecht, and K. Kaya. *Recommendations for an ambitious EU-wide solar mandate*. 2022-10. URL: https://www.oeko.de/fileadmin/oekodoc/Policy_Brief_Oeko-Institut_EU-wide_Solar_Mandate.pdf (cit. on p. 2).

[6] *Lex - 32022R0720 - en - EUR-Lex*. 2022-05. URL: https://eur-lex.europa.eu/legal-content/EN/TXT/?uri=CELEX%3A32022R0720 (cit. on p. 2).

[7] T. Castillo-Calzadilla et al. "Feasibility and simulation of a solar photovoltaic installation in DC for standalone services buildings". In: *Dyna (Bilbao)* 93 (2017-12). DOI: 10.6036/8410 (cit. on p. 2).

[8] E. C. J. R. Centre. *Joint Research Centre*. URL: https://commission.europa.eu/about-european-commission/departments-and-executive-agencies/joint-research-centre_en (cit. on p. 2).

[9] E. Commission. *Solarpower Europe note on-site solar mandates across Europe*. URL: https://api.solarpowereurope.org/uploads/SPE_Note_Solar_Mandates_in_Europe_4103dcc90d.pdf (cit. on p. 2).

[10] J. Rosell and M. Ibáñez. "Modelling power output in photovoltaic modules for outdoor operating conditions". In: *Energy Conversion and Management* 47.15 (2006), pp. 2424–2430. ISSN: 0196-8904. DOI: https://doi.org/10.1016/j.enconman.20

05.11.004. URL: https://www.sciencedirect.com/science/article/pii/S0196890405003092 (cit. on pp. 5, 6).

[11] Y. Zhang et al. "A techno-economic sizing method for grid-connected household photovoltaic battery systems". In: *Applied Energy* 269 (2020), p. 115106. ISSN: 0306-2619. DOI: https://doi.org/10.1016/j.apenergy.2020.115106. URL: https://www.sciencedirect.com/science/article/pii/S0306261920306188 (cit. on p. 6).

[12] J. A. Kratochvil, W. E. Boyson, and D. L. King. "Photovoltaic array performance model." In: (2004-08). DOI: 10.2172/919131. URL: https://www.osti.gov/biblio/919131 (cit. on p. 6).

[13] M. Tahbaz. "Estimation of the Wind Speed in Urban Areas - Height less than 10 Metres". In: *International Journal of Ventilation* 8.1 (2009), pp. 75–84. DOI: 10.1080/14733315.2006.11683833. eprint: https://doi.org/10.1080/14733315.2006.11683833. URL: https://doi.org/10.1080/14733315.2006.11683833 (cit. on pp. 6, 7).

[14] A. Diehl. *Determining module inter-row spacing*. 2022-05. URL: https://www.greentechrenewables.com/article/determining-module-inter-row-spacing (cit. on p. 7).

[15] R. Aghamolaei et al. "A comprehensive energy-oriented approach for optimization of solar potential in urban contexts: an application study for residential districts". In: *Advances in Building Energy Research* 13.2 (2019), pp. 205–219. DOI: 10.1080/17512549.2018.1488613. URL: https://doi.org/10.1080/17512549.2018.1488613 (cit. on p. 8).

[16] A. Fleischhacker et al. "Sharing Solar PV and Energy Storage in Apartment Buildings: Resource Allocation and Pricing". In: *IEEE Transactions on Smart Grid* 10.4 (2019), pp. 3963–3973. DOI: 10.1109/TSG.2018.2844877 (cit. on pp. 8, 9).

[17] M. Alam, S. Ramchurn, and A. Rogers. *Cooperative energy exchange for the efficient use of energy and resources in remote communities*. 2013-05 (cit. on p. 8).

[18] Y. Fan, D. Papadaskalopoulos, and G. Strbac. *A game theoretic modeling framework for decentralized transmission planning*. 2016. DOI: 10.1109/PSCC.2016.7540990 (cit. on p. 8).

[19] V. M. Reijnders, M. D. van der Laan, and R. Dijkstra. "Chapter 6 - Energy communities: a Dutch case study". In: *Behind and Beyond the Meter*. Ed. by F. Sioshansi. Academic Press, 2020, pp. 137–155. ISBN: 978-0-12-819951-0. DOI: https://doi.org/10.1016/B978-0-12-819951-0.00006-2. URL: https://www.sciencedirect.com/science/article/pii/B9780128199510000062 (cit. on pp. 10, 12, 21).

[20] B. Fina, H. Auer, and W. Friedl. "Profitability of PV sharing in energy communities: Use cases for different settlement patterns". In: *Energy* 189 (2019), p. 116148. ISSN: 0360-5442. DOI: https://doi.org/10.1016/j.energy.2019.116148. URL: https://www.sciencedirect.com/science/article/pii/S0360544219318432 (cit. on pp. 11, 12).

[21] C. Giotitsas, A. Pazaitis, and V. Kostakis. "A peer-to-peer approach to energy production". In: *Technology in Society* 42 (2015), pp. 28–38. ISSN: 0160-791X. DOI: https://doi.org/10.1016/j.techsoc.2015.02.002. URL: https://www.sciencedirect.com/science/article/pii/S0160791X15000251 (cit. on pp. 12, 13).

[22] Y. Du et al. "A cooperative game approach for coordinating multi-microgrid operation within distribution systems". In: *Applied Energy* 222 (2018), pp. 383–395. ISSN: 0306-2619. DOI: https://doi.org/10.1016/j.apenergy.2018.03.086. URL: https://www.sciencedirect.com/science/article/pii/S0306261918304240 (cit. on pp. 13, 14).

[23] C. Long et al. "Peer-to-peer energy trading in a community microgrid". In: *2017 IEEE Power & Energy Society General Meeting*. 2017, pp. 1–5. DOI: 10.1109/PESGM.2017.8274546 (cit. on pp. 14–16, 18, 53).

[24] R. A. Lopes et al. "A case study on the impact of nearly Zero-Energy Buildings on distribution transformer aging". In: *Energy* 157 (2018), pp. 669–678. ISSN: 0360-5442. DOI: https://doi.org/10.1016/j.energy.2018.05.148. URL: https://www.sciencedirect.com/science/article/pii/S0360544218309824 (cit. on pp. 18, 62).

[25] A. Rosner. *Lights out for yeloha - why we shut down the Solar Sharing Network*. 2016-05. URL: https://www.linkedin.com/pulse/lights-out-yeloha-why-we-shut-down-solar-sharing-network-rosner/ (cit. on p. 20).

[26] L. J. Young. *Startup profile: Yeloha brings solar into the sharing economy*. 2021-07. URL: https://spectrum.ieee.org/startup-profile-yeloha-brings-solar-into-the-sharing-economy (cit. on p. 20).

[27] R. Martin. *Renewable energy trading launched in Germany*. 2020-04. URL: https://www.technologyreview.com/2015/12/29/164103/renewable-energy-trading-launched-in-germany/ (cit. on pp. 20, 21).

[28] C. Zhang et al. "Review of Existing Peer-to-Peer Energy Trading Projects". In: *Energy Procedia* 105 (2017). 8th International Conference on Applied Energy, ICAE2016, 8-11 October 2016, Beijing, China, pp. 2563–2568. ISSN: 1876-6102. DOI: https://doi.org/10.1016/j.egypro.2017.03.737. URL: https://www.sciencedirect.com/science/article/pii/S1876610217308007 (cit. on p. 20).

[29] B. Microgrid. *Community Powered Energy*. URL: https://www.brooklyn.energy/ (cit. on p. 20).

[30] Vandebron. *Duurzame Energie van Nederlandse Bodem*. URL: https://vandebron.nl/ (cit. on p. 21).

[31] G. heeten. *267 whitepaper v0.1 - gridflex*. URL: https://gridflex.nl/wp-content/uploads/2020/09/267-whitepaper-v0.2.pdf (cit. on p. 21).

[32] P. Energy. *Power ledger whitepaper*. 2019. URL: https://www.powerledger.io/company/power-ledger-whitepaper (cit. on p. 21).

[33] P. E. Cloud. *Peer Energy Cloud*. URL: https://software-cluster.org/projects/peer-energy-cloud/ (cit. on p. 21).

[34] *Energy-Communities-map*. URL: https://energy-communities-repository.ec.europa.eu/energy-communities/energy-communities-map_en (cit. on p. 21).

[35] *Sonnenkraftwerk Henstedt-Ulzburg*. URL: https://www.sonnenkraftwerk-hu.de/ (cit. on p. 21).

[36] *Comunidad energética solar de 650 KWP en Novo Milladoiro*. 2021-07. URL: https://vagalume-energia.es/referencia/comunidad-energetica-solar/ (cit. on p. 21).

[37] *"conjuguons l'énergie au pluriel !"* URL: https://lacitoyennesolaire.wixsite.com/monsite (cit. on p. 22).

[38] K. Eroe. *Comunità Energetica Rinnovabile di Tito*. 2021-05. URL: https://www.comunirinnovabili.it/comunita-energetica-rinnovabile-di-tito/ (cit. on p. 22).

[39] IRENA. *Battery storage for renewables: Market Status and Technology Outlook*. 2015-01. URL: https://www.irena.org/-/media/Irena/Files/REmap/IRENA_Battery_Storage_report_2015.pdf?rev=4c18a2e6ed244763a194afdb995eb3e1&hash=CB20025352DB5E616C7BFC86F85FE73E (cit. on p. 23).

[40] J. F. Manwell and J. G. McGowan. "Lead acid battery storage model for hybrid energy systems". In: *Solar Energy* 50.5 (1993), pp. 399–405. ISSN: 0038-092X. DOI: https://doi.org/10.1016/0038-092X(93)90060-2. URL: https://www.sciencedirect.com/science/article/pii/0038092X93900602 (cit. on p. 23).

[41] K. Sandhu and M. Aeidapu. "Optimal sizing of PV/wind/battery Hybrid Renewable Energy System Considering Demand Side Management". In: *International Journal on Electrical Engineering and Informatics* 10 (2018-03), pp. 79–93. DOI: 10.15676/ijeei.2018.10.1.6 (cit. on pp. 23–25).

[42] A. Lüth et al. "Local electricity market designs for peer-to-peer trading: The role of battery flexibility". In: *Applied Energy* 229 (2018), pp. 1233–1243. ISSN: 0306-2619. DOI: https://doi.org/10.1016/j.apenergy.2018.08.004. URL: https://www.sciencedirect.com/science/article/pii/S0306261918311590 (cit. on pp. 25, 26).

[43] E. Barbour et al. "Community energy storage: A smart choice for the smart grid?" In: *Applied Energy* 212 (2018), pp. 489–497. ISSN: 0306-2619. DOI: https://doi.org/10.1016/j.apenergy.2017.12.056. URL: https://www.sciencedirect.com/science/article/pii/S0306261917317713 (cit. on pp. 26–29).

[44] J. Liu et al. "Energy planning of renewable applications in high-rise residential buildings integrating battery and hydrogen vehicle storage". In: *Applied Energy* 281 (2021), p. 116038. ISSN: 0306-2619. DOI: https://doi.org/10.1016/j.apenergy.2020.116038. URL: https://www.sciencedirect.com/science/article/pii/S0306261920314756 (cit. on p. 29).

[45] C. Liu et al. "Analysis and optimization of load matching in photovoltaic systems for zero energy buildings in different climate zones of China". In: *Journal of Cleaner Production* 238 (2019), p. 117914. ISSN: 0959-6526. DOI: https://doi.org/10.1016/j.jclepro.2019.117914. URL: https://www.sciencedirect.com/science/article/pii/S0959652619327842 (cit. on p. 29).

[46] E-redes. URL: https://balcaodigital.e-redes.pt/login (cit. on pp. 31, 64).

[47] 2016-01. URL: https://re.jrc.ec.europa.eu/pvg_tools/en/ (cit. on pp. 32, 54, 55).

[48] J. M. Branco et al. *Experimental analysis of original and strengthened traditional timber connections*. 1970-01. URL: https://hdl.handle.net/1822/6990 (cit. on p. 32).

[49] C. E. C. California Energy Commission. *Solar Equipment lists*. URL: https://www.energy.ca.gov/programs-and-topics/programs/solar-equipment-lists (cit. on pp. 32, 42, 51, 57).

[50] R. Lindsey and L. Dahlman. *Climate change: Global temperature*. 2023-01. URL: https://www.climate.gov/news-features/understanding-climate/climate-change-global-temperature#:~:text=Earth%E2%80%99s%5C%20temperature%5C%20has%5C%20risen%5C%20by,0.18%5C%C2%5C%B0%5C%20C)%5C%20per%5C%20decade. (cit. on p. 38).

[51] N. C. Enviromental. *Annual 2022 global climate report*. 2023-01. URL: https://www.ncei.noaa.gov/access/monitoring/monthly-report/global/202213 (cit. on p. 38).

[52] URL: https://earthengine.google.com/ (cit. on pp. 38, 54).

[53] G. Earth. URL: https://earth.google.com/web/@0,-1.1013,0a,22251752.77375655d,35y,0h,0t,0r (cit. on pp. 39, 54).

[54] A. d. ICM. *How to calculate the electrical resistance of a Wire*. 2017-02. URL: https://www.icmesp.com/en/calcular-la-resistencia-electrica-cable/ (cit. on p. 43).

[55] G. S. University. *Table of Resistivity*. URL: http://hyperphysics.phy-astr.gsu.edu/hbase/Tables/rstiv.html (cit. on p. 44).

[56] ERSE. *Preços de Energia*. URL: https://www.erse.pt/simuladores/precos-de-energia/ (cit. on pp. 45, 46).

[57] E. Energia. *Tarifas*. URL: https://ezu.pt/tarifas (cit. on p. 45).

[58] J. Jiang et al. "Optimized Operating Range for Large-Format LiFePO4/Graphite Batteries". In: *Journal of The Electrochemical Society* 161 (2013-12), A336–A341. DOI: 10.1149/2.052403jes (cit. on p. 49).

[59] E-REDES. *Secondary Substations*. 2022-12. URL: https://e-redes.opendatasoft.com/explore/dataset/postos-transformacao-distribuicao/api/ (cit. on p. 58).

I

Flowcharts of market behaviour in EC with and without a battery system

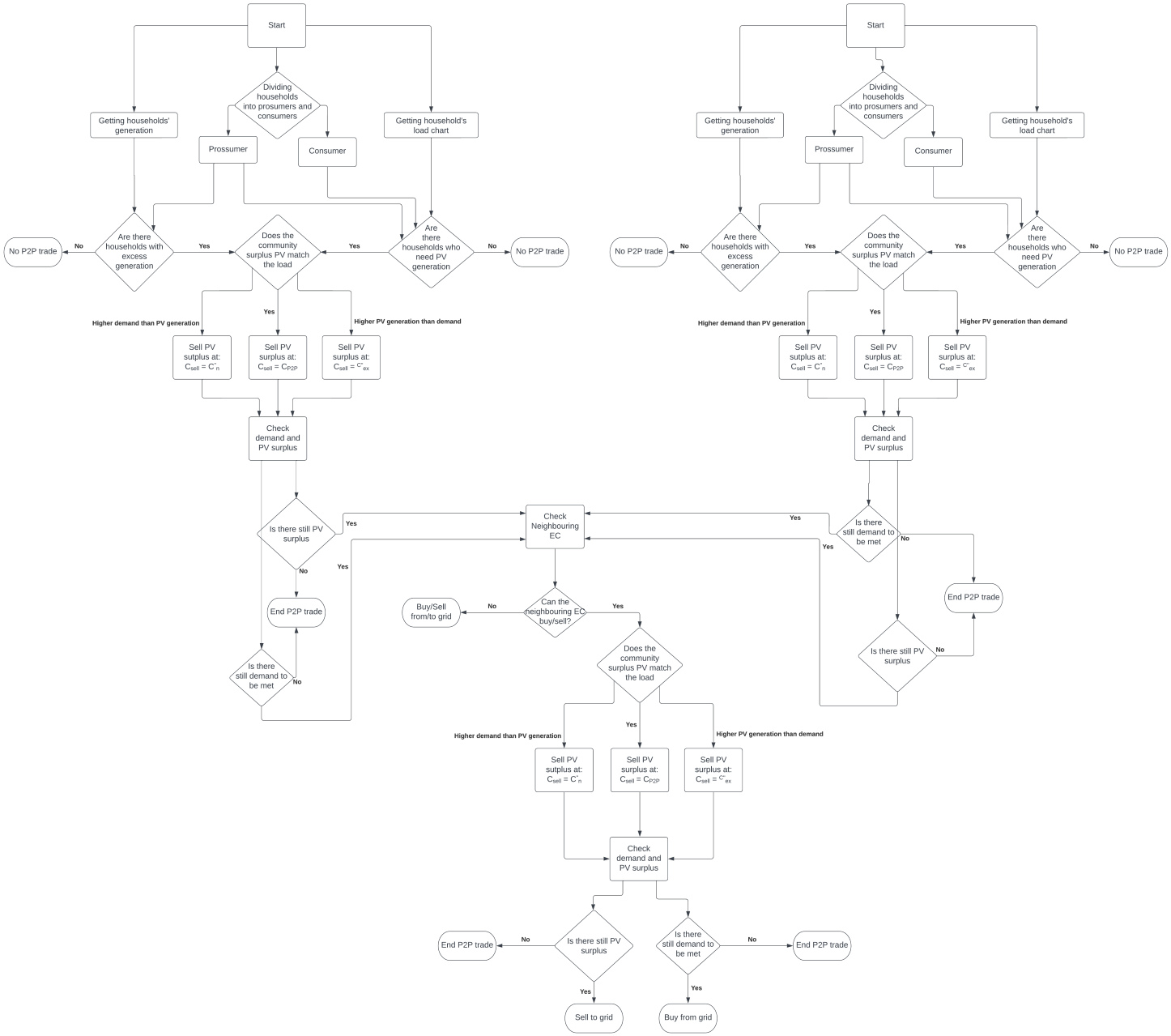

Figure I.1: Flowchart describing the process of P2P markets in a case with 2 EC's without a battery system.

II

Monthly consumption comparison

Table II.1: Relation between all months

	Relation (%)											
	Jan	Feb	Mar	Apr	May	Jun	Jul	Aug	Sep	Oct	Nov	Dec
Jan	100	97	117	114	122	119	104	103	114	135	124	88
Feb	103	100	120	117	126	122	107	106	117	139	127	90
Mar	85	83	100	98	104	102	89	88	97	116	106	75
Apr	88	85	102	100	107	104	91	90	100	118	108	77
May	82	80	96	93	100	98	85	84	93	111	101	72
Jun	84	82	98	96	103	100	87	86	95	113	104	74
Jul	96	93	112	109	117	114	100	99	109	130	119	84
Aug	97	94	114	111	119	116	101	100	110	131	120	85
Sep	88	86	103	100	107	105	92	91	100	119	109	77
Oct	74	72	87	84	90	88	77	76	84	100	92	65
Nov	81	79	95	92	99	96	84	83	92	109	100	71
Dec	114	111	133	130	139	136	119	117	130	154	141	100

III

Yearly Household Consumption

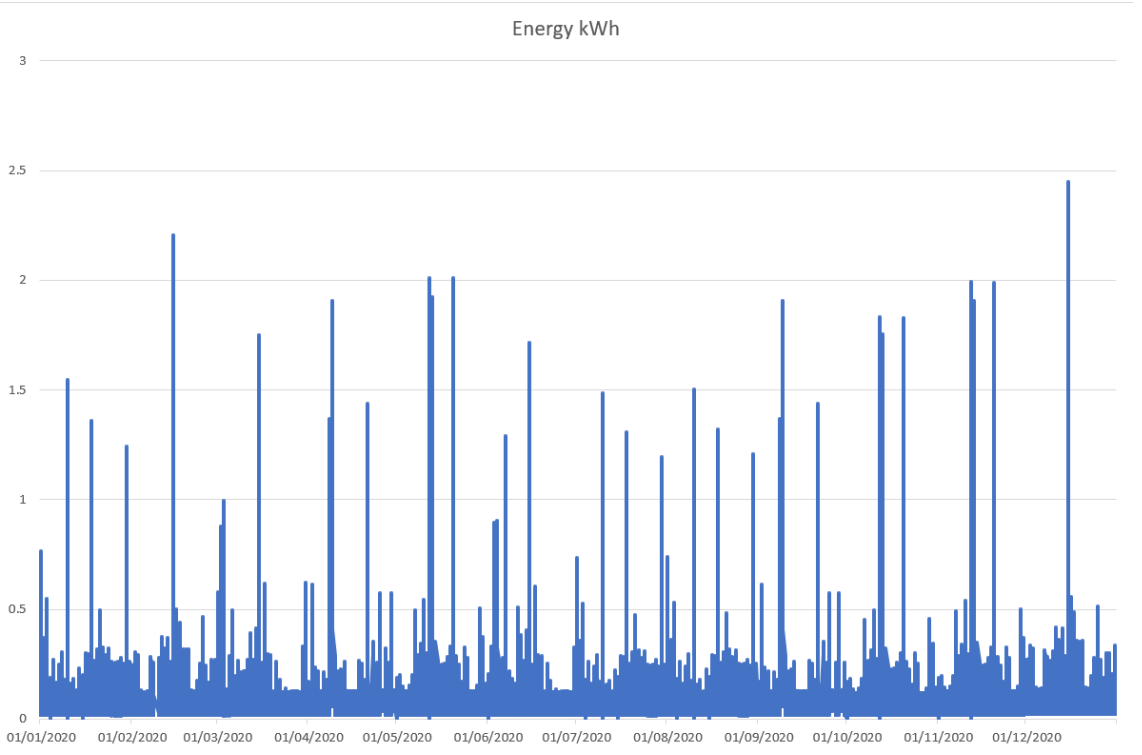

Figure III.1: Yearly consumption for household 1

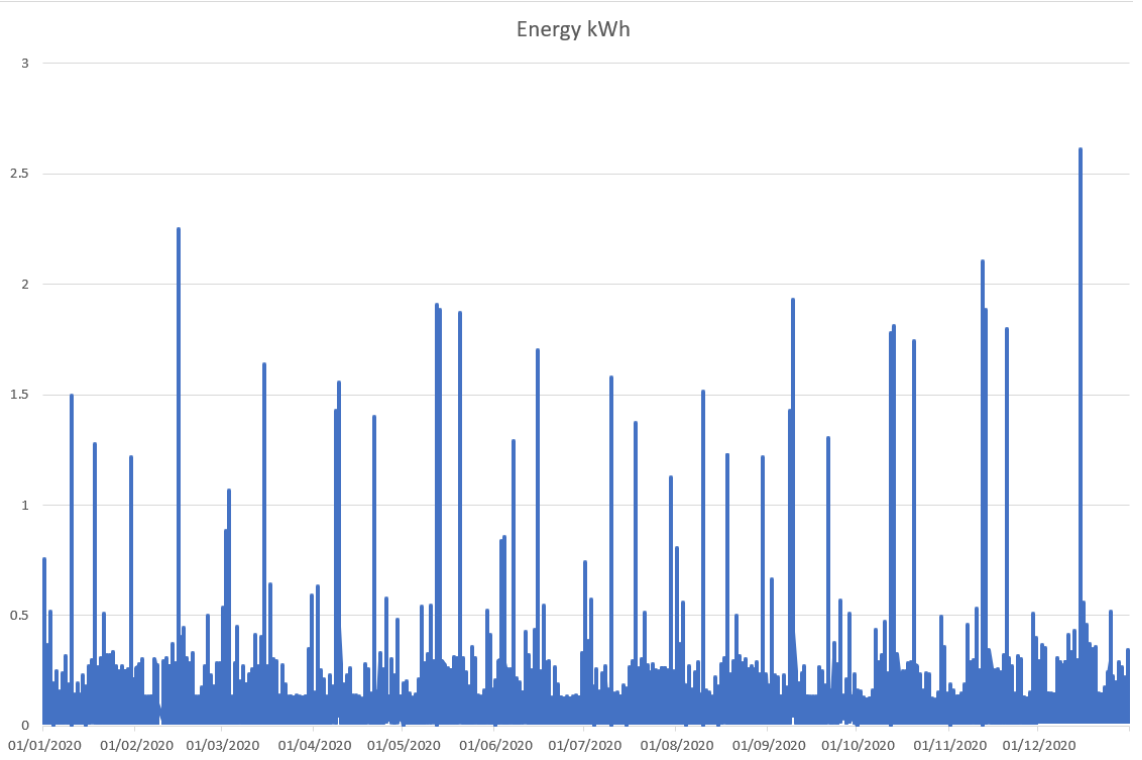

Figure III.2: Yearly consumption for household

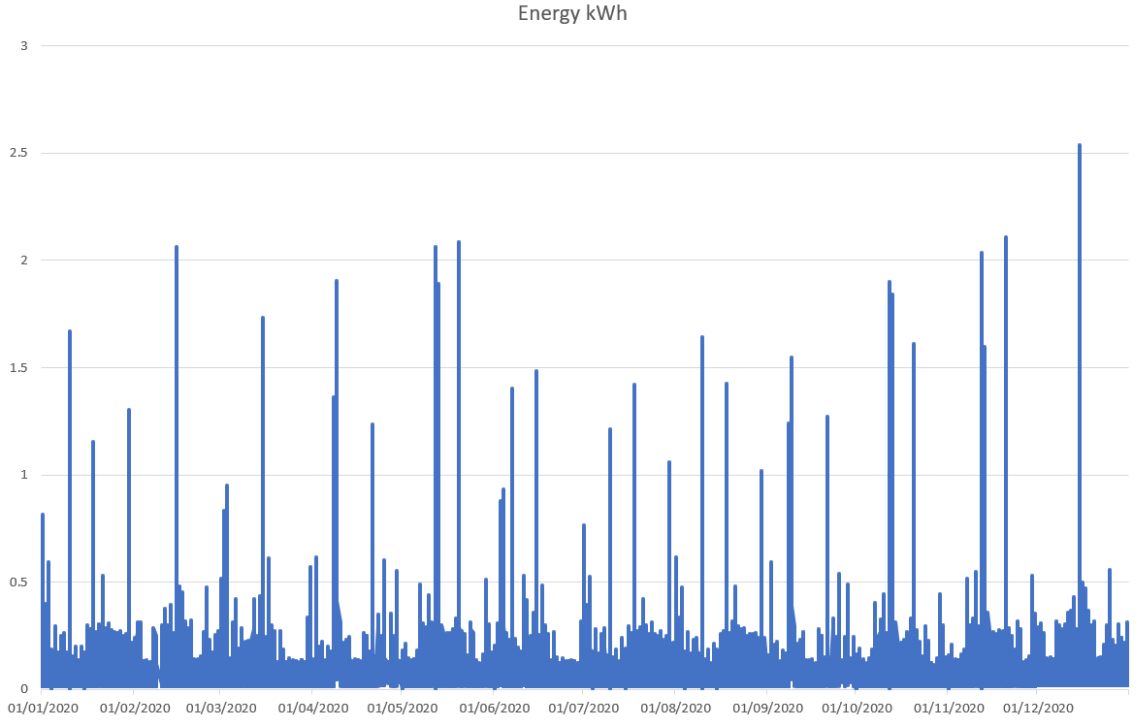

Figure III.3: Yearly consumption for household 3

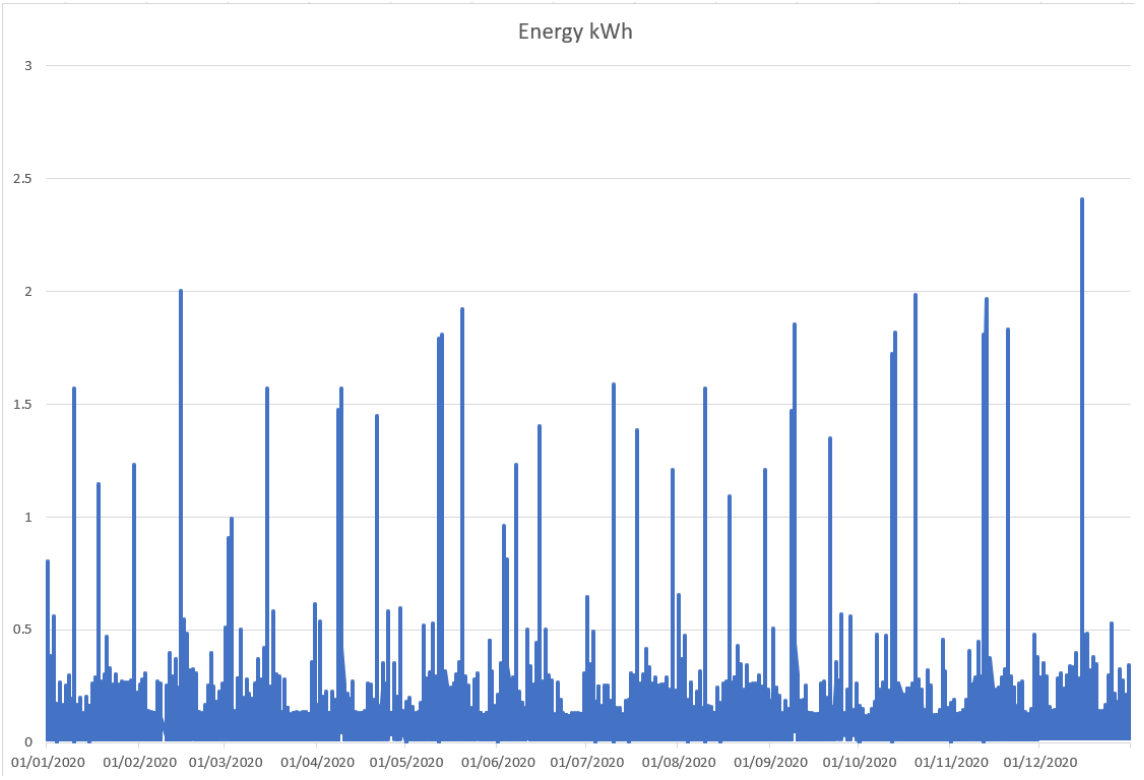

Figure III.4: Yearly consumption for household 2

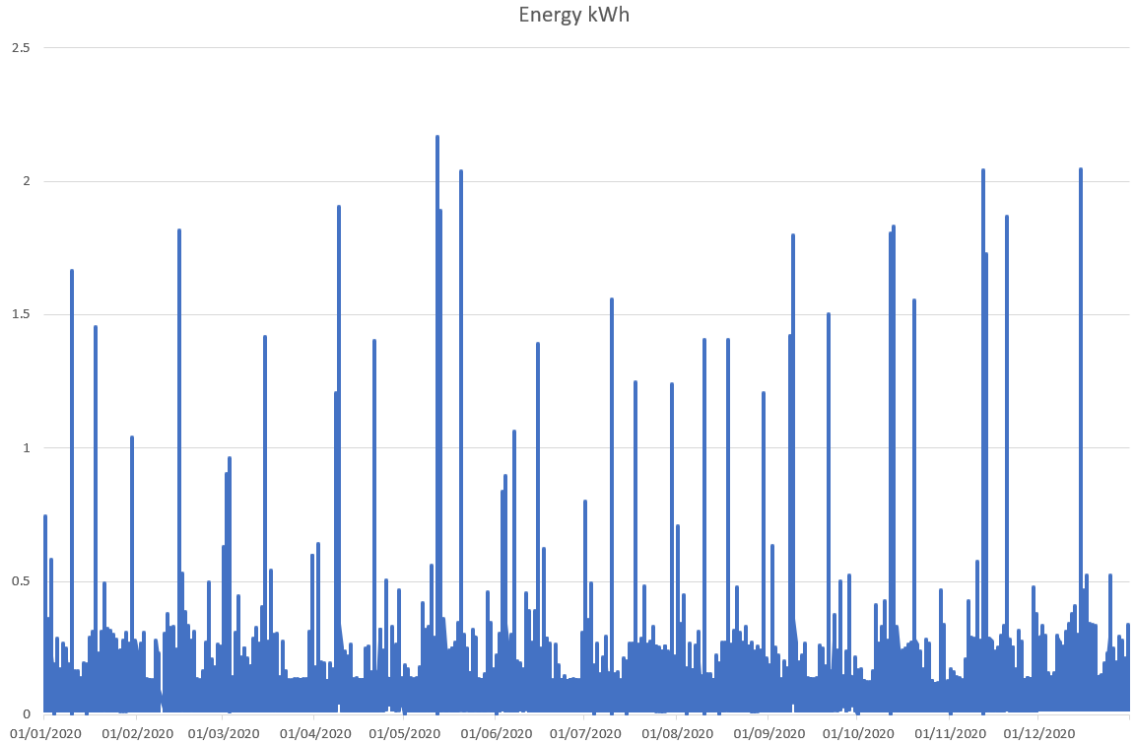

Figure III.5: Yearly consumption for household 2

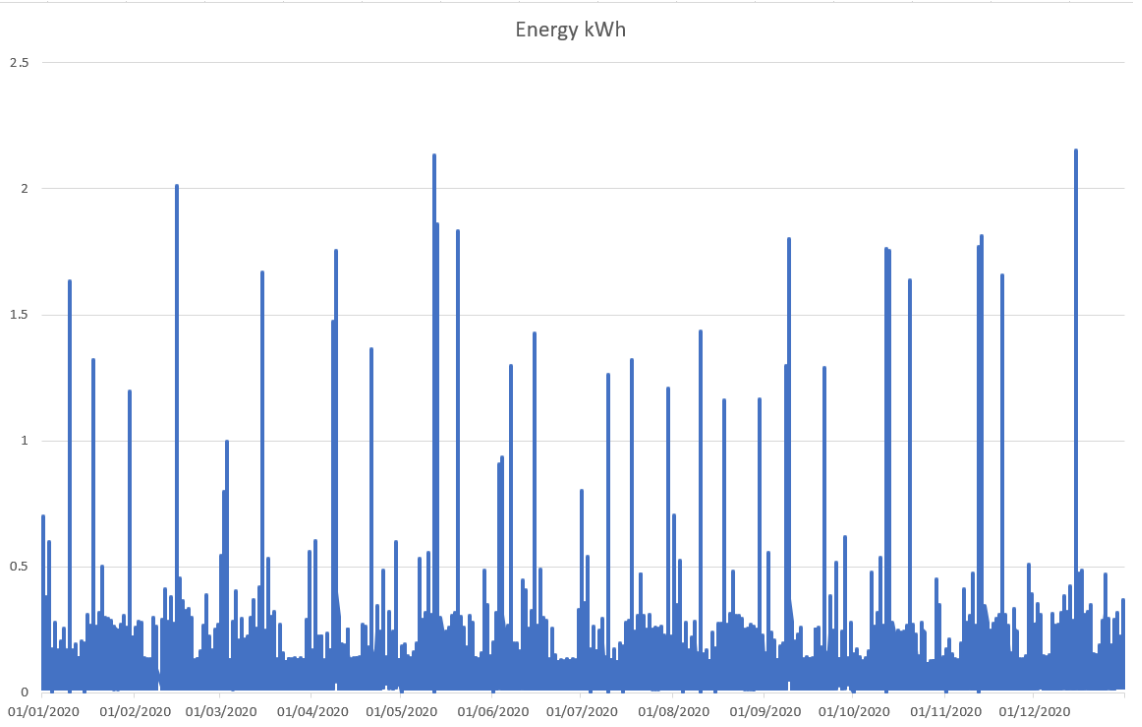

Figure III.6: Yearly consumption for household 2

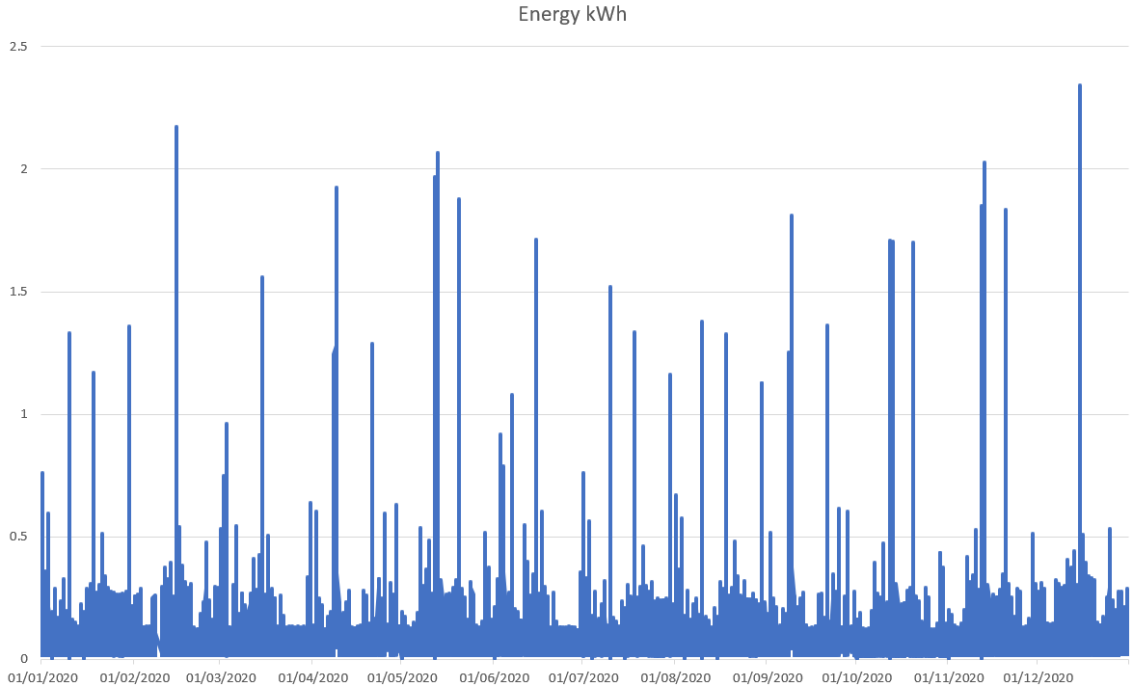

Figure III.7: Yearly consumption for household 1

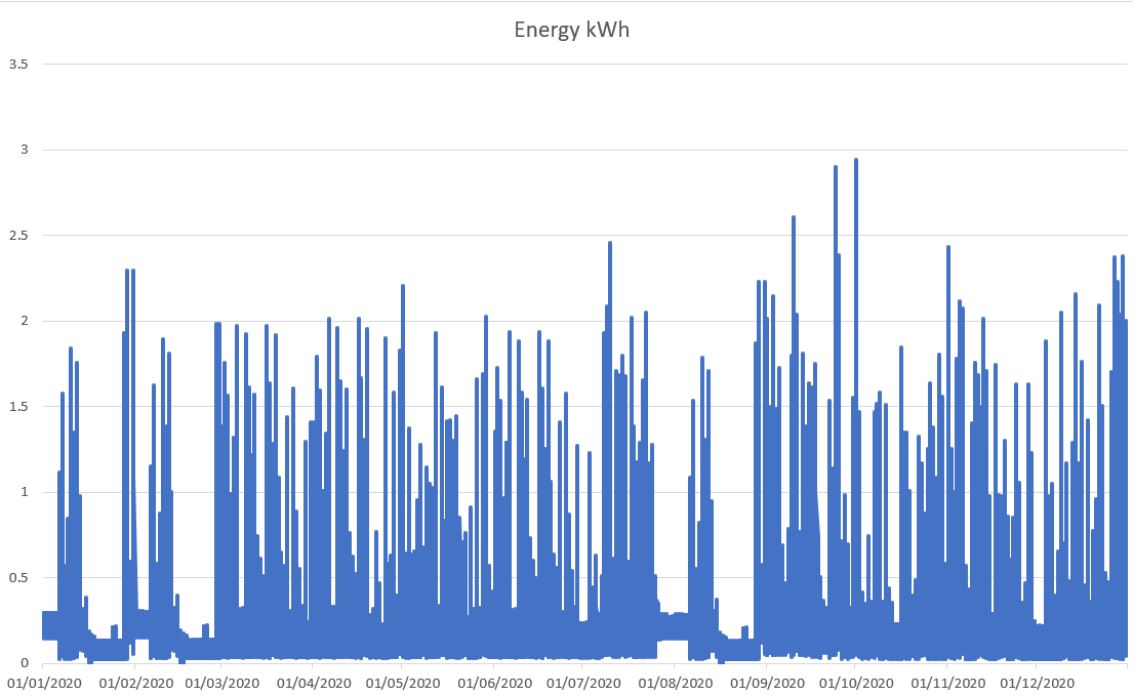

Figure III.8: Yearly consumption for household 1

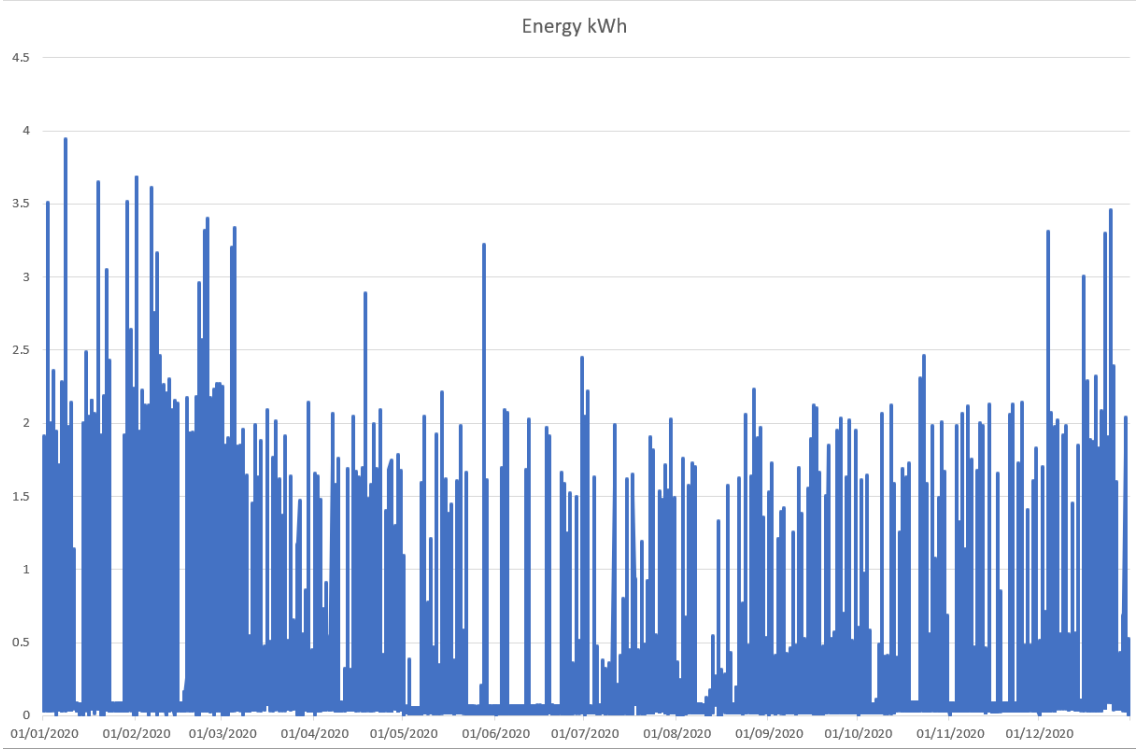

Figure III.9: Yearly consumption for household 1

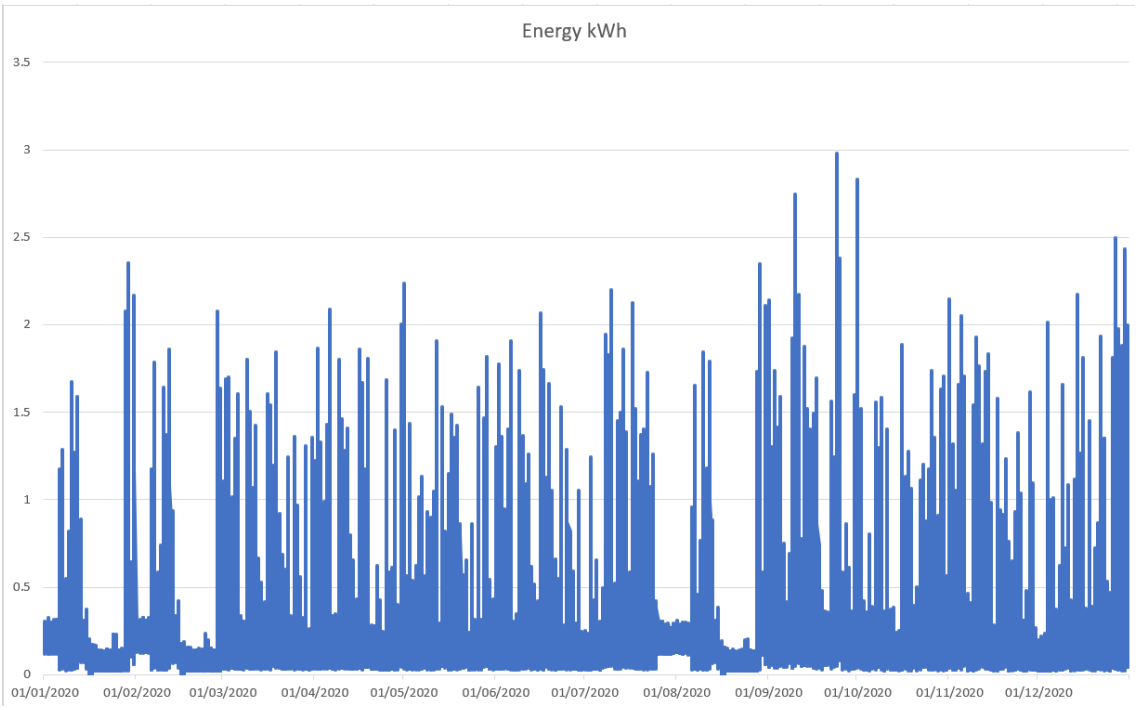

Figure III.10: Yearly consumption for household 1

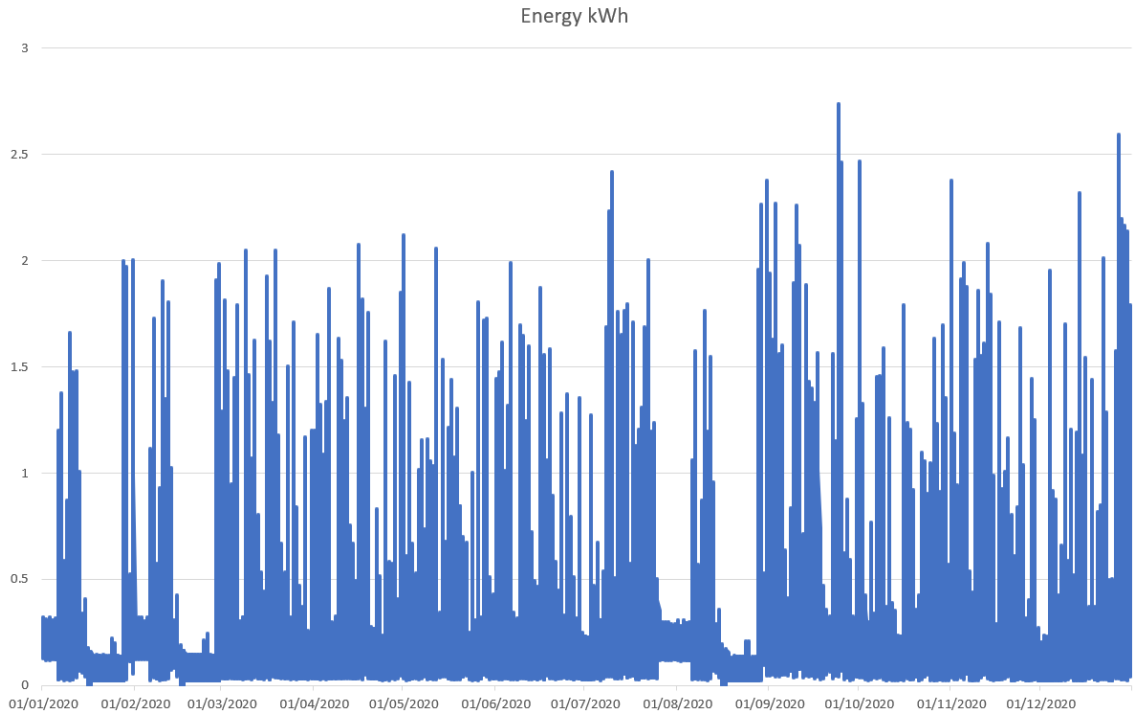

Figure III.11: Yearly consumption for household 1

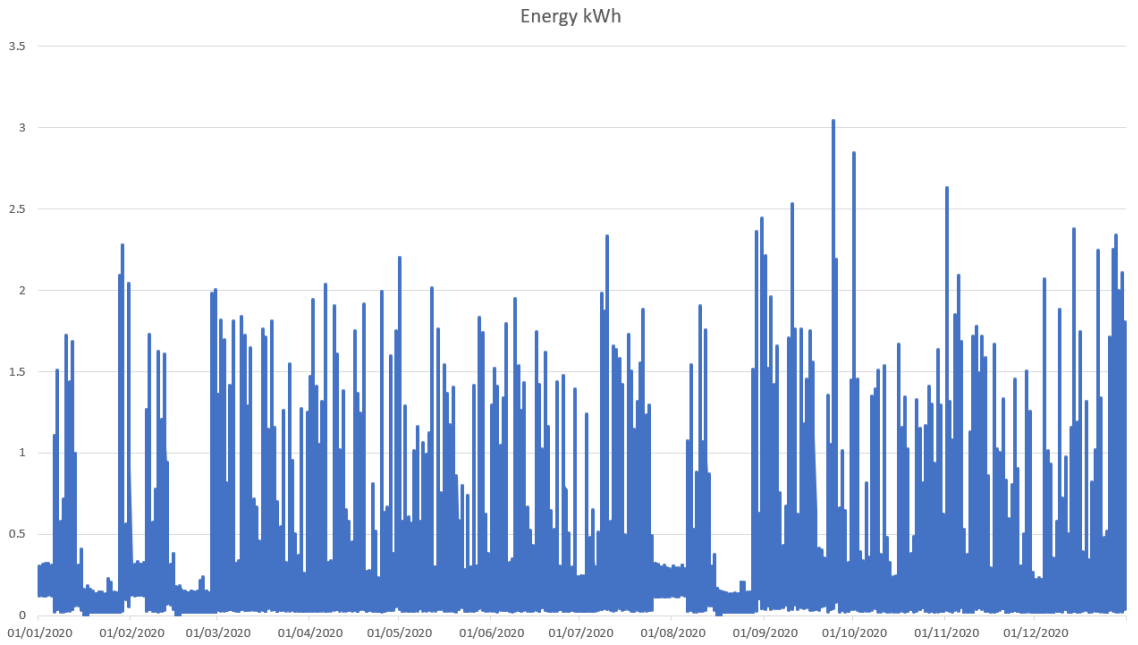

Figure III.12: Yearly consumption for household 1

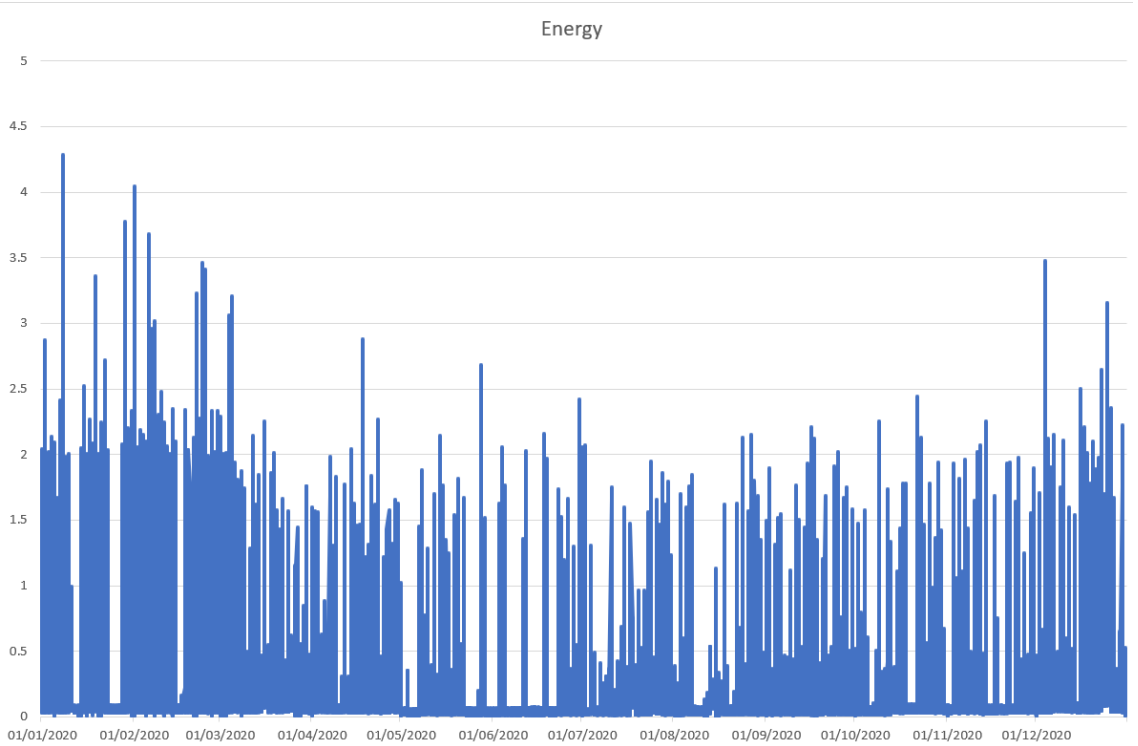

Figure III.13: Yearly consumption for household 1

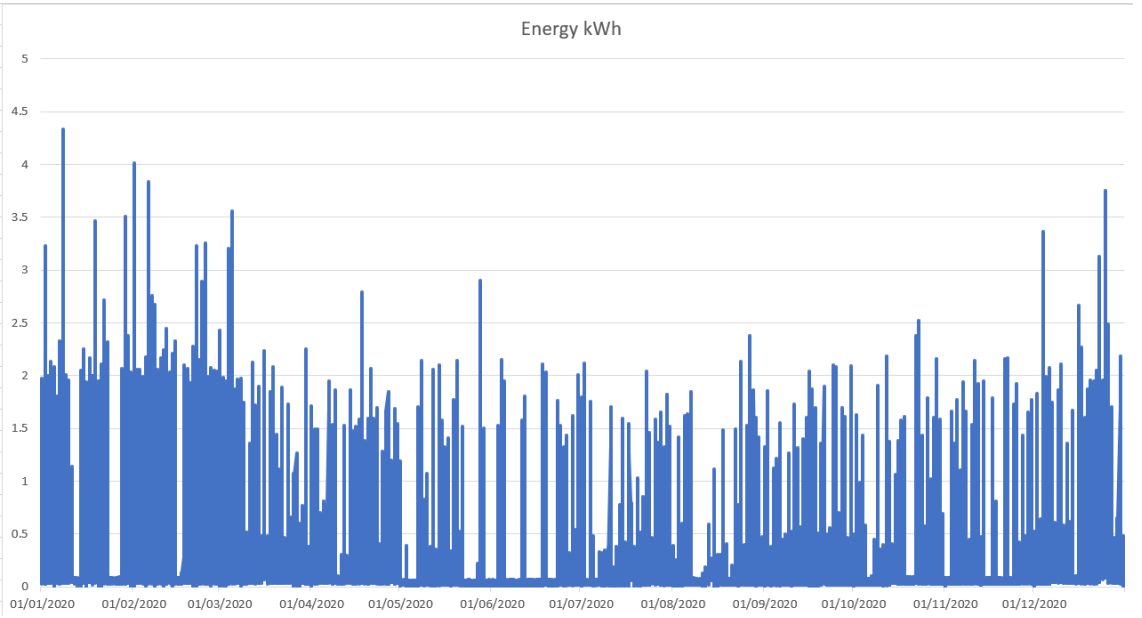

Figure III.14: Yearly consumption for household 1

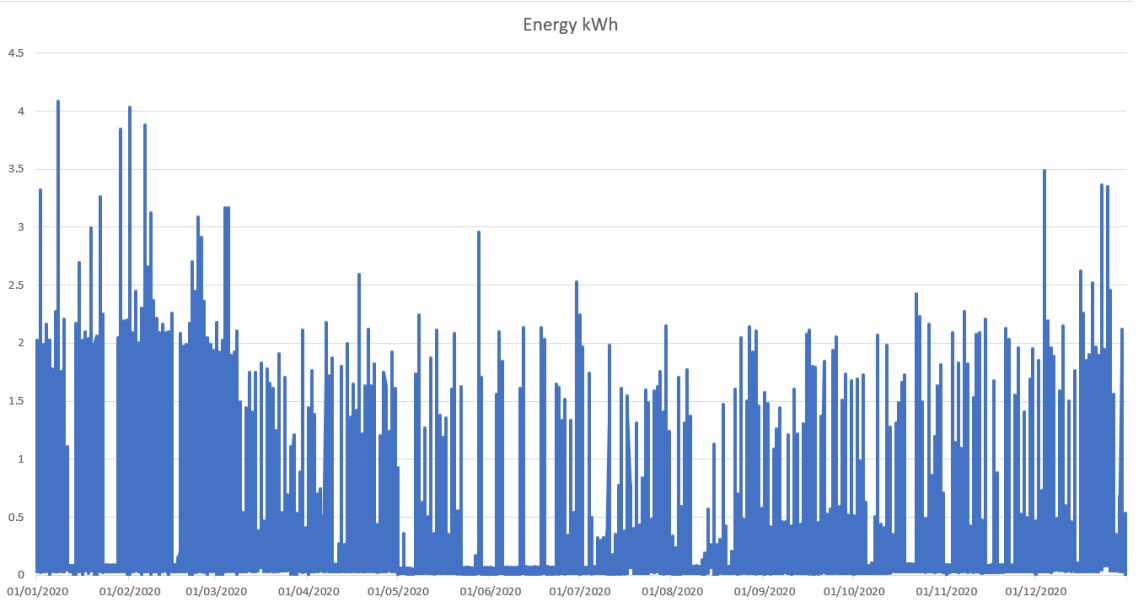

Figure III.15: Yearly consumption for household 1

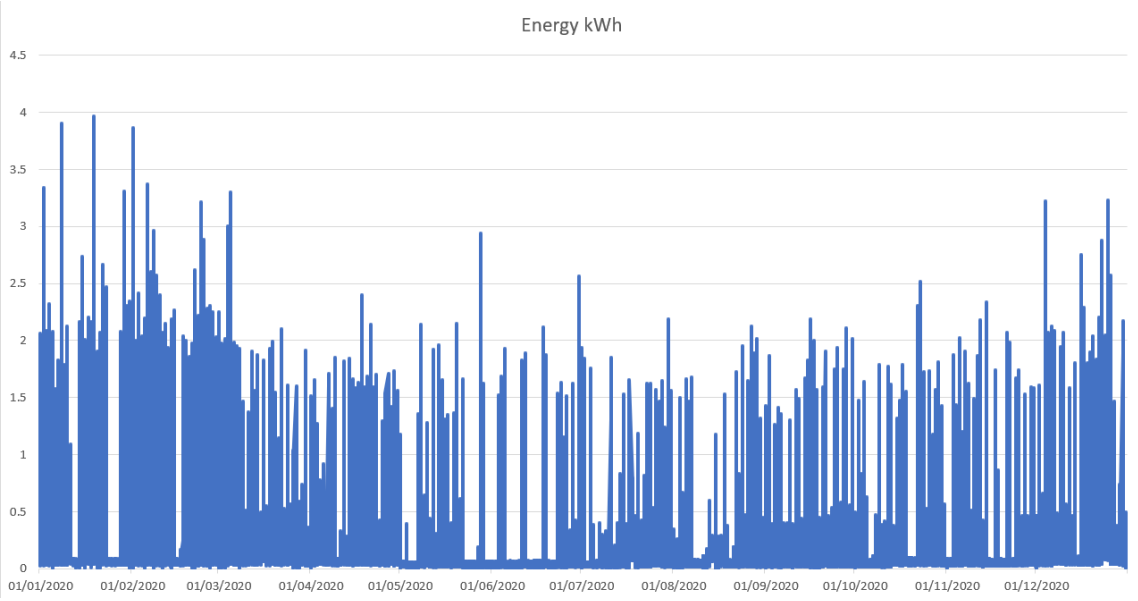

Figure III.16: Yearly consumption for household 1

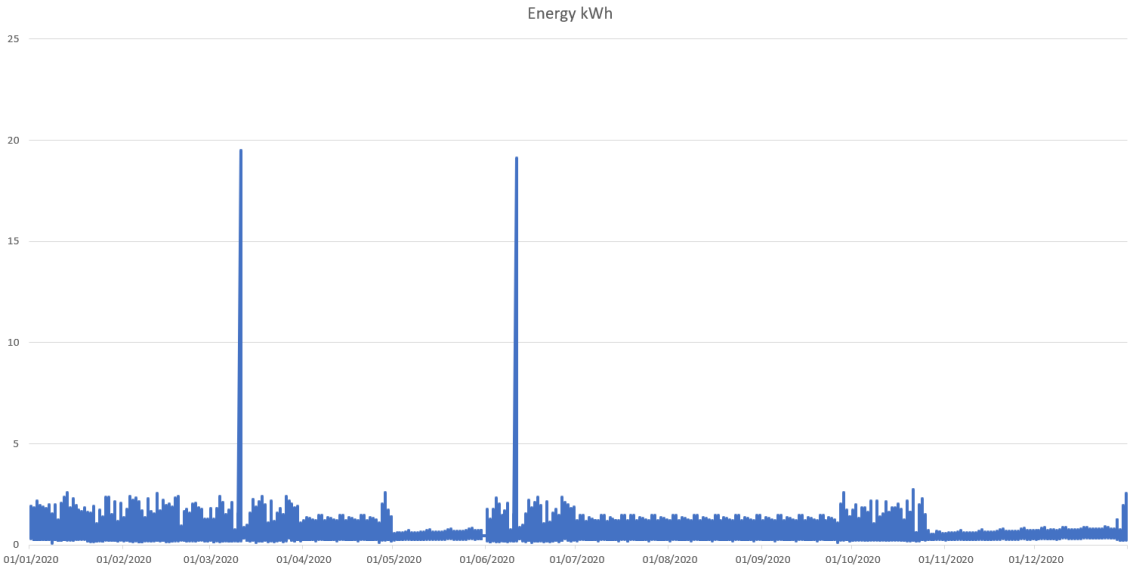

Figure III.17: Yearly consumption for household 1

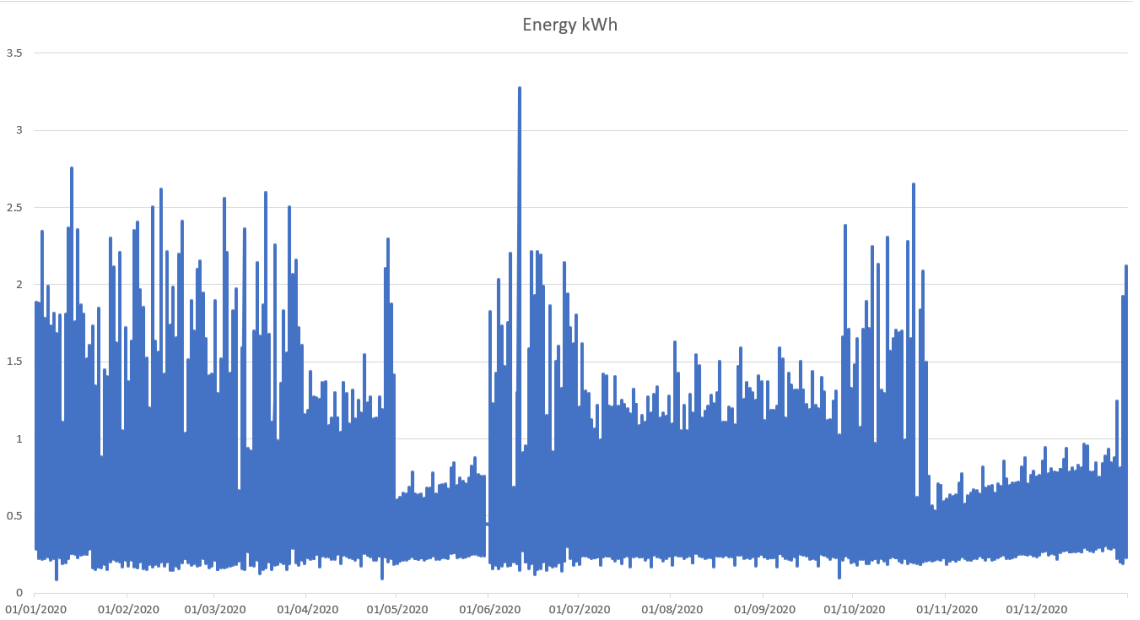

Figure III.18: Yearly consumption for household 1

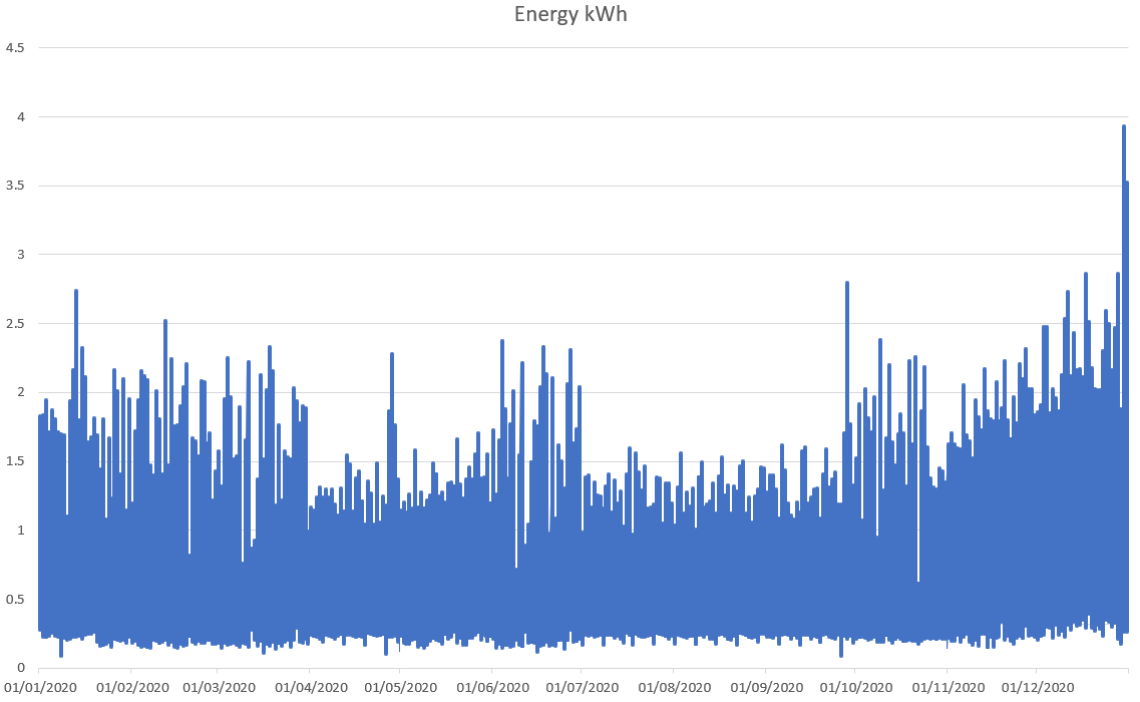

Figure III.19: Yearly consumption for household 1

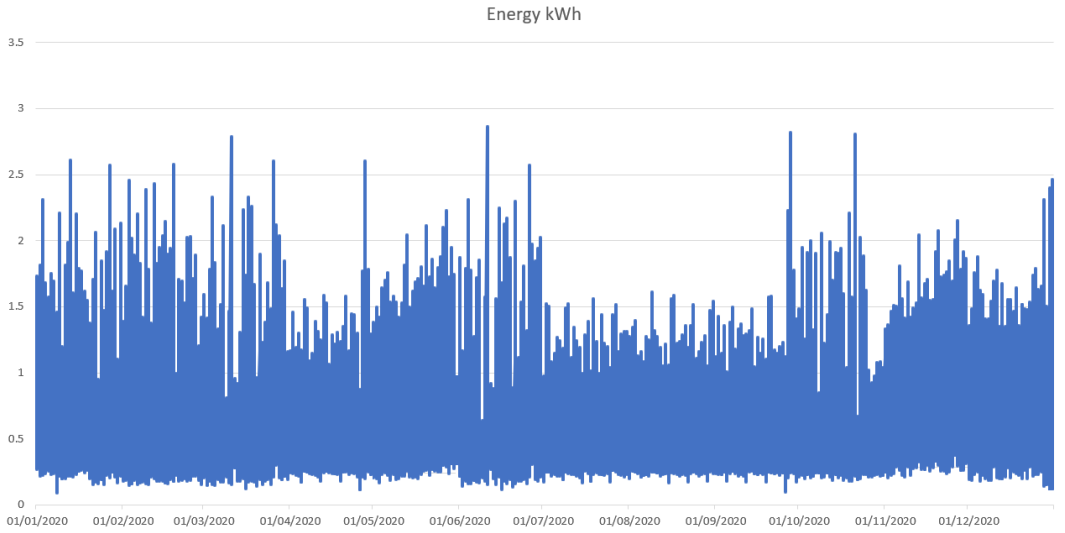

Figure III.20: Yearly consumption for household 1

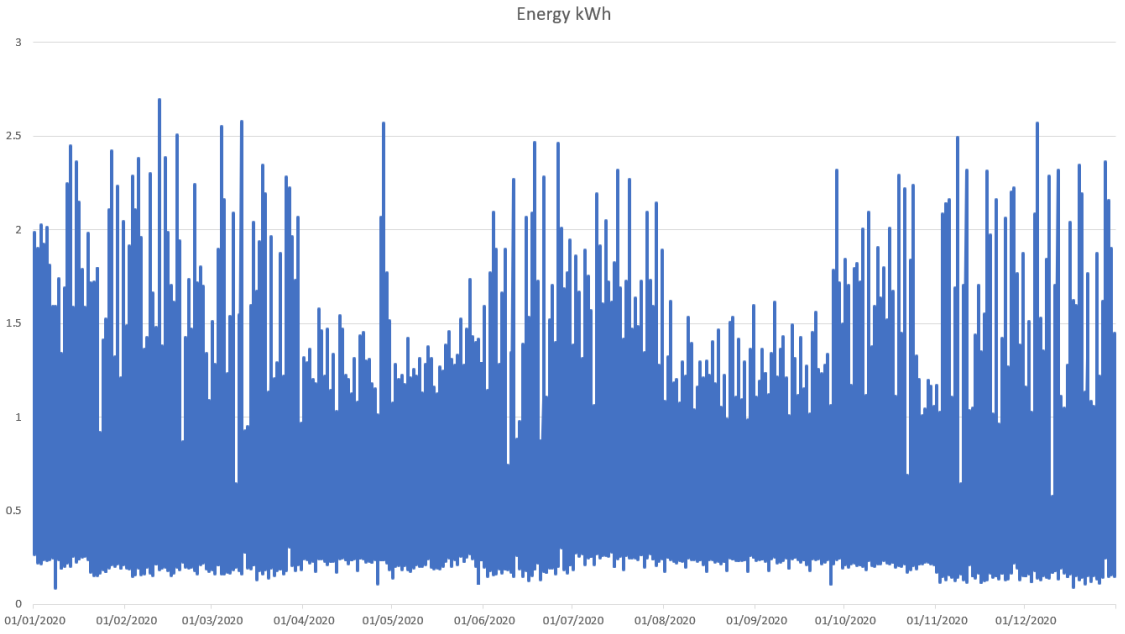

Figure III.21: Yearly consumption for household 1

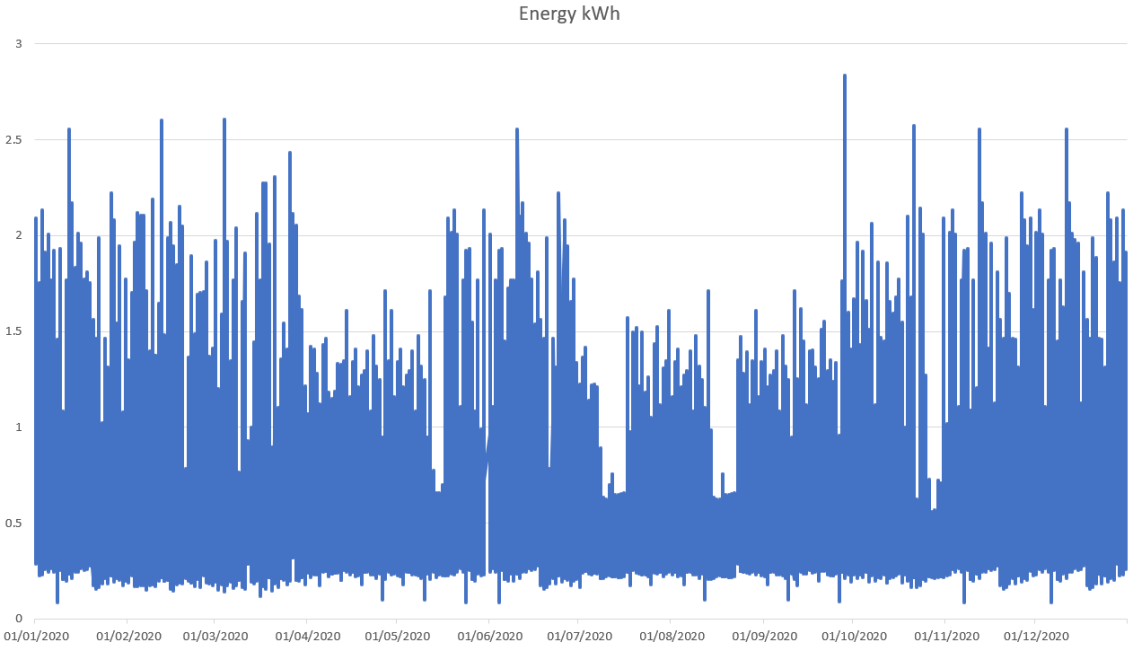

Figure III.22: Yearly consumption for household 1

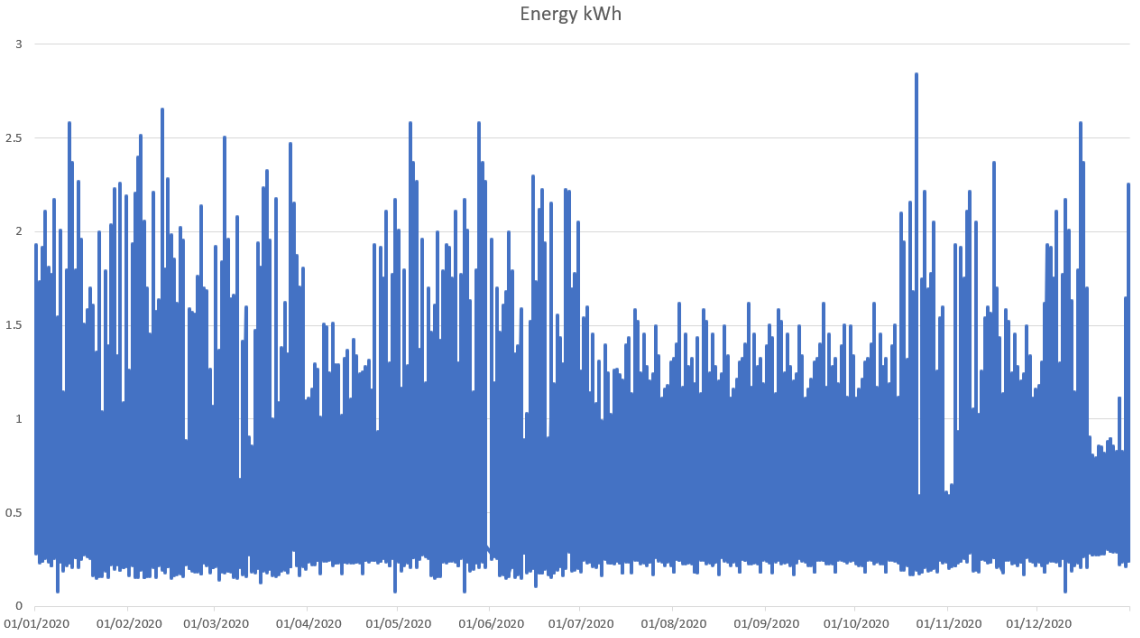

Figure III.23: Yearly consumption for household 1

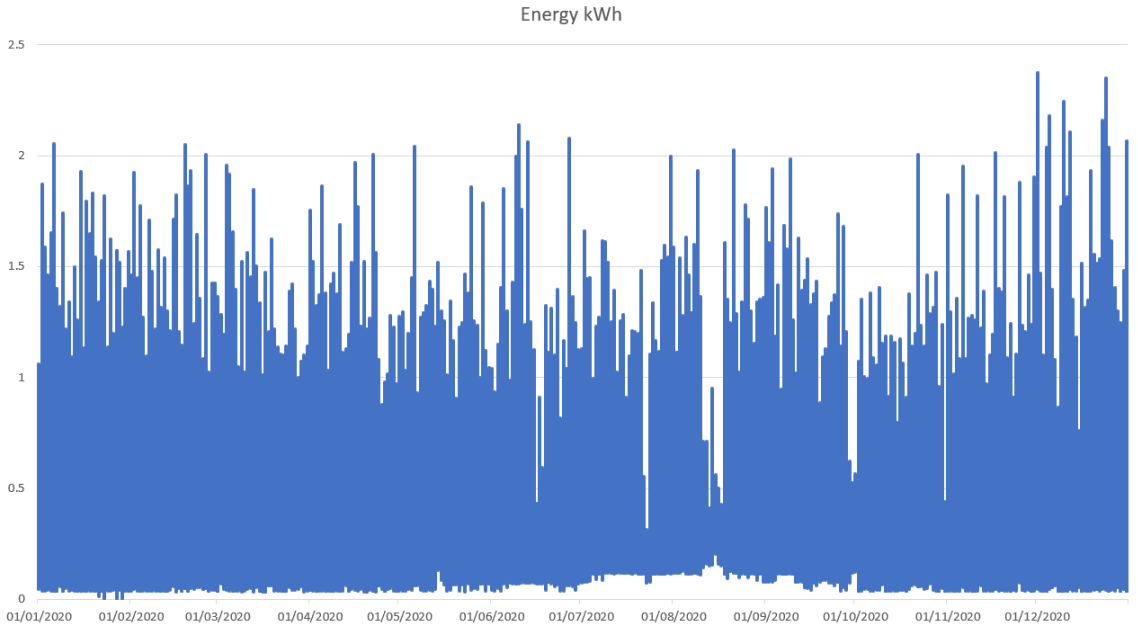

Figure III.24: Yearly consumption for household 1

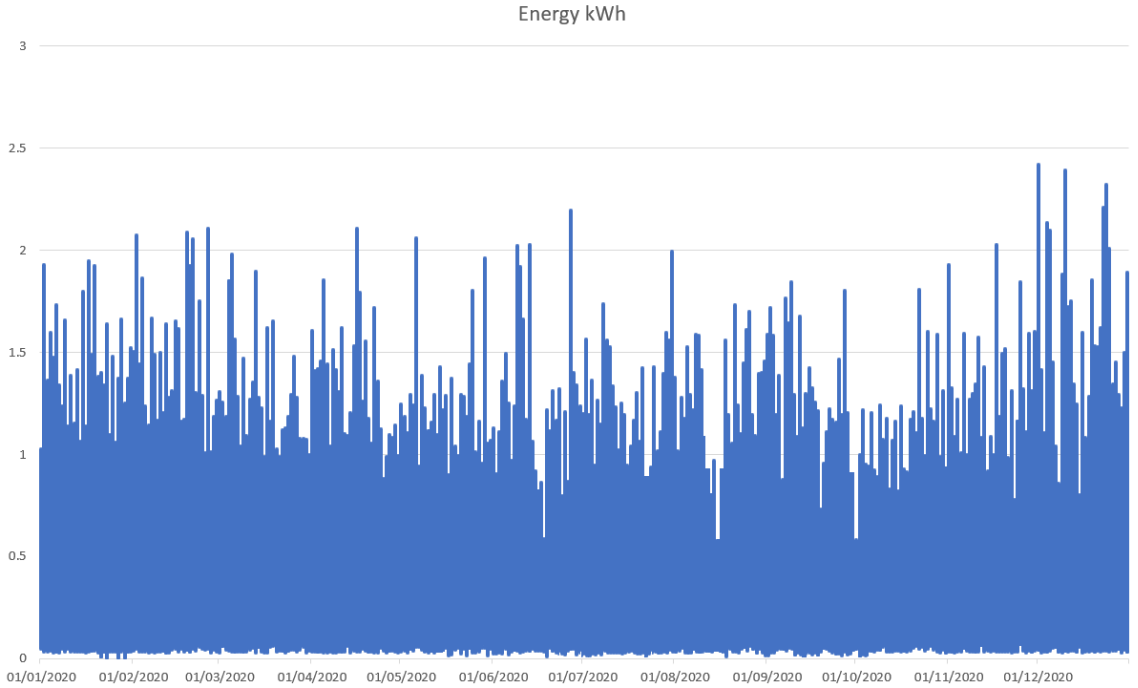

Figure III.25: Yearly consumption for household 1

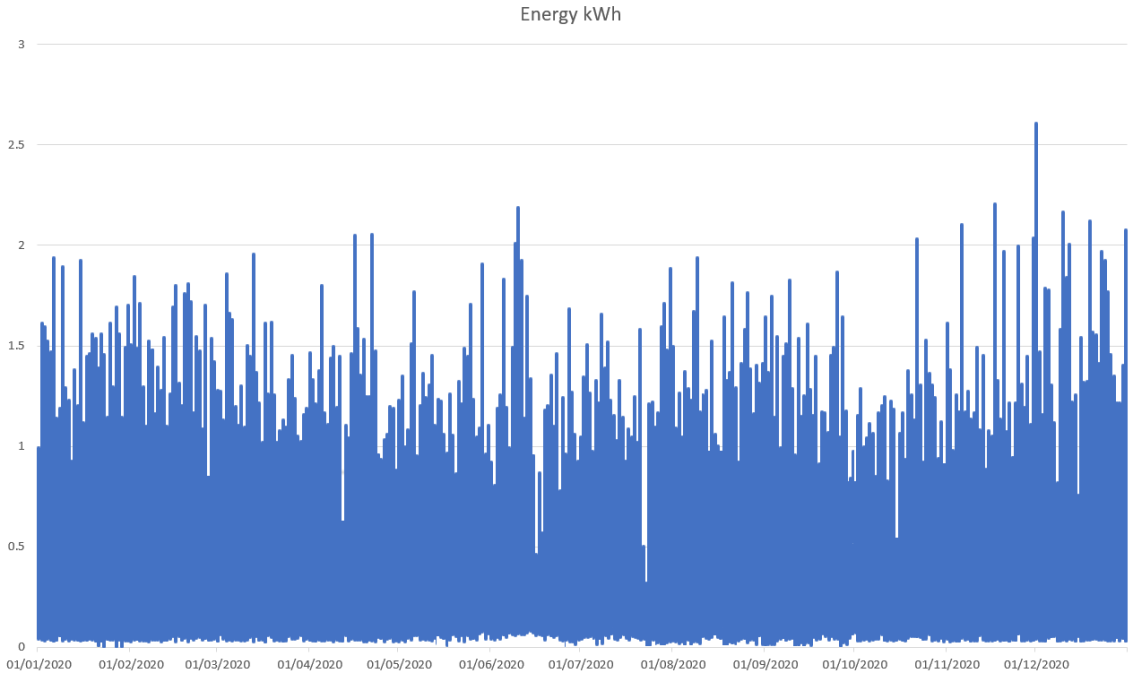

Figure III.26: Yearly consumption for household 1

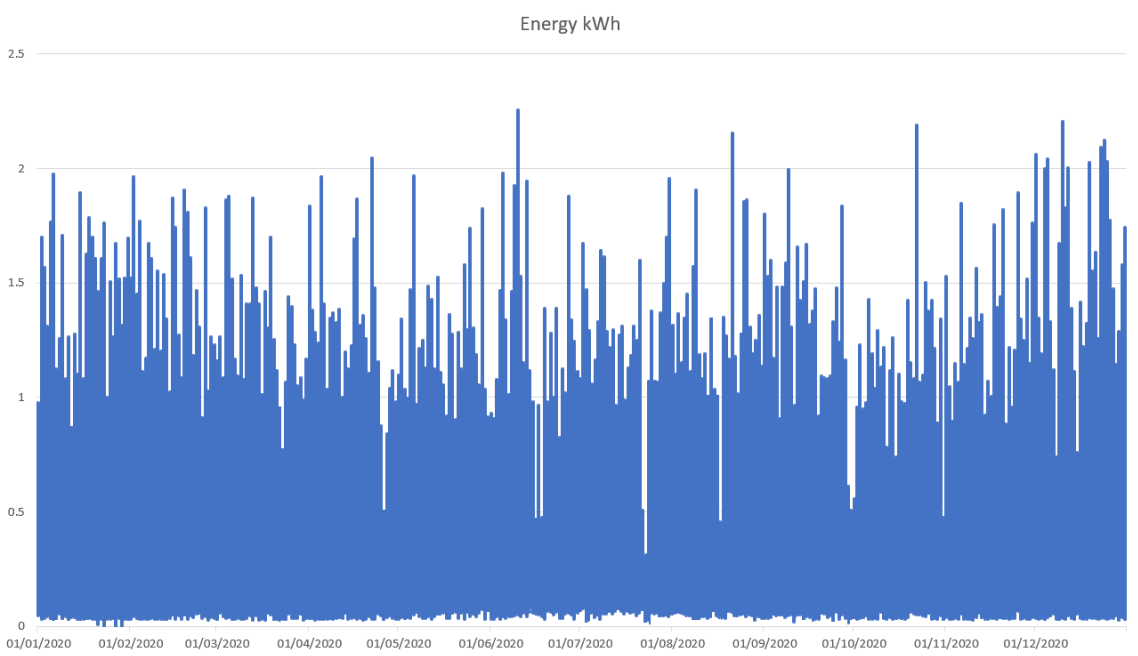

Figure III.27: Yearly consumption for household 1

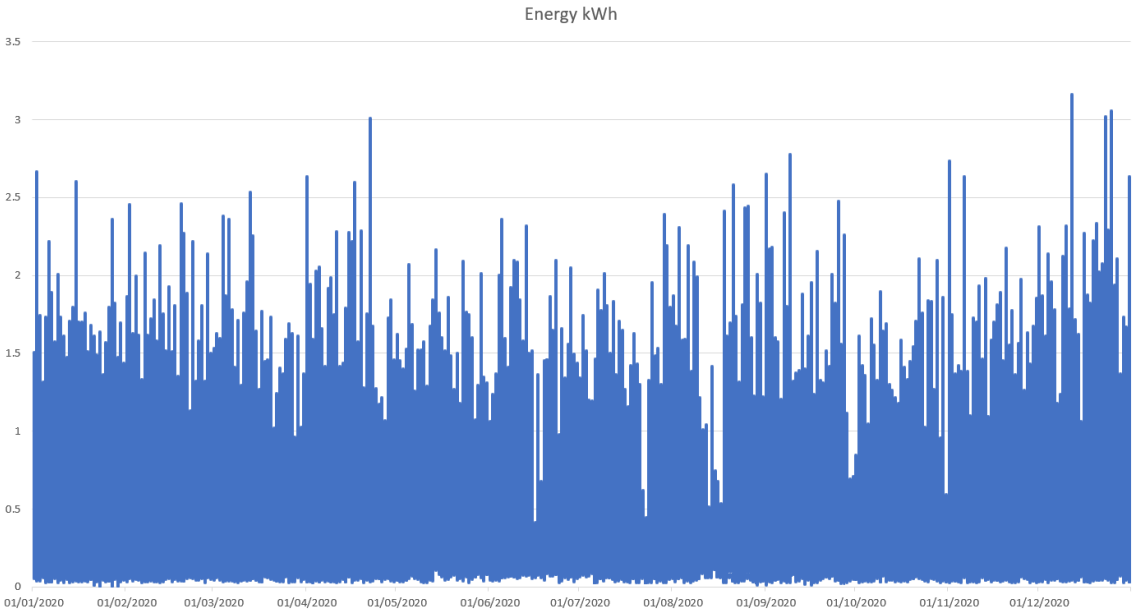

Figure III.28: Yearly consumption for household 1

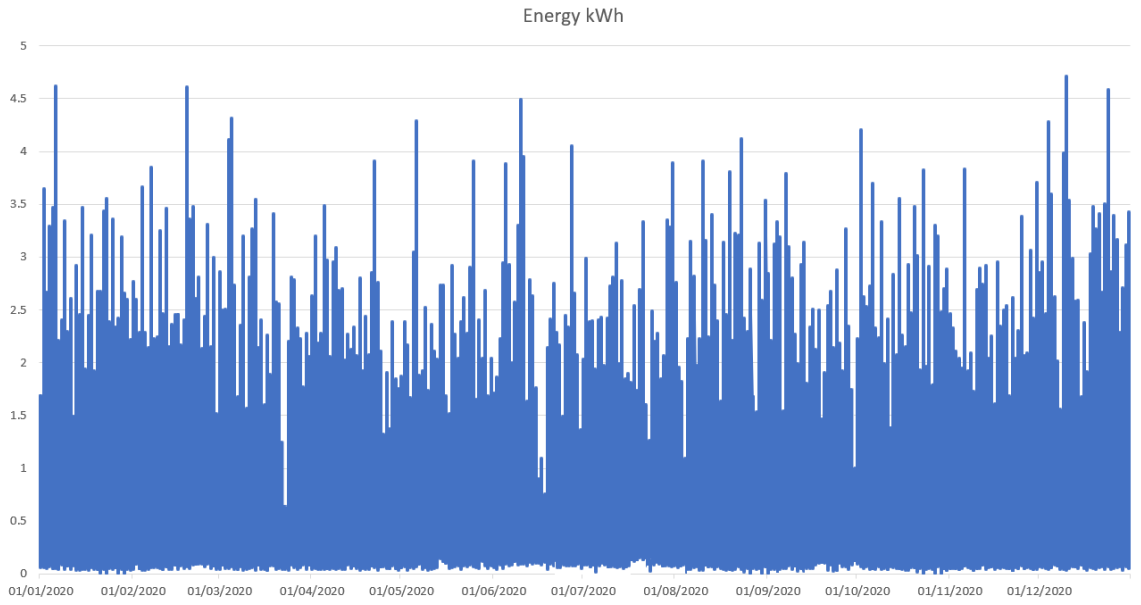

Figure III.29: Yearly consumption for household 1

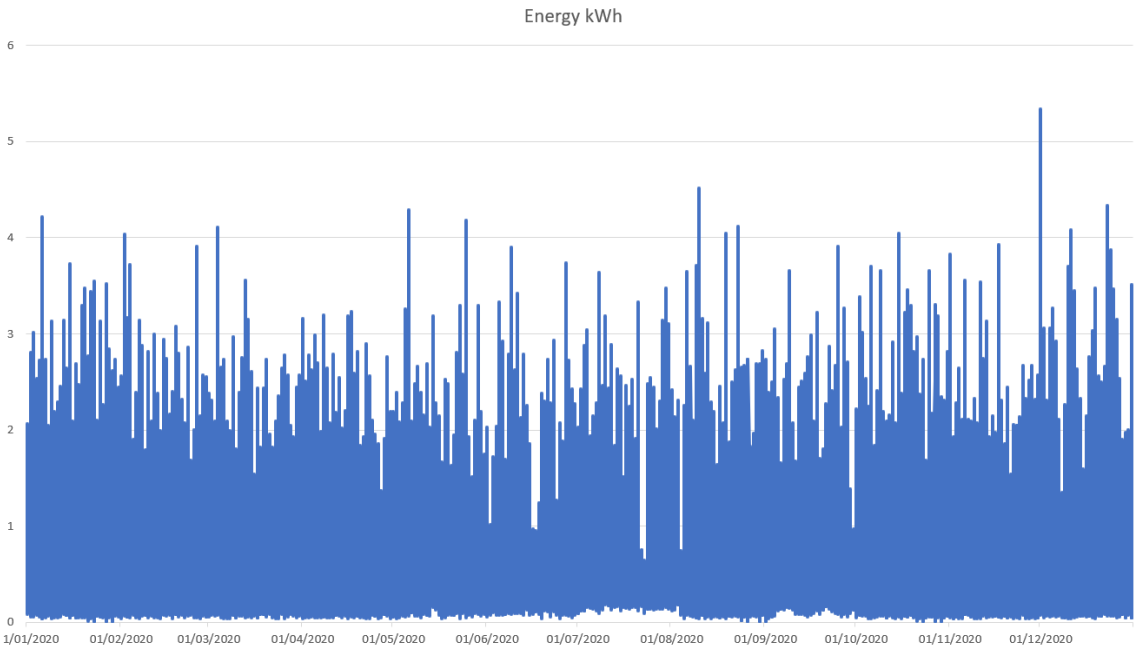

Figure III.30: Yearly consumption for household 1

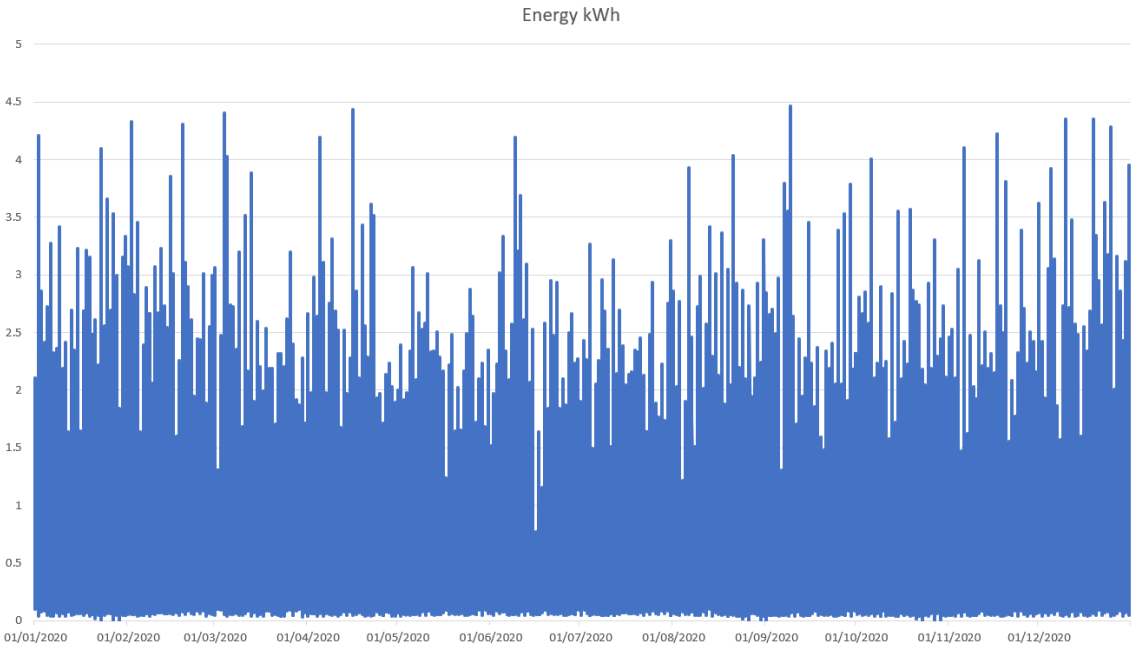

Figure III.31: Yearly consumption for household 1

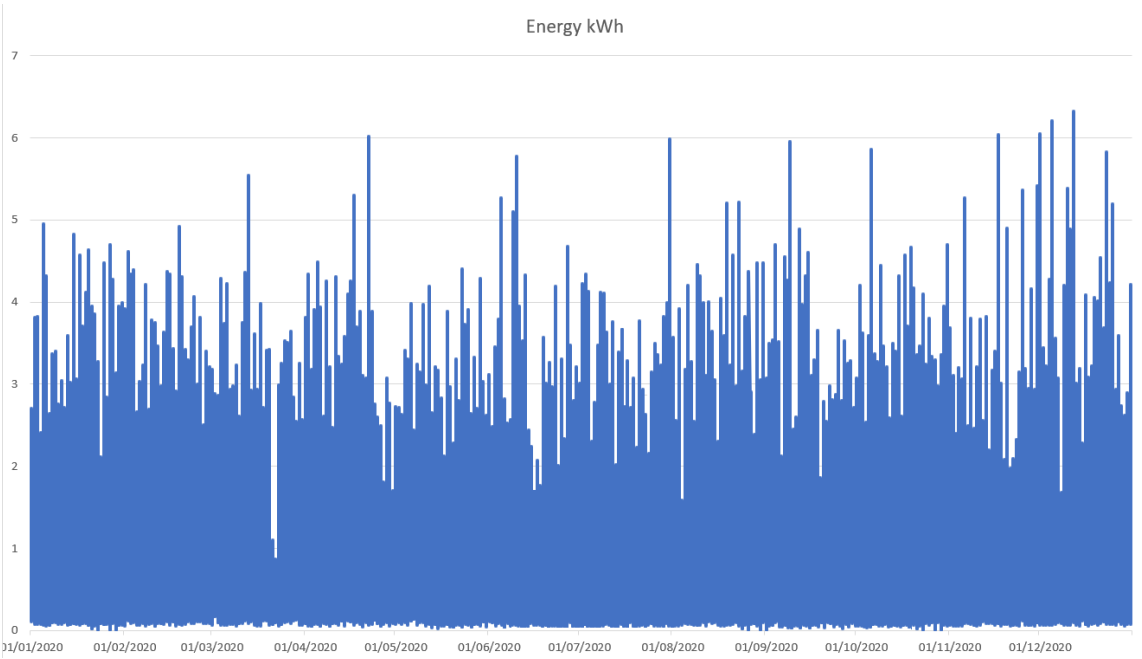

Figure III.32: Yearly consumption for household 1

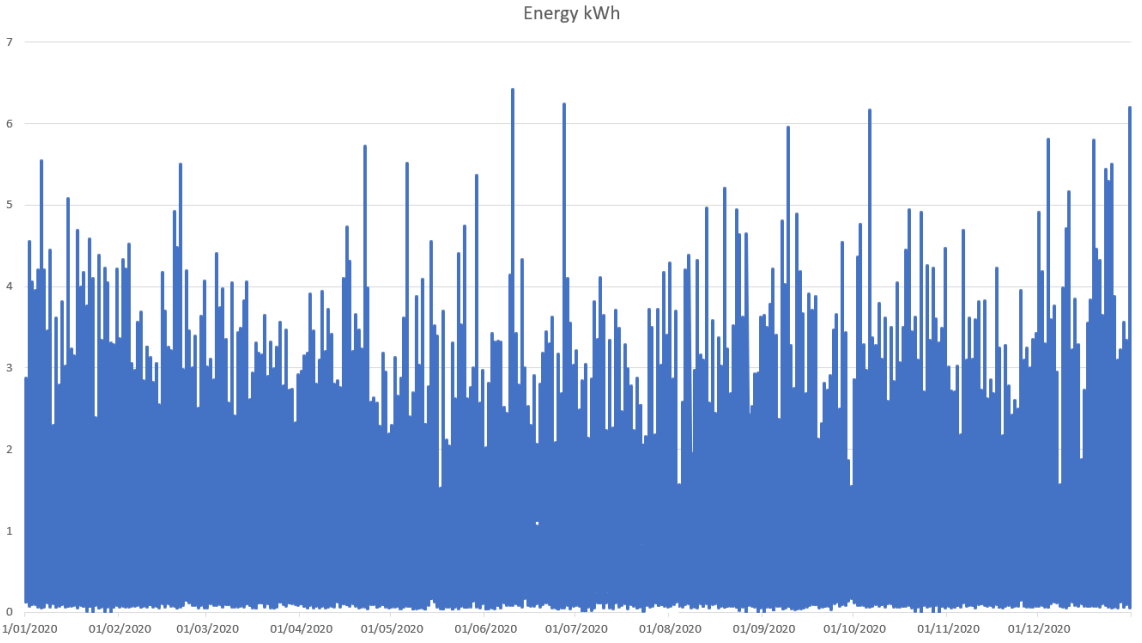

Figure III.33: Yearly consumption for household 1

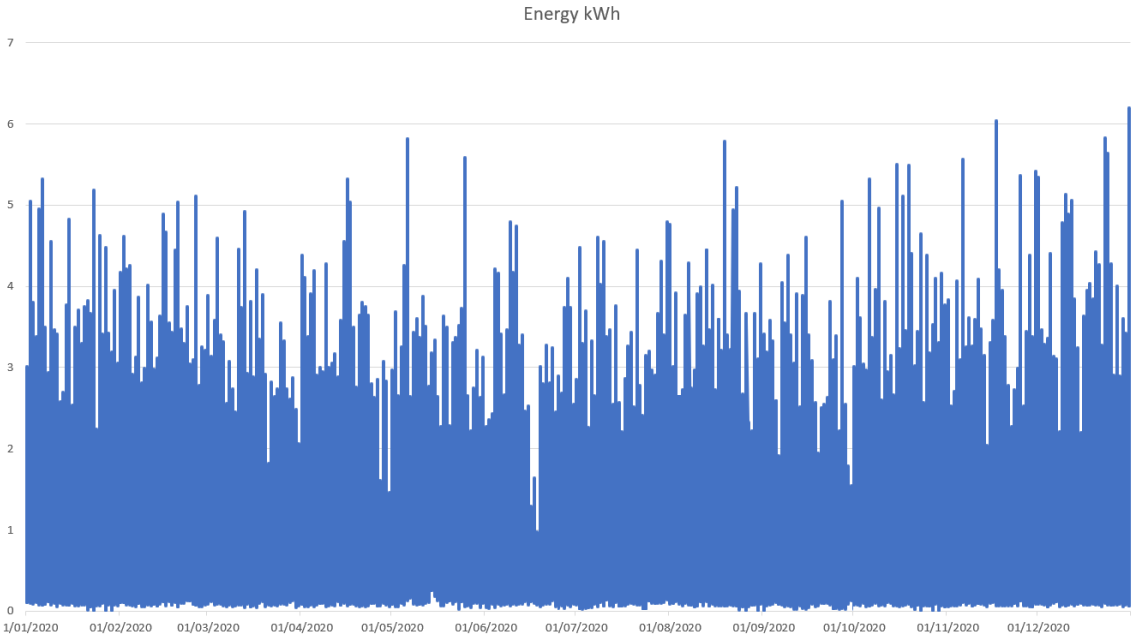

Figure III.34: Yearly consumption for household 1

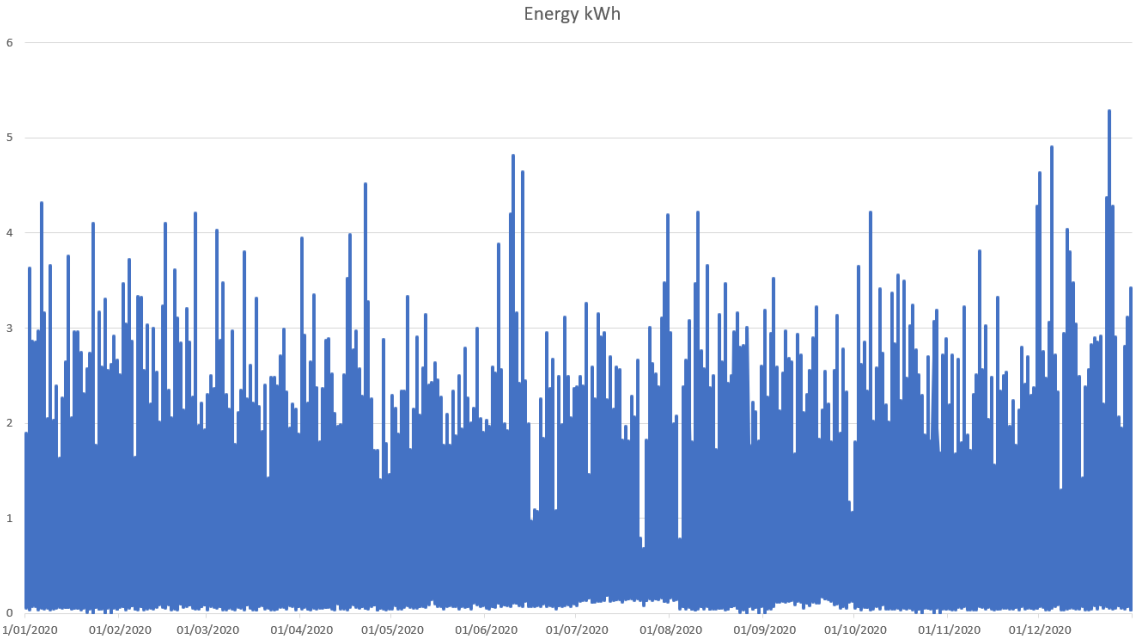

Figure III.35: Yearly consumption for household 1

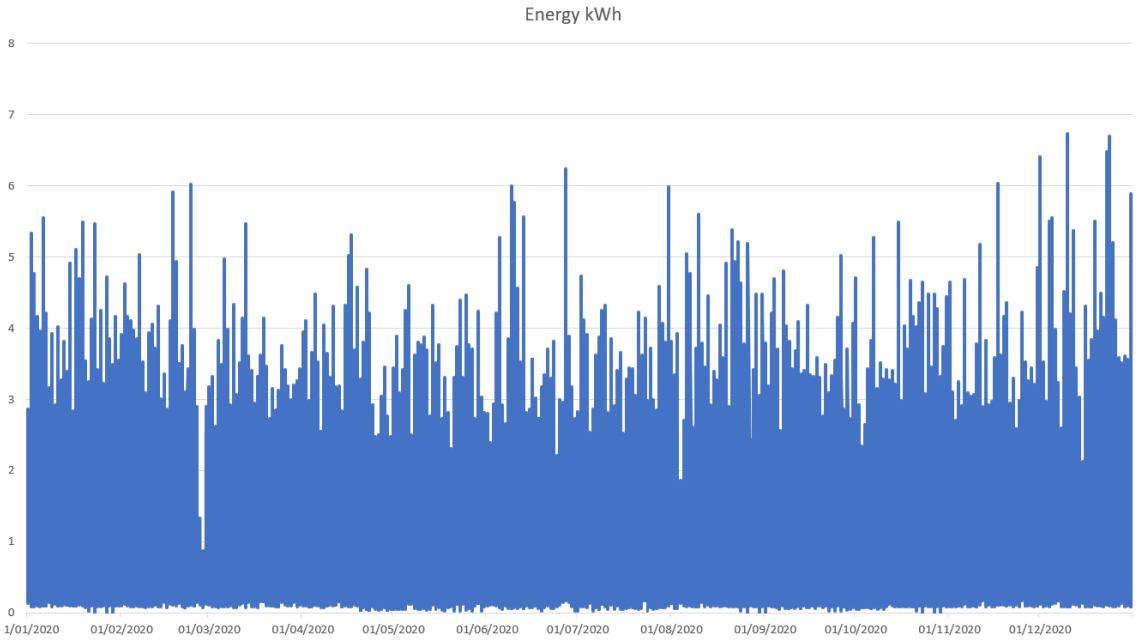

Figure III.36: Yearly consumption for household 1

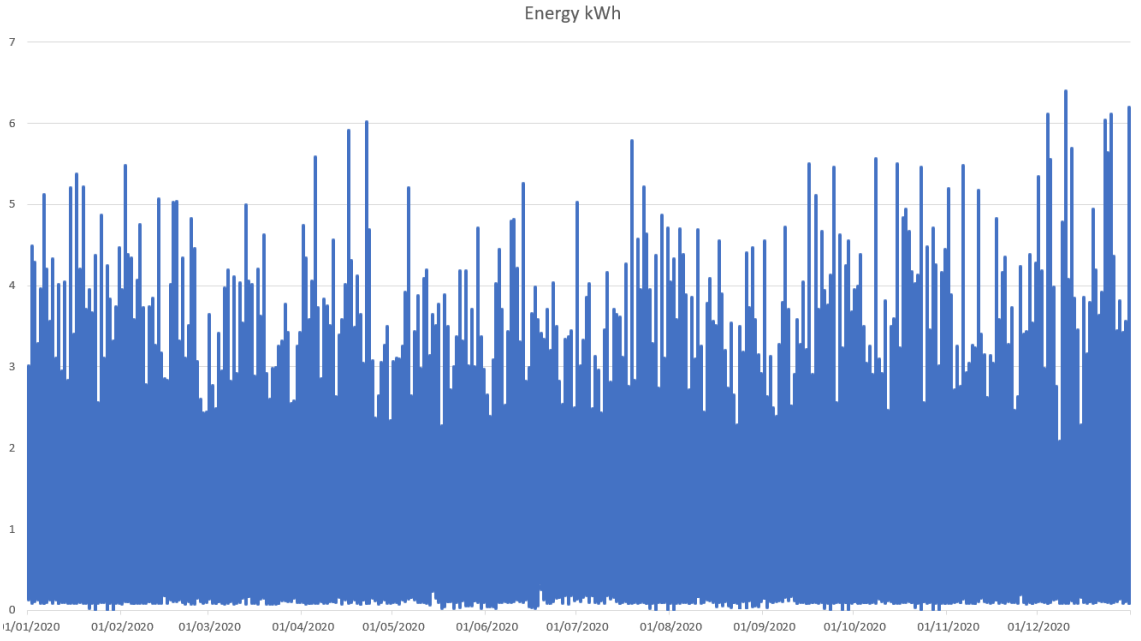

Figure III.37: Yearly consumption for household 1

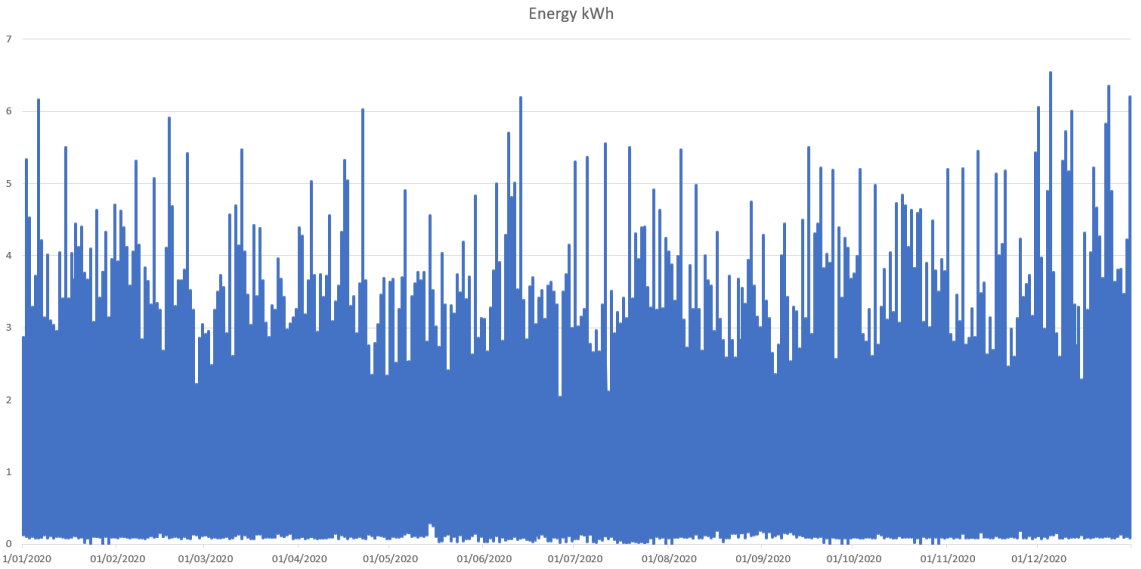

Figure III.38: Yearly consumption for household 1

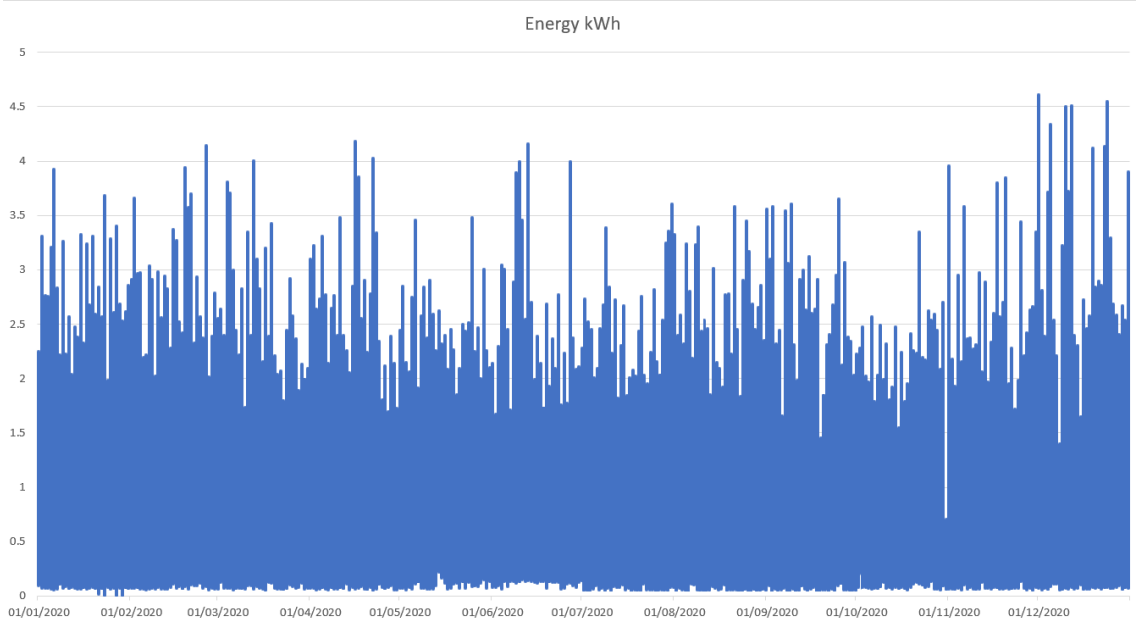

Figure III.39: Yearly consumption for household 1

IV

Number of Modules Per Household

Table IV.1: Number of PV modules per household

Household	North Modules	South Modules	East Modules	West Modules
1	-	1	-	-
2	-	1	-	-
3	-	1	-	-
4	-	1	-	-
5	-	-	1	-
6	-	-	1	-
7	-	-	1	-
8	-	-	2	-
9	-	2	-	-
10	-	2	-	-
11	-	-	2	-
12	-	2	-	-
13	-	2	-	-
14	-	2	-	-
15	-	2	-	-
16	-	2	-	-
17	-	5	-	-
18	-	5	-	-
19	-	5	-	-
20	-	5	-	-
21	-	5	-	-
22	-	5	-	-
23	-	5	-	-
24	-	5	-	-
25	-	3	-	-
26	-	-	3	-
27	-	3	-	-
28	-	3	-	-
29	-	3	-	-
30	-	3	-	-
31	-	3		-
32	-	3	-	-
33	-	5	-	-
34	-	-	4	-
35	-	-	4	-
36	-	-	4	-
37	-	-	3	2
38	-	-	4	1
39	-	-	3	3
40	-	-	3	3

V

Performance indicators for the individual households

Table V.1: Individual approach

Household	SSR (%)	SCR (%)
1	0.29	0.44
2	0.29	0.43
3	0.29	0.43
4	0.29	0.43
5	0.32	0.33
6	0.32	0.33
7	0.32	0.33
8	0.36	0.41
9	0.22	0.34
10	0.33	0.50
11	0.33	0.50
12	0.33	0.50
13	0.25	0.28
14	0.25	0.27
15	0.25	0.27
16	0.25	0.27
17	0.39	0.36
18	0.39	0.34
19	0.39	0.34
20	0.39	0.34

Table V.2: Individual with storage approach

	LM		Batt		Total	
Household	SSR (%)	SCR (%)	SSR (%)	SCR (%)	SSR (%)	SCR (%)
1	0.29	0.44	0.28	0.43	0.57	0.87
2	0.29	0.43	0.29	0.43	0.58	0.85
3	0.29	0.43	0.29	0.43	0.58	0.85
4	0.29	0.43	0.29	0.43	0.59	0.85
5	0.32	0.33	0.48	0.50	0.79	0.83
6	0.32	0.33	0.48	0.50	0.79	0.83
7	0.32	0.33	0.48	0.50	0.79	0.83
8	0.36	0.41	0.40	0.46	0.76	0.87
9	0.22	0.34	0.21	0.33	0.42	0.67
10	0.33	0.50	0.25	0.38	0.58	0.88
11	0.33	0.50	0.25	0.38	0.58	0.88
12	0.33	0.50	0.25	0.38	0.58	0.88
13	0.25	0.28	0.31	0.33	0.56	0.61
14	0.25	0.27	0.33	0.36	0.59	0.63
15	0.25	0.27	0.33	0.36	0.58	0.63
16	0.25	0.27	0.33	0.36	0.59	0.63
17	0.39	0.36	0.50	0.46	0.89	0.81
18	0.39	0.34	0.55	0.48	0.94	0.82
19	0.39	0.34	0.55	0.48	0.94	0.82
20	0.39	0.34	0.55	0.48	0.94	0.82

Table V.3: Energy community approach - 16 households

	LM		P2P		Total	
Household	SSR (%)	SCR (%)	SSR (%)	SCR (%)	SSR (%)	SCR (%)
1	0.29	0.44	0.10	0.15	0.39	0.59
2	0.00	0.00	0.32	0.00	0.32	0.00
3	0.29	0.43	0.07	0.11	0.37	0.53
4	0.29	0.43	0.05	0.07	0.34	0.50
5	0.00	0.00	0.29	0.00	0.29	0.00
6	0.32	0.33	0.02	0.02	0.34	0.35
7	0.32	0.33	0.02	0.02	0.33	0.35
8	0.00	0.00	0.29	0.00	0.29	0.00
9	0.22	0.34	0.02	0.03	0.24	0.38
10	0.00	0.00	0.26	0.00	0.26	0.00
11	0.00	0.00	0.23	0.00	0.23	0.00
12	0.33	0.50	0.04	0.07	0.38	0.57
13	0.00	0.00	0.11	0.00	0.11	0.00
14	0.25	0.27	0.001	0.002	0.25	0.28
15	0.25	0.27	0.001	0.001	0.25	0.28
16	0.25	0.27	0.0004	0.0005	0.25	0.28
21	0.34	0.49	0.03	0.04	0.37	0.53
22	0.00	0.00	0.25	0.00	0.25	0.00
23	0.34	0.49	0.02	0.02	0.35	0.51
24	0.34	0.49	0.01	0.01	0.35	0.50
25	0.00	0.00	0.24	0.00	0.24	0.00
26	0.37	0.46	0.03	0.03	0.39	0.49
27	0.33	0.58	0.02	0.04	0.35	0.62
28	0.00	0.00	0.20	0.00	0.20	0.00
29	0.36	0.51	0.004	0.006	0.37	0.52
30	0.36	0.51	0.004	0.005	0.37	0.52
31	0.36	0.51	0.003	0.004	0.37	0.51
32	0.36	0.51	0.003	0.004	0.37	0.51
33	0.00	0.00	0.15	0.00	0.15	0.00
34	0.00	0.00	0.15	0.00	0.15	0.00
35	0.38	0.42	0.004	0.004	0.39	0.43
36	0.00	0.00	0.13	0.00	0.13	0.00

Table V.4: Energy community approach - 17 households

	LM		P2P		Total	
Household	SSR (%)	SCR (%)	SSR (%)	SCR (%)	SSR (%)	SCR (%)
1	0.00	0.00	0.35	0.00	0.35	0.00
2	0.29	0.43	0.10	0.14	0.39	0.57
3	0.00	0.00	0.34	0.00	0.34	0.00
4	0.29	0.43	0.06	0.09	0.35	0.51
5	0.00	0.00	0.29	0.00	0.29	0.00
6	0.32	0.33	0.03	0.03	0.34	0.36
7	0.00	0.00	0.26	0.00	0.26	0.00
8	0.36	0.41	0.05	0.06	0.42	0.47
9	0.00	0.00	0.14	0.00	0.14	0.00
10	0.33	0.50	0.07	0.10	0.40	0.60
11	0.33	0.50	0.05	0.08	0.39	0.58
12	0.33	0.50	0.04	0.06	0.37	0.56
13	0.00	0.00	0.13	0.00	0.13	0.00
14	0.25	0.27	0.01	0.01	0.26	0.28
15	0.25	0.27	0.004	0.004	0.26	0.28
16	0.25	0.27	0.003	0.003	0.26	0.28
17	0.00	0.00	0.173	0.000	0.17	0.00
21	0.00	0.00	0.25	0.00	0.25	0.00
22	0.34	0.49	0.03	0.04	0.36	0.53
23	0.00	0.00	0.25	0.00	0.25	0.00
24	0.34	0.49	0.01	0.02	0.35	0.51
25	0.00	0.00	0.22	0.00	0.22	0.00
26	0.37	0.46	0.01	0.01	0.38	0.47
27	0.00	0.00	0.18	0.00	0.18	0.00
28	0.33	0.58	0.01	0.02	0.34	0.60
29	0.00	0.00	0.17	0.00	0.17	0.00
30	0.36	0.51	0.002	0.003	0.37	0.51
31	0.36	0.51	0.002	0.003	0.37	0.51
32	0.36	0.51	0.002	0.002	0.37	0.51
33	0.00	0.00	0.13	0.00	0.13	0.00
34	0.35	0.55	0.001	0.002	0.35	0.55
35	0.38	0.42	0.003	0.003	0.38	0.43
36	0.38	0.42	0.002	0.002	0.38	0.42
37	0.00	0.00	0.15	0.00	0.15	0.00

Table V.5: Energy community approach - 18 households

	LM		P2P		Total	
Household	SSR (%)	SCR (%)	SSR (%)	SCR (%)	SSR (%)	SCR (%)
1	0.00	0.00	0.39	0.00	0.39	0.00
2	0.29	0.43	0.11	0.16	0.41	0.59
3	0.00	0.00	0.36	0.00	0.36	0.00
4	0.29	0.43	0.08	0.11	0.37	0.54
5	0.32	0.33	0.05	0.05	0.37	0.38
6	0.00	0.00	0.31	0.00	0.31	0.00
7	0.32	0.33	0.03	0.03	0.34	0.36
8	0.36	0.41	0.08	0.10	0.45	0.51
9	0.00	0.00	0.27	0.00	0.27	0.00
10	0.00	0.00	0.32	0.00	0.32	0.00
11	0.33	0.50	0.07	0.11	0.40	0.61
12	0.00	0.00	0.28	0.00	0.28	0.00
13	0.25	0.28	0.02	0.02	0.27	0.30
14	0.25	0.27	0.01	0.01	0.27	0.29
15	0.00	0.00	0.13	0.00	0.13	0.00
16	0.25	0.27	0.004	0.004	0.26	0.28
17	0.39	0.36	0.01	0.01	0.40	0.37
18	0.00	0.00	0.22	0.00	0.22	0.00
21	0.00	0.00	0.29	0.00	0.29	0.00
22	0.34	0.49	0.03	0.04	0.36	0.53
23	0.00	0.00	0.24	0.00	0.24	0.00
24	0.34	0.49	0.01	0.01	0.35	0.50
25	0.32	0.60	0.04	0.08	0.37	0.69
26	0.00	0.00	0.21	0.00	0.21	0.00
27	0.33	0.58	0.02	0.04	0.35	0.62
28	0.33	0.58	0.02	0.03	0.34	0.61
29	0.00	0.00	0.19	0.00	0.19	0.00
30	0.00	0.00	0.17	0.00	0.17	0.00
31	0.36	0.51	0.003	0.004	0.37	0.51
32	0.00	0.00	0.16	0.00	0.16	0.00
33	0.34	0.57	0.002	0.003	0.34	0.57
34	0.35	0.55	0.001	0.002	0.35	0.55
35	0.00	0.00	0.13	0.00	0.13	0.00
36	0.38	0.42	0.003	0.004	0.39	0.43
37	0.35	0.39	0.01	0.01	0.36	0.40
38	0.00	0.00	0.14	0.00	0.14	0.00

Table V.6: Energy community approach - 19 households

	LM		P2P		Total	
Household	SSR (%)	SCR (%)	SSR (%)	SCR (%)	SSR (%)	SCR (%)
1	0.00	0.00	0.41	0.00	0.41	0.00
2	0.00	0.00	0.41	0.00	0.41	0.00
3	0.29	0.43	0.10	0.14	0.39	0.57
4	0.00	0.00	0.35	0.00	0.35	0.00
5	0.32	0.33	0.07	0.07	0.38	0.40
6	0.32	0.33	0.06	0.06	0.38	0.39
7	0.00	0.00	0.33	0.00	0.33	0.00
8	0.36	0.41	0.08	0.09	0.45	0.51
9	0.22	0.34	0.13	0.20	0.34	0.55
10	0.00	0.00	0.36	0.00	0.36	0.00
11	0.33	0.50	0.09	0.13	0.42	0.63
12	0.33	0.50	0.07	0.10	0.40	0.60
13	0.00	0.00	0.23	0.00	0.23	0.00
14	0.25	0.27	0.03	0.04	0.29	0.31
15	0.25	0.27	0.02	0.02	0.27	0.30
16	0.00	0.00	0.15	0.00	0.15	0.00
17	0.39	0.36	0.01	0.01	0.40	0.37
18	0.39	0.34	0.01	0.01	0.40	0.35
19	0.00	0.00	0.24	0.00	0.24	0.00
21	0.00	0.00	0.28	0.00	0.28	0.00
22	0.00	0.00	0.27	0.00	0.27	0.00
23	0.34	0.49	0.02	0.03	0.36	0.52
24	0.00	0.00	0.23	0.00	0.23	0.00
25	0.32	0.60	0.05	0.09	0.37	0.70
26	0.37	0.46	0.02	0.02	0.38	0.48
27	0.00	0.00	0.21	0.00	0.21	0.00
28	0.33	0.58	0.02	0.04	0.35	0.63
29	0.36	0.51	0.01	0.02	0.38	0.53
30	0.00	0.00	0.19	0.00	0.19	0.00
31	0.36	0.51	0.01	0.01	0.37	0.52
32	0.36	0.51	0.01	0.01	0.37	0.52
33	0.00	0.00	0.15	0.00	0.15	0.00
34	0.35	0.55	0.01	0.01	0.35	0.56
35	0.38	0.42	0.002	0.003	0.38	0.43
36	0.00	0.00	0.14	0.00	0.14	0.00
37	0.35	0.39	0.01	0.01	0.36	0.39
38	0.35	0.39	0.01	0.01	0.35	0.39
39	0.00	0.00	0.11	0.00	0.11	0.00

Table V.7: Energy community with Storage approach - 16 households

	LM		P2P		Total	
Household	SSR (%)	SCR (%)	SSR (%)	SCR (%)	SSR (%)	SCR (%)
1	0.00	0.00	0.41	0.00	0.41	0.00
2	0.00	0.00	0.41	0.00	0.41	0.00
3	0.29	0.43	0.10	0.14	0.39	0.57
4	0.00	0.00	0.35	0.00	0.35	0.00
5	0.32	0.33	0.07	0.07	0.38	0.40
6	0.32	0.33	0.06	0.06	0.38	0.39
7	0.00	0.00	0.33	0.00	0.33	0.00
8	0.36	0.41	0.08	0.09	0.45	0.51
9	0.22	0.34	0.13	0.20	0.34	0.55
10	0.00	0.00	0.36	0.00	0.36	0.00
11	0.33	0.50	0.09	0.13	0.42	0.63
12	0.33	0.50	0.07	0.10	0.40	0.60
13	0.00	0.00	0.23	0.00	0.23	0.00
14	0.25	0.27	0.03	0.04	0.29	0.31
15	0.25	0.27	0.02	0.02	0.27	0.30
16	0.00	0.00	0.15	0.00	0.15	0.00
17	0.39	0.36	0.01	0.01	0.40	0.37
18	0.39	0.34	0.01	0.01	0.40	0.35
19	0.00	0.00	0.24	0.00	0.24	0.00
20	0.00	0.00	0.23	0.00	0.23	0.00
21	0.00	0.00	0.29	0.00	0.29	0.00
22	0.00	0.00	0.03	0.00	0.03	0.00
23	0.34	0.49	0.26	0.38	0.60	0.87
24	0.00	0.00	0.02	0.00	0.02	0.00
25	0.39	0.41	0.05	0.05	0.44	0.46
26	0.33	0.58	0.23	0.40	0.55	0.98
27	0.00	0.00	0.02	0.00	0.02	0.00
28	0.33	0.58	0.02	0.03	0.35	0.62
29	0.36	0.51	0.20	0.28	0.56	0.79
30	0.00	0.00	0.01	0.00	0.01	0.00
31	0.36	0.51	0.01	0.01	0.37	0.52
32	0.36	0.51	0.18	0.25	0.54	0.76
33	0.00	0.00	0.01	0.00	0.01	0.00
34	0.38	0.48	0.004	0.005	0.38	0.48
35	0.35	0.55	0.16	0.25	0.50	0.79
36	0.00	0.00	0.00	0.00	0.00	0.00
37	0.33	0.46	0.01	0.02	0.35	0.48
38	0.35	0.39	0.16	0.18	0.51	0.57
39	0.36	0.47	0.003	0.004	0.36	0.47
40	0.00	0.00	0.12	0.00	0.12	0.00

Table V.8: Energy community with Storage approach - 16 households

	LM		P2P		Batt		Total	
Household	SSR (%)	SCR (%)	SSR (%)	SCR (%)	SSR (%)	SCR (%)	SSR (%)	SCR (%)
1	0.29	0.44	0.10	0.15	0.17	0.26	0.56	0.85
2	0.00	0.00	0.32	0.00	0.20	0.00	0.51	0.00
3	0.29	0.43	0.07	0.11	0.19	0.27	0.56	0.81
4	0.29	0.43	0.05	0.07	0.20	0.00	0.55	0.50
5	0.00	0.00	0.29	0.00	0.21	0.31	0.50	0.31
6	0.32	0.33	0.02	0.02	0.21	0.00	0.55	0.35
7	0.32	0.33	0.02	0.02	0.21	0.22	0.54	0.56
8	0.00	0.00	0.29	0.00	0.20	0.46	0.49	0.46
9	0.22	0.34	0.02	0.03	0.13	0.00	0.37	0.38
10	0.00	0.00	0.26	0.00	0.26	0.39	0.51	0.39
11	0.00	0.00	0.23	0.00	0.28	0.00	0.51	0.00
12	0.33	0.50	0.04	0.07	0.23	0.35	0.61	0.92
13	0.00	0.00	0.11	0.00	0.22	0.00	0.33	0.00
14	0.25	0.27	0.001	0.002	0.15	0.17	0.41	0.44
15	0.25	0.27	0.001	0.001	0.15	0.16	0.40	0.44
16	0.25	0.27	0.0004	0.0005	0.15	0.16	0.40	0.43

Table V.9: Energy community with Storage approach - 17 households

LM	LM		P2P		Batt		Total	
Household	SSR (%)	SCR (%)	SSR (%)	SCR (%)	SSR (%)	SCR (%)	SSR (%)	SCR (%)
1	0.00	0.00	0.35	0.00	0.19	0.27	0.54	0.27
2	0.29	0.43	0.10	0.14	0.20	0.00	0.58	0.57
3	0.00	0.00	0.34	0.00	0.20	0.29	0.54	0.29
4	0.29	0.43	0.06	0.09	0.21	0.00	0.56	0.51
5	0.00	0.00	0.29	0.00	0.22	0.34	0.51	0.34
6	0.32	0.33	0.03	0.03	0.22	0.00	0.56	0.36
7	0.00	0.00	0.26	0.00	0.22	0.24	0.48	0.24
8	0.36	0.41	0.05	0.06	0.21	0.47	0.63	0.94
9	0.00	0.00	0.14	0.00	0.13	0.00	0.27	0.00
10	0.33	0.50	0.07	0.10	0.27	0.39	0.67	0.99
11	0.33	0.50	0.05	0.08	0.28	0.00	0.67	0.58
12	0.33	0.50	0.04	0.06	0.24	0.37	0.61	0.93
13	0.00	0.00	0.13	0.00	0.23	0.00	0.36	0.00
14	0.25	0.27	0.01	0.01	0.15	0.17	0.41	0.45
15	0.25	0.27	0.004	0.004	0.15	0.16	0.41	0.44
16	0.25	0.27	0.003	0.003	0.15	0.16	0.40	0.44
17	0.00	0.00	0.173	0.000	0.160	0.180	0.33	0.18

Table V.10: Energy community with Storage approach - 18 households

	LM		P2P		Batt		Total	
Household	SSR (%)	SCR (%)	SSR (%)	SCR (%)	SSR (%)	SCR (%)	SSR (%)	SCR (%)
1	0.00	0.00	0.39	0.00	0.15	0.00	0.54	0.00
2	0.29	0.43	0.11	0.16	0.14	0.21	0.55	0.80
3	0.00	0.00	0.36	0.00	0.16	0.00	0.52	0.00
4	0.29	0.43	0.08	0.11	0.16	0.24	0.53	0.77
5	0.32	0.33	0.05	0.05	0.16	0.17	0.53	0.55
6	0.00	0.00	0.31	0.00	0.18	0.00	0.49	0.00
7	0.32	0.33	0.03	0.03	0.17	0.17	0.51	0.53
8	0.36	0.41	0.08	0.10	0.16	0.19	0.61	0.69
9	0.00	0.00	0.27	0.00	0.12	0.00	0.39	0.00
10	0.00	0.00	0.32	0.00	0.21	0.00	0.53	0.00
11	0.33	0.50	0.07	0.11	0.20	0.30	0.60	0.91
12	0.00	0.00	0.28	0.00	0.24	0.00	0.51	0.00
13	0.25	0.28	0.02	0.02	0.14	0.15	0.41	0.45
14	0.25	0.27	0.01	0.01	0.15	0.16	0.42	0.45
15	0.00	0.00	0.13	0.00	0.20	0.00	0.33	0.00
16	0.25	0.27	0.004	0.004	0.143	0.155	0.40	0.43
17	0.39	0.36	0.01	0.01	0.20	0.18	0.60	0.55
18	0.00	0.00	0.22	0.00	0.25	0.00	0.47	0.00

Table V.11: Energy community with Storage approach - 19 households

	LM		P2P		Batt		Total	
Household	SSR (%)	SCR (%)	SSR (%)	SCR (%)	SSR (%)	SCR (%)	SSR (%)	SCR (%)
1	0.00	0.00	0.41	0.00	0.19	0.00	0.60	0.00
2	0.00	0.00	0.41	0.00	0.20	0.00	0.60	0.00
3	0.29	0.43	0.10	0.14	0.21	0.30	0.60	0.87
4	0.00	0.00	0.35	0.00	0.22	0.00	0.58	0.00
5	0.32	0.33	0.07	0.07	0.21	0.22	0.60	0.62
6	0.32	0.33	0.06	0.06	0.22	0.23	0.59	0.62
7	0.00	0.00	0.33	0.00	0.24	0.00	0.56	0.00
8	0.36	0.41	0.08	0.09	0.21	0.24	0.66	0.75
9	0.22	0.34	0.13	0.20	0.14	0.23	0.49	0.77
10	0.00	0.00	0.36	0.00	0.25	0.00	0.61	0.00
11	0.33	0.50	0.09	0.13	0.25	0.37	0.66	1.00
12	0.33	0.50	0.07	0.10	0.26	0.39	0.65	0.99
13	0.00	0.00	0.23	0.00	0.21	0.00	0.43	0.00
14	0.25	0.27	0.03	0.04	0.20	0.21	0.48	0.53
15	0.25	0.27	0.02	0.02	0.20	0.22	0.47	0.51
16	0.00	0.00	0.15	0.00	0.26	0.00	0.41	0.00
17	0.39	0.36	0.01	0.01	0.26	0.23	0.66	0.60
18	0.39	0.34	0.01	0.01	0.26	0.23	0.66	0.57
19	0.00	0.00	0.24	0.00	0.31	0.00	0.55	0.00

Table V.12: Energy community with Storage approach - 20 households

	LM		P2P		Batt		Total	
Household	SSR (%)	SCR (%)	SSR (%)	SCR (%)	SSR (%)	SCR (%)	SSR (%)	SCR (%)
1	0.00	0.00	0.41	0.00	0.12	0.00	0.53	0.00
2	0.00	0.00	0.41	0.00	0.13	0.00	0.53	0.00
3	0.29	0.43	0.10	0.14	0.13	0.19	0.52	0.76
4	0.00	0.00	0.35	0.00	0.14	0.00	0.49	0.00
5	0.32	0.33	0.07	0.07	0.13	0.13	0.51	0.53
6	0.32	0.33	0.06	0.06	0.13	0.14	0.51	0.53
7	0.00	0.00	0.33	0.00	0.15	0.00	0.48	0.00
8	0.36	0.41	0.08	0.09	0.16	0.18	0.60	0.68
9	0.22	0.34	0.13	0.20	0.10	0.16	0.44	0.71
10	0.00	0.00	0.36	0.00	0.18	0.00	0.54	0.00
11	0.33	0.50	0.09	0.13	0.19	0.29	0.61	0.92
12	0.33	0.50	0.07	0.10	0.20	0.31	0.60	0.91
13	0.00	0.00	0.23	0.00	0.16	0.00	0.38	0.00
14	0.25	0.27	0.03	0.04	0.16	0.17	0.45	0.48
15	0.25	0.27	0.02	0.02	0.16	0.17	0.43	0.47
16	0.00	0.00	0.15	0.00	0.21	0.00	0.36	0.00
17	0.39	0.36	0.01	0.01	0.19	0.17	0.59	0.54
18	0.39	0.34	0.01	0.01	0.20	0.17	0.60	0.52
19	0.00	0.00	0.24	0.00	0.20	0.30	0.44	0.30
20	0.00	0.00	0.23	0.00	0.24	0.00	0.47	0.00

Table V.13: Multiple energy communities approach - 16 households

	LM		P2P		Total	
Household	SSR	SCR	SSR	SCR	SSR	SCR
1	0.29	0.44	0.13	0.19	0.41	0.63
2	0.00	0.00	0.38	0.00	0.38	0.00
3	0.29	0.43	0.11	0.15	0.40	0.58
4	0.29	0.43	0.09	0.13	0.38	0.56
5	0.00	0.00	0.35	0.00	0.35	0.00
6	0.32	0.33	0.06	0.06	0.38	0.39
7	0.32	0.33	0.06	0.06	0.38	0.39
8	0.00	0.00	0.36	0.00	0.36	0.00
9	0.22	0.34	0.06	0.10	0.28	0.44
10	0.00	0.00	0.35	0.00	0.35	0.00
11	0.00	0.00	0.31	0.00	0.31	0.00
12	0.33	0.50	0.07	0.10	0.40	0.61
13	0.00	0.00	0.18	0.00	0.18	0.00
14	0.25	0.27	0.03	0.04	0.29	0.31
15	0.25	0.27	0.03	0.03	0.28	0.31
16	0.25	0.27	0.02	0.03	0.28	0.30
21	0.34	0.49	0.03	0.04	0.37	0.53
22	0.00	0.00	0.23	0.00	0.23	0.00
23	0.34	0.49	0.02	0.02	0.35	0.51
24	0.34	0.49	0.01	0.02	0.35	0.51
25	0.00	0.00	0.22	0.00	0.22	0.00
26	0.37	0.46	0.03	0.04	0.40	0.49
27	0.33	0.58	0.03	0.05	0.35	0.63
28	0.00	0.00	0.20	0.00	0.20	0.00
29	0.36	0.51	0.01	0.01	0.37	0.52
30	0.36	0.51	0.01	0.01	0.37	0.52
31	0.36	0.51	0.01	0.01	0.37	0.52
32	0.36	0.51	0.01	0.01	0.37	0.52
33	0.00	0.00	0.15	0.00	0.15	0.00
34	0.00	0.00	0.16	0.00	0.16	0.00
35	0.38	0.42	0.01	0.01	0.39	0.43
36	0.00	0.00	0.14	0.00	0.14	0.00

Table V.14: Multiple energy communities approach - 17 households

	LM		P2P		Total	
Household	SSR	SCR	SSR	SCR	SSR	SCR
1	0.00	0.00	0.39	0.00	0.39	0.00
2	0.29	0.43	0.12	0.18	0.42	0.61
3	0.00	0.00	0.39	0.00	0.39	0.00
4	0.29	0.43	0.10	0.14	0.39	0.57
5	0.00	0.00	0.35	0.00	0.35	0.00
6	0.32	0.33	0.07	0.07	0.39	0.40
7	0.00	0.00	0.34	0.00	0.34	0.00
8	0.36	0.41	0.08	0.09	0.44	0.50
9	0.00	0.00	0.20	0.00	0.20	0.00
10	0.33	0.50	0.10	0.14	0.43	0.65
11	0.33	0.50	0.08	0.13	0.41	0.63
12	0.33	0.50	0.07	0.11	0.40	0.61
13	0.00	0.00	0.20	0.00	0.20	0.00
14	0.25	0.27	0.04	0.04	0.29	0.32
15	0.25	0.27	0.03	0.03	0.29	0.31
16	0.25	0.27	0.03	0.03	0.28	0.30
17	0.00	0.00	0.25	0.00	0.25	0.00
21	0.00	0.00	0.25	0.00	0.25	0.00
22	0.34	0.49	0.02	0.03	0.36	0.52
23	0.00	0.00	0.21	0.00	0.21	0.00
24	0.34	0.49	0.01	0.01	0.35	0.50
25	0.00	0.00	0.20	0.00	0.20	0.00
26	0.37	0.46	0.02	0.03	0.39	0.49
27	0.00	0.00	0.18	0.00	0.18	0.00
28	0.33	0.58	0.01	0.03	0.34	0.61
29	0.00	0.00	0.18	0.00	0.18	0.00
30	0.36	0.51	0.00	0.00	0.37	0.52
31	0.36	0.51	0.00	0.00	0.37	0.51
32	0.36	0.51	0.00	0.00	0.37	0.51
33	0.00	0.00	0.13	0.00	0.13	0.00
34	0.35	0.55	0.00	0.00	0.35	0.55
35	0.38	0.42	0.01	0.01	0.39	0.43
36	0.38	0.42	0.00	0.01	0.39	0.43
37	0.00	0.00	0.14	0.00	0.14	0.00

Table V.15: Multiple energy communities approach - 18 households

	LM		P2P		Total	
Household	SSR	SCR	SSR	SCR	SSR	SCR
1	0.00	0.00	0.42	0.00	0.42	0.00
2	0.29	0.43	0.14	0.20	0.43	0.63
3	0.00	0.00	0.40	0.00	0.40	0.00
4	0.29	0.43	0.11	0.15	0.40	0.58
5	0.32	0.33	0.08	0.09	0.40	0.42
6	0.00	0.00	0.36	0.00	0.36	0.00
7	0.32	0.33	0.07	0.08	0.39	0.41
8	0.36	0.41	0.10	0.11	0.46	0.52
9	0.00	0.00	0.26	0.00	0.26	0.00
10	0.00	0.00	0.38	0.00	0.38	0.00
11	0.33	0.50	0.10	0.15	0.43	0.65
12	0.00	0.00	0.35	0.00	0.35	0.00
13	0.25	0.28	0.09	0.09	0.34	0.37
14	0.25	0.27	0.05	0.06	0.31	0.33
15	0.00	0.00	0.19	0.00	0.19	0.00
16	0.25	0.27	0.03	0.03	0.29	0.31
17	0.39	0.36	0.01	0.01	0.40	0.37
18	0.00	0.00	0.27	0.00	0.27	0.00
21	0.00	0.00	0.25	0.00	0.25	0.00
22	0.34	0.49	0.02	0.03	0.36	0.52
23	0.00	0.00	0.23	0.00	0.23	0.00
24	0.34	0.49	0.01	0.02	0.35	0.51
25	0.32	0.60	0.05	0.09	0.37	0.70
26	0.00	0.00	0.22	0.00	0.22	0.00
27	0.33	0.58	0.03	0.06	0.36	0.64
28	0.33	0.58	0.03	0.05	0.36	0.63
29	0.00	0.00	0.21	0.00	0.21	0.00
30	0.00	0.00	0.20	0.00	0.20	0.00
31	0.36	0.51	0.01	0.01	0.37	0.52
32	0.00	0.00	0.18	0.00	0.18	0.00
33	0.34	0.57	0.01	0.01	0.35	0.58
34	0.35	0.55	0.01	0.01	0.35	0.56
35	0.00	0.00	0.15	0.00	0.15	0.00
36	0.38	0.42	0.01	0.01	0.39	0.43
37	0.35	0.39	0.02	0.02	0.36	0.40
38	0.00	0.00	0.15	0.00	0.15	0.00

Table V.16: Multiple energy communities approach - 19 households

	LM		P2P		Total	
Household	SSR	SCR	SSR	SCR	SSR	SCR
1	0.00	0.00	0.42	0.00	0.42	0.00
2	0.00	0.00	0.42	0.00	0.42	0.00
3	0.29	0.43	0.13	0.19	0.42	0.61
4	0.00	0.00	0.39	0.00	0.39	0.00
5	0.32	0.33	0.10	0.10	0.41	0.43
6	0.32	0.33	0.09	0.09	0.41	0.42
7	0.00	0.00	0.37	0.00	0.37	0.00
8	0.24	0.28	0.10	0.11	0.34	0.39
9	0.32	0.51	0.11	0.17	0.43	0.68
10	0.00	0.00	0.40	0.00	0.40	0.00
11	0.33	0.50	0.10	0.16	0.44	0.66
12	0.21	0.32	0.10	0.15	0.31	0.47
13	0.00	0.00	0.27	0.00	0.27	0.00
14	0.25	0.27	0.09	0.10	0.35	0.38
15	0.25	0.27	0.07	0.08	0.32	0.35
16	0.00	0.00	0.20	0.00	0.20	0.00
17	0.37	0.34	0.02	0.02	0.39	0.35
18	0.39	0.34	0.01	0.01	0.40	0.35
19	0.00	0.00	0.28	0.00	0.28	0.00
21	0.00	0.00	0.28	0.00	0.28	0.00
22	0.00	0.00	0.26	0.00	0.26	0.00
23	0.34	0.49	0.02	0.03	0.36	0.52
24	0.00	0.00	0.24	0.00	0.24	0.00
25	0.31	0.58	0.06	0.12	0.38	0.70
26	0.37	0.46	0.04	0.04	0.40	0.50
27	0.00	0.00	0.25	0.00	0.25	0.00
28	0.29	0.51	0.04	0.07	0.33	0.58
29	0.36	0.51	0.03	0.04	0.39	0.55
30	0.00	0.00	0.22	0.00	0.22	0.00
31	0.36	0.51	0.02	0.03	0.38	0.54
32	0.52	0.74	0.02	0.02	0.54	0.76
33	0.00	0.00	0.18	0.00	0.18	0.00
34	0.35	0.55	0.01	0.02	0.36	0.57
35	0.38	0.42	0.01	0.01	0.39	0.43
36	0.00	0.00	0.18	0.00	0.18	0.00
37	0.35	0.39	0.01	0.01	0.36	0.40
38	0.45	0.50	0.01	0.01	0.46	0.51
39	0.00	0.00	0.14	0.00	0.14	0.00

Table V.17: Multiple energy communities approach - 20 households

	LM		P2P		Total	
Household	SSR	SCR	SSR	SCR	SSR	SCR
1	0.00	0.00	0.43	0.00	0.43	0.00
2	0.00	0.00	0.42	0.00	0.42	0.00
3	0.29	0.43	0.12	0.18	0.42	0.61
4	0.00	0.00	0.39	0.00	0.39	0.00
5	0.32	0.33	0.09	0.10	0.41	0.43
6	0.32	0.33	0.09	0.09	0.40	0.42
7	0.00	0.00	0.37	0.00	0.37	0.00
8	0.36	0.41	0.10	0.11	0.46	0.52
9	0.22	0.34	0.12	0.18	0.33	0.53
10	0.00	0.00	0.40	0.00	0.40	0.00
11	0.33	0.50	0.10	0.16	0.44	0.66
12	0.33	0.50	0.10	0.14	0.43	0.65
13	0.00	0.00	0.27	0.00	0.27	0.00
14	0.25	0.27	0.09	0.09	0.34	0.37
15	0.25	0.27	0.06	0.07	0.32	0.34
16	0.00	0.00	0.20	0.00	0.20	0.00
17	0.39	0.36	0.02	0.02	0.41	0.37
18	0.39	0.34	0.01	0.01	0.40	0.35
19	0.00	0.00	0.29	0.00	0.29	0.00
20	0.00	0.00	0.28	0.00	0.28	0.00
21	0.00	0.00	0.25	0.00	0.25	0.00
22	0.34	0.49	0.02	0.03	0.36	0.52
23	0.00	0.00	0.24	0.00	0.24	0.00
24	0.34	0.49	0.02	0.02	0.35	0.51
25	0.32	0.60	0.06	0.11	0.38	0.71
26	0.00	0.00	0.25	0.00	0.25	0.00
27	0.33	0.58	0.04	0.07	0.37	0.66
28	0.33	0.58	0.03	0.06	0.36	0.64
29	0.00	0.00	0.22	0.00	0.22	0.00
30	0.36	0.51	0.02	0.02	0.38	0.54
31	0.36	0.51	0.02	0.02	0.38	0.53
32	0.00	0.00	0.20	0.00	0.20	0.00
33	0.34	0.57	0.01	0.02	0.35	0.59
34	0.35	0.55	0.01	0.02	0.36	0.57
35	0.00	0.00	0.17	0.00	0.17	0.00
36	0.38	0.42	0.01	0.01	0.39	0.43
37	0.35	0.39	0.01	0.02	0.36	0.40
38	0.00	0.00	0.17	0.00	0.17	0.00
39	0.36	0.47	0.01	0.01	0.37	0.48
40	0.00	0.00	0.13	0.00	0.13	0.00

VI

Electricity bill for the individual households

Table VI.1: Energy bill for the individual approach

Household	No PV (€)	Individual (€)
1	504,30	298.39
2	443.42	239.49
3	412.47	208.69
4	472.79	268.89
5	512.55	246.49
6	532.86	266.84
7	517.50	251.34
8	901.47	337.27
9	953.69	608.79
10	855.80	426.76
11	897.51	468.46
12	846.90	417.83
13	807.72	296.77
14	937.72	428.51
15	859.68	348.79
16	758.87	378.08
17	2072.58	543.78
18	1963.40	452.88
19	1564.21	523.90
20	1863.25	507.61

Table VI.2: Energy bill for the individual with storage approach

Household	No PV (€)	Individual with Storage (€)
1	504,30	173.01
2	443.42	154.51
3	412.47	163.80
4	472.79	167.93
5	512.55	60.07
6	532.86	60.28
7	517.50	59.86
8	901.47	164.06
9	953.69	433.60
10	855.80	326.87
11	897.51	332.66
12	846.90	324.80
13	807.72	228.65
14	937.72	264.53
15	859.68	235.09
16	758.87	214.30
17	2072.58	11.44
18	1963.40	132.03
19	1564.21	103.85
20	1863.25	114.44

Table VI.3: Energy bill for the multiple energy community approach

		No PV (€)		Energy Community (€)									
Household		EC 1	EC 2	EC 1	EC 2	EC 1	EC 2	EC 1	EC 2	EC 1	EC 2	EC 1	EC 2
1	21	504.30	2060.31	160.74	721.17	242.31	1315.77	254.83	1308.26	249.63	2655.53	250.09	1325.23
2	22	443.42	1114.90	281.69	828.45	92.27	592.33	193.27	593.81	226.95	613.10	250.29	603.33
3	23	412.47	1966.03	88.47	277.17	254.24	1344.35	254.16	1345.06	123.26	1352.40	98.80	1351.90
4	24	472.79	1883.55	142.54	829.71	87.46	545.06	195.55	541.77	368.21	485.89	258.37	533.42
5	25	512.55	2014.33	295.95	658.43	257.91	902.50	235.49	457.73	149.88	203.31	141.48	460.03
6	26	532.86	1448.09	126.28	230.56	44.45	262.14	260.58	880.13	191.48	899.88	224.38	895.24
7	27	517.55	1394.74	251.75	630.49	261.27	900.84	222.24	441.06	618.99	441.01	260.37	435.26
8	28	901.47	1354.60	296.73	785.93	77.85	482.91	149.40	470.28	144.64	238.56	151.88	467.79
9	29	953.69	1110.99	273.13	203.56	340.88	754.05	360.73	741.73	168.95	736.53	144.73	736.03
10	30	855.80	1069.35	503.65	196.83	185.59	247.73	507.05	744.86	310.16	265.53	502.66	242.72
11	31	897.51	1160.99	390.97	436.24	189.79	245.74	206.20	270.65	390.45	278.23	190.08	241.93
12	32	846.90	1071.73	346.42	387.29	187.67	284.26	525.50	751.09	183.69	1393.52	187.23	739.74
13	33	807.72	2132.14	245.75	1308.44	489.90	1414.70	448.29	718.49	307.70	478.12	468.92	707.21
14	34	937.72	1681.58	149.36	845.31	83.35	487.91	346.16	525.13	232.70	159.66	156.92	524.34
15	35	859.68	1451.58	74.93	476.48	95.57	172.97	533.48	1101.31	254.82	1111.53	57.383	1088.31
16	36	758.87	1506.58	142.49	907.48	85.95	251.57	169.93	190.69	174.48	262.80	534.857	175.974
17	37	2072.58	1864.31	-	-	1270.56	1369.60	260.64	288.29	1296.09	279.83	252.569	280.869
18	38	1561.21	2066.03	-	-	-	-	1286.25	1388.06	1047.66	1874.89	127.02	1384.89
19	39	1564.21	2363.18	-	-		-	-	-	1287.15	1289.30	1295.93	628.79
20	40	1863.25	2490.42	-	-	-	-		-	-	-	1328.38	1794.88

Table VI.4: Energy bill for the energy community approach

Household	No PV (€)	Energy Community (€)				
1	504.30	89.59	222.10	225.40	208.33	314.66
2	443.42	207.46	91.18	86.10	202.59	230.26
3	412.47	90.15	225.22	220.73	79.45	94.57
4	472.79	91.94	99.67	95.09	205.64	227.48
5	512.55	215.26	231.03	144.79	131.00	140.09
6	532.86	47.62	149.08	227.12	132.48	29.63
7	517.55	46.06	233.25	144.95	209.95	232.01
8	901.47	404.07	94.48	89.53	71.47	62.06
9	953.69	195.06	440.59	45.82	181.41	189.15
10	855.80	411.38	186.11	437.57	399.12	430.32
11	897.51	423.95	193.49	180.74	159.48	167.95
12	846.90	254.85	195.42	448.53	158.63	168.50
13	807.72	417.53	505.25	121.09	444.27	459.25
14	937.72	154.67	148.29	139.27	112.96	74.40
15	859.68	156.97	150.98	523.90	122.33	85.654
16	758.87	157.92	152.23	150.90	489.46	511.649
17	2072.58		1087.59	319.03	157.64	24.932
18	1561.21			1058.02	106.02	109.96
19	1564.21				963.17	377.97
20	1863.25					1063.54

Table VI.5: Energy bill for the energy community approach

		No PV (€)		Energy Community (€)									
Household		EC 1	EC 2	EC 1	EC 2	EC 1	EC 2	EC 1	EC 2	EC 1	EC 2	EC 1	EC 2
1	21	504.30	2060.31	160.74	721.17	242.31	1315.77	254.83	1308.26	249.63	2655.53	250.09	1325.23
2	22	443.42	1114.90	281.69	828.45	92.27	592.33	193.27	593.81	226.95	613.10	250.29	603.33
3	23	412.47	1966.03	88.47	277.17	254.24	1344.35	254.16	1345.06	123.26	1352.40	98.80	1351.90
4	24	472.79	1883.55	142.54	829.71	87.46	545.06	195.55	541.77	368.21	485.89	258.37	533.42
5	25	512.55	2014.33	295.95	658.43	257.91	902.50	235.49	457.73	149.88	203.31	41.48	460.03
6	26	532.86	1448.09	126.28	230.56	44.45	262.14	260.58	880.13	191.48	899.88	24.38	895.24
7	27	517.55	1394.74	251.75	630.49	261.27	900.84	222.24	441.06	618.99	441.01	260.37	435.26
8	28	901.47	1354.60	296.73	785.93	77.85	482.91	149.40	470.28	144.64	238.56	51.88	467.79
9	29	953.69	1110.99	273.13	203.56	340.88	754.05	360.73	741.73	168.95	736.53	84.73	736.03
10	30	855.80	1069.35	503.65	196.83	185.59	247.73	507.05	744.86	310.16	265.53	502.66	242.72
11	31	897.51	1160.99	390.97	436.24	189.79	245.74	206.20	270.65	390.45	278.23	190.08	241.93
12	32	846.90	1071.73	346.42	387.29	187.67	284.26	525.50	751.09	183.69	1393.52	187.23	739.74
13	33	807.72	2132.14	245.75	1308.44	489.90	1414.70	448.29	718.49	307.70	478.12	468.92	707.21
14	34	937.72	1681.58	149.36	845.31	83.35	487.91	346.16	525.13	232.70	159.66	56.92	524.34
15	35	859.68	1451.58	74.93	476.48	95.57	172.97	533.48	1101.31	254.82	1111.53	57.383	1088.31
16	36	758.87	1506.58	142.49	907.48	85.95	251.57	169.93	190.69	174.48	262.80	534.857	175.974
17	37	2072.58	1864.31	-	-	1270.56	1369.60	260.64	288.29	1296.09	279.83	52.569	280.869
18	38	1561.21	2066.03	-	-	-	-	1286.25	1388.06	1047.66	1874.89	127.02	1384.89
19	39	1564.21	2363.18	-	-		-	-	-	1287.15	1289.30	1295.93	628.79
20	40	1863.25	2490.42	-	-	-	-		-	-	-	1328.38	1794.88

VII

Datasheet

APsystems
ALTENERGY POWER

Branchenführer für **Mikrowechselrichter - Solartechnologie**

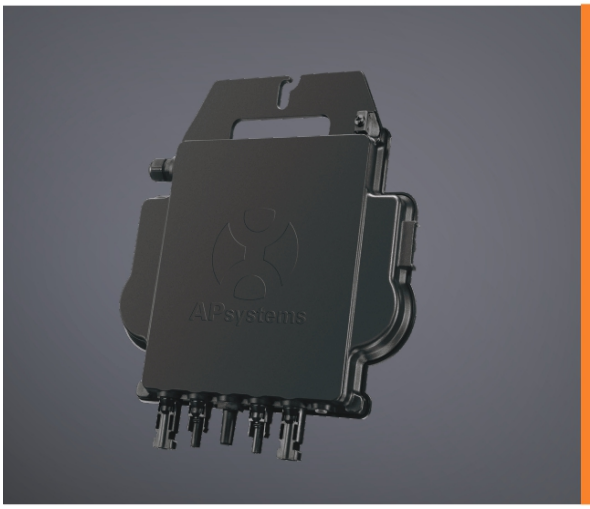

DS3

Der leistungsstärkste Dual- Mikrowechselrichter

- Ein Mikrowechselrichter kann 2 Panels bedienen
- Maximale dauerhafte Ausgangsleistung 600VA, 730VA, 880VA, oder 960VA
- Zwei Eingangskanäle mit unabhängigen MPPTs
- Reactive Power Control
- Maximale Zuverlässigkeit, IP67
- Verschlüsselte ZigBee-Kommunikation
- VDE Relais integriert

PRODUCT PRODUKTMERKMALE

Die dritte Generation der Dual-Mikro-wechselrichter von APsystems erreicht beispiellose Ausgangsleistungen von 600, 730 VA, 880 VA, bzw. 960VA um sich an die heutige und künftige Generation von Hochleistungspanelen anzupassen. Mit 2 unabhängigen MPPT und verschlüsselten Zigbee-Signalen profitieren DS3-S, DS3-L, DS3, und DS3-H von einer völlig neuen Architektur und sind vollständig abwärtskompatibel mit den QS1- und YC600-Mikrowechselrichtern.

Das innovative und kompakte Design macht das Produkt leichter und maximiert die Stromproduktion. Die Komponenten sind mit Silikon vergossen, um die Belastung der Elektronik zu reduzieren, die Wärmeableitung zu erleichtern, und die Wasserdichtheit zu verbessern. Strenge Testmethoden, einschließlich beschleunigter Lebensdauertests, gewährleisten eine maximale Zuverlässigkeit des Systems. Eine 24/7-Energie-überwachung über Apps oder ein webbasiertes Portal erleichtert die Ferndiagnose und -wartung.

Die neue DS3-Serie interagiert mit Stromnetzen durch eine Funktion, die als RPC (Reactive Power Control) bezeichnet wird, um Photovoltaik-Leistungsspitzen im Netz besser zu bewältigen. Mit einer Leistung und einem Wirkungsgrad von 97.3% sowie einer einzigartigen Integration mit 20% weniger Komponenten, setzen APsystems DS3-S, DS3-L, DS3 & DS3-H neue Maßstäbe für private und gewerbliche PV.

VERDRAHTUNGSSCHEMA

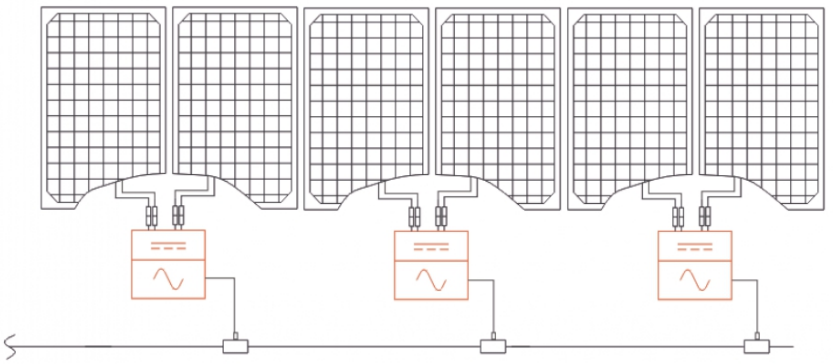

2022/08/22 Rev1.0

Figure VII.1: Micro inverter datasheet 1

Datenblatt | DS3 Mikrowechselrichter Series

Modell	DS3-S	DS3-L	DS3	DS3-H
Region		EMEA		
Eingangsdaten (DC)				
Empfohlener PV-Modulleistungsbereich (STC)	255Wp-550Wp+		300Wp-620Wp+	330Wp-660Wp+
MPPT Spannungsbereich(1)	28V-45V			
Betriebsspannungsbereich	16V-60V			
Maximale Eingangsspannung	60V			
Maximale Eingangsstromstärke	18A x 2	18A x 2	20A x 2	20A x 2
Isc PV	22.5A x 2	22.5A x 2	25A x 2	25A x 2
Ausgangsdaten (AC)				
Maximale Ausgangsleistung	600VA	730VA	880VA	960VA
Nennausgangsspannung(2)	230V/184V-253V			
Nennausgangsstrom	2.6A	3.2A	3.8A	4.2A
Nennausgangsfrequenz(2)	50Hz/48Hz-51Hz			
Leistungsfaktor (Standard/Regelbereich)	0.99/0.8 untererregt... 0.8 übreerregt			
Maximalanzahl Einheiten je Stromkreis bei 2.5mm²(3)	8	7	5	5
Wirkungsgrad				
Max. Wirkungsgrad	97.3%			
Nennwirkungsgrad MPPT	99.5%			
Nachtverbrauch	20mW			
Mechanische Daten				
Betriebstemperaturbereich(4)	- 40 °C to + 65 °C			
Lagertemperaturbereich	- 40 °C to + 85 °C			
Abmessungen (B x H x T)	263mm x 218mm x 41.2mm		263mm x 218mm x 42.5mm	
Gewicht	2.7kg		3.1kg	
AC Bus Cable	2.5mm²(23A)			
DC Connector Type	Stäubli MC4 PV-ADBP4-S2&ADSP4-S2			
Kühlung	Natürliche Konvektion - Keine Lüfter			
Gehäuseschutzart	IP67			
Funktionen				
Kommunikation (Wechselrichter/ECU)(5)	Encrypted ZigBee			
Transformatordesign	Hochfrequenz- Transformatoren, galvanisch getrennt			
Überwachung	Energy Management Analysis (EMA) system			
Garantie(6)	Standardmäßig 10 Jahre, optional 20 Jahre			
Zertifikate und Konformitäte				
Sicherheit, EMC und Netzkonformität	EN 62109-1/-2; EN 61000-1/-2/-3/-4; VDE-AR-N 4105; G98; G99; G98/NI; G99/NI	EN 62109-1/-2; EN 61000-1/-2/-3/-4; EN 50549-1; PN-EN 50549-1; DIN V VDE V 0126-1-1; VFR 2019; UTE C15-712-1; CEI 0-21; UNE 217002; NTS; RD647; VDE-AR-N 4105; G98; G99; G98/NI; G99/NI		

(1) Die MPPT-Spannungsbereiche können bei früheren DS3-Modellen unterschiedlich sein, mit einem Bereich von 34 - 45 V für Mikrowechselrichter, die nicht an eine ECU angeschlossen sind, und einem Bereich von 30 - 45 V für Geräte, die mit einer ECU aufgerüstet wurden.
(2) Der Nennspannungs-/Frequenzbereich kann auf Wunsch des Versorgungsunternehmens über den Nennwert hinaus erweitert werden.
(3) Die Grenzen können variieren. Beziehen Sie sich auf die lokalen Anforderungen, um die Anzahl der Mikrowechselrichter pro Stromzweig in Ihrer Region zu definieren.
(4) Der Wechselrichter wechselt in gedrosselten Betrieb bei unzureichender Wärmeabfuhr.
(5) Für eine stabile Kommunikation wird empfohlen, nicht mehr als 80 Mikrowechselrichter mit einer einzelnen ECU zu verbinden.
(6) Um Anspruch auf die beste Garantie zu haben, müssen die Mikrowechselrichter von APsystems über das EMA-Portal überwacht werden. Bitte beachten Sie unsere Garantiebedingungen auf emea.APsystems.com

Niederlassungen in Europa:

APsystems
Karspeldreef 8, 1101 CJ, Amsterdam, The Netherlands
Tel: +31 (0)85 3018499
Email : emea@apsystems.com

APsystems
C/Bulnea 244c rue du Point du Jour
01000 Saint Denis lès Bourg
Email : emea@apsystems.com | Tel: +33-4-81 65 60 40

Figure VII.2: Micro inverter datasheet 2

www.jinkosolar.com

Jinko Solar
Building Your Trust in Solar

TR 72M
510-530 Watt
Mono-facial

Tiling Ribbon (TR) Technology

Positive power tolerance of 0~+3%

(Draft)

TIGER Pro

KEY FEATURES

TR technology + Half Cell
TR technology with Half cell aims to eliminate the cell gap to increase module efficiency (mono-facial up to 21.41%)

MBB instead of 5BB
MBB technology decreases the distance between bus bars and finger grid line which is benefit to power increase.

Higher lifetime Power Yield
2.0% first year degradation,
0.55% linear degradation

Best Warranty
12 year product warranty,
25 year linear power warranty

Strengthened Mechanical Support
5400 Pa snow load, 2400 Pa wind load

PV CYCLE · TÜVRheinland CERTIFIED · CE

POSITIVE QUALITY Continuous Quality Assurance · CLEAN ENERGY COUNCIL MEMBER

ISO9001:2015, ISO14001:2015, ISO45001:2018 certified factory

IEC61215, IEC61730 certified product

LINEAR PERFORMANCE WARRANTY

12 Year Product Warranty • 25 Year Linear Power Warranty
0.55% Annual Degradation Over 25 years

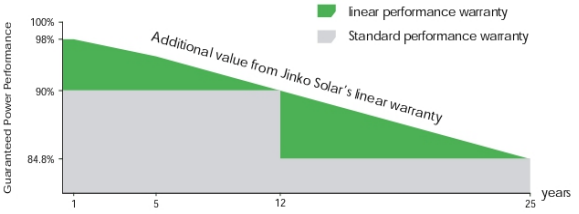

Figure VII.3: PV module datasheet 1

Engineering Drawings

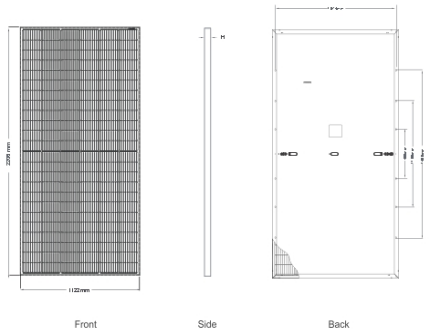

Electrical Performance & Temperature Dependence

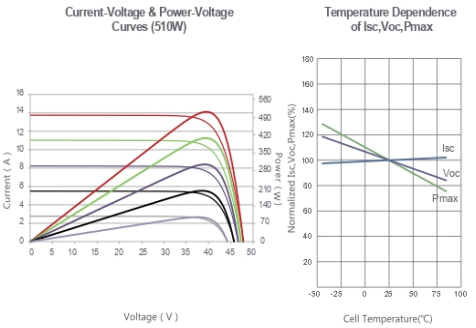

Packaging Configuration

(Two pallets = One stack)

31pcs/pallets, 62pcs/stack, 620pcs/ 40'HQ Container

Mechanical Characteristics

Cell Type	P type Mono-crystalline
No.of cells	144 (2×72)
Dimensions	2206×1122×35mm (86.85×44.17×1.38 inch)
Weight	28.2 kg (62.17 lbs)
Front Glass	3.2mm,Anti-Reflection Coating, High Transmission, Low Iron, Tempered Glass
Frame	Anodized Aluminium Alloy
Junction Box	IP67 Rated
Output Cables	TUV 1×4.0mm² (+): 290mm , (-): 145 mm or Customized Length

SPECIFICATIONS

Module Type	JKM510M-7TL4-V		JKM515M-7TL4-V		JKM520M-7TL4-V		JKM525M-7TL4-V		JKM530M-7TL4-V	
	STC	NOCT	STC	NOCT	STC	NOCT	STC	NOCT	STC	NOCT
Maximum Power (Pmax)	510Wp	379Wp	515Wp	383Wp	520Wp	387Wp	525Wp	391Wp	530Wp	394Wp
Maximum Power Voltage (Vmp)	41.40V	38.25V	41.50V	38.35V	41.60V	38.46V	41.70V	38.56V	41.80V	38.66V
Maximum Power Current (Imp)	12.32A	9.92A	12.41A	9.99A	12.50A	10.06A	12.59A	10.13A	12.68A	10.20A
Open-circuit Voltage (Voc)	48.94V	46.10V	49.04V	46.19V	49.14V	46.28V	49.24V	46.38V	49.34V	46.47V
Short-circuit Current (Isc)	13.05A	10.54A	13.14A	10.61A	13.23A	10.69A	13.32A	10.76A	13.41A	10.83A
Module Efficiency STC (%)	20.60%		20.81%		21.03%		21.21%		21.41%	
Operating Temperature(℃)	-40℃~+85℃									
Maximum system voltage	1500VDC (IEC)									
Maximum series fuse rating	25A									
Power tolerance	0~+3%									
Temperature coefficients of Pmax	-0.35%/℃									
Temperature coefficients of Voc	-0.28%/℃									
Temperature coefficients of Isc	0.048%/℃									
Nominal operating cell temperature (NOCT)	45±2℃									

*STC: Irradiance 1000W/m² Cell Temperature 25°C AM=1.5

NOCT: Irradiance 800W/m² Ambient Temperature 20°C AM=1.5 Wind Speed 1m/s

* Power measurement tolerance: ± 3%

TR JKM510-530M-7TL4-V-D4.1-EN

Figure VII.4: PV module datasheet 2

Figure VII.5: 10kWh / 15kWh Battery datasheet 1

A1-ESS-G2

A1-HYB-G2

- Up to 200% oversizing allowed
- Up to 3 MPPTs
- Maximum 16A PV input current
- Microgrid supported
- Optional revenue grade metering
- Up to 4 systems in parallel①
- Peak efficiency: 98%
- Integrated arc fault protection and rapid shutdown transmitter

T-BAT-SYS-HV-5.0

- Long life & Safe LPF battery
- Up to 4 battery modules stackable, 20kWh each system
- Modular design & Quick installation
- Floor or wall mounted

A1-BI-200-G2

- Maximum 160A AC current
- Flexible home backup
- Up to 4 systems in parallel
- 64A generator supported
- Built-in energy management meter
- Smart load management②
- Heat pump extendable③
- EV charger extendable④

A1-HYB-G2

	A1-HYB-3.8-G2	A1-HYB-5.0-G2	A1-HYB-6.0-G2	A1-HYB-7.6-G2
INPUT PV				
Maximum recommended PV power [W]	7600	10000	10000	15200
Maximum DC voltage [V]	550			
Nominal DC operating voltage [V]	360			
Maximum input current [A]	A: 16 / B: 16	A: 16 / B: 16	A: 16 / B: 16	A: 16 / B: 16 / C: 16
Maximum short circuit current [A]	A: 20 / B: 20	A: 20 / B: 20	A: 20 / B: 20	A: 20 / B: 20 / C: 20
MPPT voltage range [V]	90-500			
Start input voltage [V]	120			
No. of MPP trackers, Strings per MPP tracker	2, 1 / 1	2, 1 / 1	2, 1 / 1	3, 1 / 1 / 1
DC disconnection switch	YES			
INPUT/OUTPUT AC				
Nominal AC power [VA]	3816	5016	6000	7608
Maximum apparent AC power [VA]	3816	5016	6000	7608
Nominal AC voltage [V] / Nominal AC frequency [Hz]	240 / 50, 60			
Nominal AC current [A]	15.9	20.9	25	31.7
Displacement power factor	0.8 leading to 0.8 lagging			
Total harmonic distortion (THD, rated power)	< 3%			
INPUT/OUTPUT BAT				
Battery type	Li-ion			
Maximum output power [W]	3816	5016	6000	7600
Maximum charge / discharge current [A]	54	54	54	54
Reverse-polarity protection	YES			
Cycle efficiency charging to discharging (PCS)	88.5%	90.5%	91.5%	92.5%
ADDITIONAL FEATURES				
AFCI	YES			
Revenue grade metering, ANSI C12.20	Optional			
Rapid shutdown transmitter	Integrated PLC controller to RSD			
EFFICIENCY				
CEC weighted efficiency	97.50%			
Maximum inverter efficiency	98.00%			
POWER CONSUMPTION				
Internal consumption (night) [W]	< 3			
STANDARD				
Safety	UL1741, UL1741 SA, UL1699B, CSA - C22.2 No. 1071-01, Canadian AFCI according to T.I.L. M-07			
Emissions	FCC Part 15 Class B			
Grid connection standards	IEEE1547, Rule 21, Rule14 (HI)			
INSTALLATION SPECIFICATIONS				
Protection class	NEMA 4X			
Operating temperature range [°F / °C]	-13 to +140 / -25 to +60			
De-rating start temperature [°F / °C]	113 / 45 or above			
Storage temperature range [°F / °C]	-13 to +167 / -25 to +75			
Relative humidity [%]	0 to 95			
Altitude [ft / m]	9843 / 3000 MAX			
Typical noise emission [dBA]	< 30			
Over voltage category	IV (electric supply side), II (PV side)			
GENERAL				
Dimensions (W x H x D) [in / mm]	33.1 x 15.7 x 5.7 / 840 x 400 x 145			
Weight [lb / kg]	75 / 34			
Cooling	Natural convection			
Topology	Transformerless			
Communication interfaces	RS485, CAN, WIFI (optional) / 4G (optional), Dry Contact			
Warranty	12 years			

A1-AC-G2

	A1-AC-3.8K-G2	A1-AC-5.0K-G2	A1-AC-6.0K-G2	A1-AC-7.6K-G2
INPUT/OUTPUT AC				
Nominal AC power [VA]	3816	5016	6000	7608
Maximum apparent AC power [VA]	3816	5016	6000	7608
Nominal AC voltage [V] / Nominal AC frequency [Hz]	240 / 50, 60			
Nominal AC current [A]	15.9	20.9	25	31.7
Displacement power factor	0.8 leading to 0.8 lagging			
Total harmonic distortion (THD, rated power)	< 3%			
NPUT/OUTPUT BAT				
Battery type	Li-ion			
Maximum output power [W]	3816	5016	6000	7600
Maximum charge / discharge current [A]	54	54	54	54
Reverse-polarity protection	YES			
Cycle efficiency charging to discharging (PCS)	88.5%	90.5%	91.5%	92.5%
ADDITIONAL FEATURES				
Revenue grade metering, ANSI C12.20	Optional			
Efficiency				
Maximum inverter efficiency	98.00%			
POWER CONSUMPTION				
Internal consumption (night) [W]	< 3			
STANDARD				
Safety	UL1741, UL1741 SA, CSA - C22.2 No. 1071-01			
Emissions	FCC Part 15 Class B			
Grid connection standards	IEEE1547, Rule 21, Rule14 (HI)			
INSTALLATION SPECIFICATIONS				
Protection class	NEMA 4X			
Operating temperature range [°F / °C]	-13 to +140 / -25 to +60			
De-rating start temperature [°F / °C]	113 / 45 or above			
Storage temperature range [°F / °C]	-13 to +167 / -25 to +75			
Relative humidity [%]	0 to 95			
Altitude [ft / m]	9843 / 3000 MAX			
Typical noise emission [dBA]	< 30			
Over voltage category	IV (electric supply side)			
GENERAL				
Dimensions (WxHxD) [in / mm]	33.1 x 15.7 x 5.7 / 840 x 400 x 145			
Weight [lb / kg]	75 / 34			
Cooling	Natural convection			
Topology	Transformerless			
Communication interfaces	RS485, CAN, WIFI (optional) / 4G (optional), Dry Contact			
Warranty	12 years			

T-BAT-SYS-HV-5.0

	T-BAT H 10.0	T-BAT H 15.0	T-BAT H 20.0
MODEL			
Battery type	100Ah Lithium (LFP)		
Components	TBMS-MCS60060 + 2*TP-HS50	TBMS-MCS60060 + 3*TP-HS50	TBMS-MCS60060 + 4*TP-HS50
NOMINAL CHARACTER			
Voltage [V]	102.4	153.6	204.8
Operating voltage range [V]	90 - 116	135 - 174	180 - 232
Total energy [kWh]	10	15	20
Usable energy [kWh]④	9	13.5	18
Battery roundtrip efficiency [%]⑤	95%		
Maximum power [kW]	5.5	8.3	11.1
Maximum charge / discharge current [A]	54		
Cycle life (90% DOD)	6000 cycles		
Warranty	12 years (Details refer to SolaX Power warranty statement)		
INSTALLATION SPECIFICATIONS			
Charge / Discharge temperature range [°F / °C]	Charge: 32 to 127.4 / 0 to 53, Discharge: 14 to 127.4 / -10 to 53		
Storage temperature range [°F / °C]	3 months: 41 to 122 / -20 to 50, 1 year: 32 to 104 / 0 to 40		
Relative humidity [%]	0 to 100		
Altitude [ft / m]	9843 / 3000 MAX		
Protection class	NEMA 4X		
STANDARD			
Certification	UN38.3, UL1973, UL9540, UL9540A		
Hazardous materials classification	Class 9		
GENERAL			
Cooling	Natural convection		
Dimensions (W x H x D) [in / mm] - TBMS-MCS60060 (BMS)	33.5 x 5.2 x 5.8 / 850 x 133 x 148		
Dimensions (W x H x D) [in / mm] - TP-HS50 (BAT)	33.5 x 23.6 x 5.8 / 850 x 600 x 148	33.5 x 35.4 x 5.8 / 850 x 900 x 148	33.5 x 47.2 x 5.8 / 850 x 1200 x 148
Dimensions (W x H x D) [in / mm] - Base	33.5 x 2.2 x 5.8 / 850 x 55 x 148		
Weight [lb / kg]	TBMS-MCS60060: 22 / 10 + 2*TP-HS50: 238 / 108	TBMS-MCS60060: 22 / 10 + 3*TP-HS50: 357 / 162	TBMS-MCS60060: 22 / 10 + 4* TP-HS50: 476 / 216

A1-BI-200-G2

GRID INPUT	
Nominal AC input voltage [V]	120 / 240
Nominal AC frequency [Hz]	50 / 60
Maximum AC input current [A]	160
OUTPUT TO MAIN PANEL IN GRID TIED OPERATION	
Nominal AC output voltage [V]	120 / 240
Maximum AC input current [A]	160
OUTPUT TO MAIN PANEL IN BACKUP OPERATION	
Nominal AC output voltage [V]	120 / 240
Imbalance compensation in backup operation [VA]	5000
Split phase imbalance output current [A]	41.7
Maximum AC output current [A]	126.8
INPUT FROM INVERTER	
Maximum number of inverter inputs	4
Maximum AC power [W]	7600
Maximum continuous input current @240V [A]	31.7
Maximum inverter input AC circuit breaker [A]	40 (optional)
Upgradability	Up to 4 x 40A circuit breaker
GENERATOR	
Maximum AC power [W]	15000
Maximum continuous input current [A]	63
Auto generator start	Yes
GENERAL	
Dimensions (HxWxD) [in / mm]	27.8 x 17.7 x 5.9 / 706 x 450 x 151
Weight [lb / kg]	69.4 / 31.5
Energy meter accuracy	1%
Communication interfaces	RS485, CAN, Dry Contact
Cooling	Fan
Warranty	12 years
STANDARD	
Safety	UL1741, CSA 22.2 NO.107
Emissions	FCC part 15 Class B
INSTALLATION SPECIFICATIONS	
Altitude [ft / m]	9843 / 3000 MAX
Operating temperature range [°F / °C]	-13 to +140 / -25 to +60
Protection class	NEMA 3R
Typical noise emission [dBA]	< 50

① To be released in Q4 2022. ② To be released in Q2 2023. ③ To be released in Q3 2023.
④ Test Conditions: 90% DOD, 0.2C charge & discharge at + 25 °C. ⑤ Maximum Charge/Discharge power may be variant with different inverter models.

*V1.2 Information may be subject to change without notice.

Figure VII.6: 10kWh / 15kWh Battery datasheet 2

AmpliPHI 3.8™ BATTERY

simpliphi
Power. On Your Terms.™

SimpliPhi Power's AmpliPHI 3.8™ Battery utilizes the safest Lithium Ion chemistry available, Lithium Ferro Phosphate (LFP). No cobalt or explosive hazards that put customers at risk. By eliminating cobalt, the risk of thermal runaway, fire propagation, operating temperature constraints, and toxic coolants are reduced. The AmpliPHI features a Battery Management System (BMS) with closed loop communications pre-configured for industry leading inverters that reports SOC and other critical real-time data, optimizing the value of storage and functionality within balance-of-system equipment. Combined with our proven overcurrent protection (OCPD) and accessible 100 Amp DC breaker On/Off switch, installation time is reduced and safety is increased during set-up for residential and commercial systems, on and off-grid. Designed to scale up to 75 batteries, the AmpliPHI integrates seamlessly with Sol-Ark and SMA, with other inverter brands being added soon.

AmpliPHI 3.8 kWh Module	AmpliPHI 48V
SKU	AmpliPHI-3.8-48
DC Voltages - Nominal	51.2 VDC
Amp-Hours	75 Ah
Rated kWh Capacity	3.8 kWh DC @ 100% DOD 3.04 kWh DC @ 80% DOD
Maximum Quantity Per System	75 (285kWh)
MAX Discharge Rate (10 minutes)	100 Amps DC (5.1 kW DC)
MAX Continuous Discharge Rate	37.5 Amps DC (1.9 kW DC)
MAX Continuous Charge Rate	37.5 Amps DC (1.9 kW DC)
DC Voltage Range[1]	48 VDC to 56 VDC
Depth of Discharge[1]	up to 100%
Charging Temperature[1]	32° to 120° F (0° to 49° C)
Operating Temperature[1]	-4° to 140° F (-20° to 60° C)
Storage Temperature	6 months: 14° to 77° F (-10° to 25° C) 3 months: -4° to 113° F (-20° to 45° C)
Self-Discharge Rate	< 1% per month
Cycle Life	10,000+ cycles (@ 80% DOD)
Memory Effect	None
Warranty	10 Years
Weight	86 lbs. (39.0 kg)
Dimensions (W x H x D)	13.5 x 14 x 8 in. (15.5" H w/terminals) / 0.88 ft3 (34.3 x 35.6 x 20.3 cm / 0.025 m3)
Model Number	AmpliPHI3.8-48

1. Max operating ranges. Refer to Installation Manual for recommended conditions.
• All specifications listed are typical/nominal and subject to change without notice.
• UN 3480, Lithium ion batteries, 9, II
• UL, CE, UN/DOT and RoHS compliant components - UL 1642, UL 1973, UL 9540A Test Approved
• Designed and manufactured in California, USA

Intertek

Power. On Your Terms.™

805-640-6700 | SIMPLIPHIPOWER.COM |
REV202110071710

Figure VII.7: 3.8kWh Battery datasheet 1

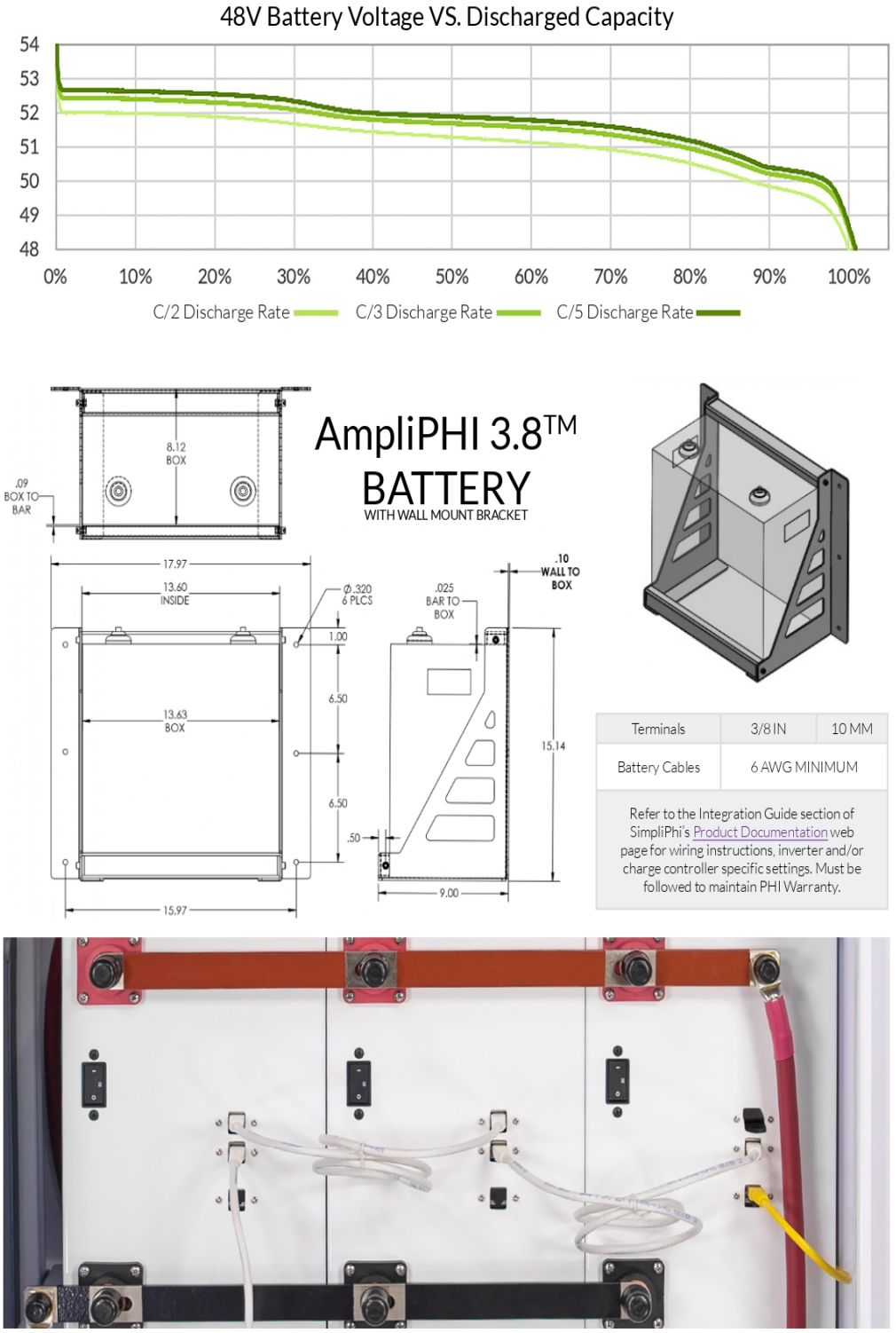

Figure VII.8: 3.8kWh Battery datasheet 2